Title
Fundamentals of saturation kinetics--application to iopanic acid in the dog

Author
Staubus, Alfred Elsworth

Publication Date
1974

Peer reviewed|Thesis/dissertation

FUNDAMENTALS OF SATURATION KINETICS - APPLICATION TO IOPANIC ACID IN THE DOG

by

Alfred Elsworth Staubus
Pharm.D., University of California, San Francisco, 1971

DISSERTATION

Submitted in partial satisfaction of the requirements for the degree of

DOCTOR OF PHILOSOPHY

in

PHARMACEUTICAL CHEMISTRY

in the

GRADUATE DIVISION

(San Francisco)

of the

UNIVERSITY OF CALIFORNIA

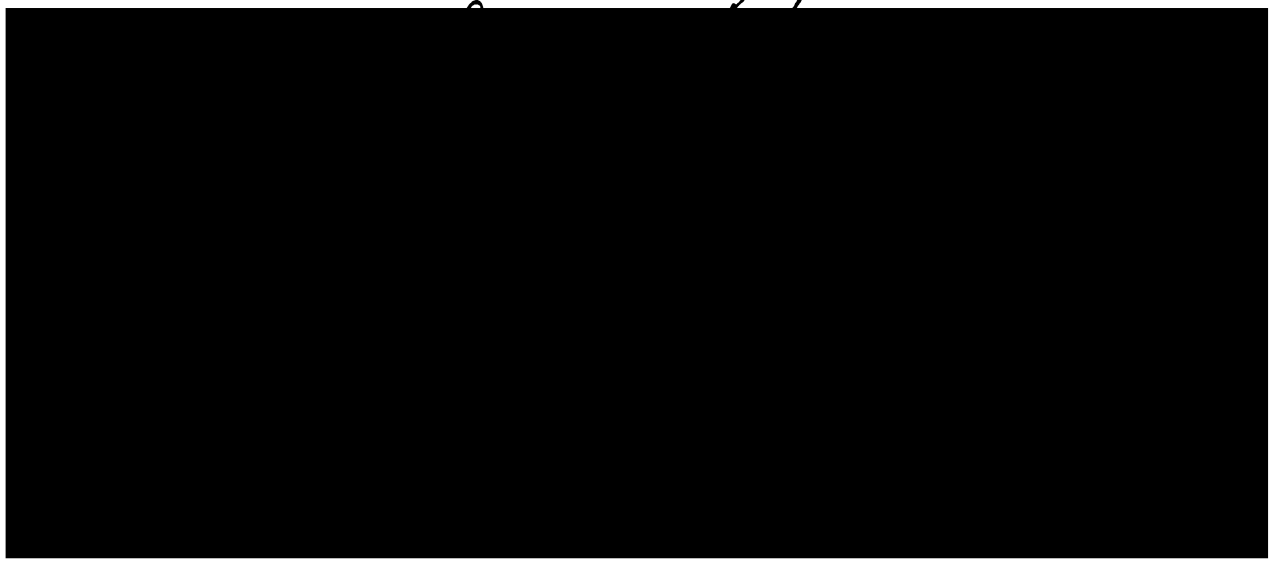

ABSTRACT

The fundamental saturation kinetics of multiple compartmental models at distribution equilibrium were developed and tested using iopanoic acid infusions in mongrel dogs. The theoretical considerations of saturated capacity-limited systems resulted in the simplification and refinement of a multiple infusion technique that permits the estimation of the apparent maximum velocity, Vm, of the capacity-limited step and the estimation of the apparent steady state volume of distribution, Vd. This multiple infusion technique should theoretically be applicable to any drug undergoing a saturable elimination without a significant concomitant first-order process. For such drugs, this multiple infusion technique permits the estimation of Vm and Vd using blood data alone, without necessitating sampling either bile or urine.

Zero-order infusions of iopanoic acid at rates greater than the apparent maximum velocity results in eventual linear accumulation of drug in the body. Such accumulation is apparent by a linear increase in blood concentration with time. The linear blood concentration-

time slope, $\frac{dC}{dt}$, is a function of the infusion rate (k_o), the apparent maximum velocity (Vm), and the apparent steady state volume of distribution (Vd):

$$\frac{dC}{dt} = \frac{k_o - Vm}{Vd}$$

Post-infusion linear decay curves are observed when the drug is at distribution equilibrium above an apparent saturation threshold of approximately 45 mg of iopanoic acid per liter. The slope of the linear decay curve is equal to - Vm/Vd.

Using this multiple infusion technique, we studied the effect of concomitant infusions of taurocholate on the Vm and Vd of iopanoic acid. A five-fold increase in the infusion rate of taurocholate resulted in an average increase of 40 percent in the Vm of iopanoic acid. There was no significant change in the apparent steady state volume of distribution of iopanoic acid.

In dealing with capacity-limited systems, the concept of clearance was examined.

Clearance in first-order systems is independent of concentration and is defined in terms of volume per unit time. However, application of this definition to saturated, capacity-limited systems (with no significant parallel first-order elimination) loses meaning. In such systems, the

clearance varies with concentration and no longer becomes a characteristic parameter of the particular drug. It may be more appropriate under these saturated conditions to relate the clearance of the drug to the actual amount cleared per unit time, Vm. We suggest that this term, Vm, be called the zero-order mass clearance constant with units of amount per unit time. It is virtually independent of drug concentration. For equivalent clarity, the clearance of a drug during first-order kinetics could then be referred to as the first-order volume clearance constant with, of course, units of volume per unit time.

ACKNOWLEDGMENTS

I would like to express special appreciation to the following people:

To my wife Angela for her loving assistance and companionship during my graduate education.

To Dr. Sidney Riegelman for his guidance, support and friendship. He provided the ideal environment for scientific inquiry and development. I am grateful to have been a student of his.

To Dr. James A. Nelson for his enthusiasm, friendship and collaboration that resulted in a very productive and meaningful experience.

To Dr. Leslie Z. Benet for his warm professional and personal relationship during my graduate education.

To the members of the faculty and the School of Pharmacy for their encouragement and instruction.

To Miss Lucy Roman for her many long hours of dog-sitting, friendship and humor.

To Betsy and all the other warm, beautiful people who made my graduate years a little bit easier.

TABLE OF CONTENTS

TITLE PAGE i

ACKNOWLEDGMENTS ii

TABLE OF CONTENTS iii

CHAPTER I - INTRODUCTION 1

-Cholecystography - Definition and Use . . 1
-Iopanoic Acid Synthesis 4
-Iopanoic Acid Cholecystographic Activity and Toxicity 4
-Iopanoic Acid Physical Properties 5
-Gastro-Intestinal Absorption of Iopanoic Acid 6
-Plasma Protein Binding 7
-Possible Mechanistic Aspects of Hepatic Uptake 8
-Glucuronidation and Biliary Excretion . . 10
-Pharmacokinetics of Iopanoic Acid by Previous Workers 13
-The Dog as an Experimental Model for Cholecystographic Investigation 16

CHAPTER II - THEORETICAL ASPECTS OF SATURATED CAPACITY-LIMITED SYSTEMS 18

-One Compartment Model 23
-Two Compartment Models 30
-Two Compartment-Metabolic Rate-Limited Model 30
-Biliary Excretion 36
-The Two Compartment Volume Constant . . . 36
-The Two Compartment Post-Infusion Period . 39
-Estimation of Vm 40
-Two Compartment Transport Rate-Limited Model 43
-Two Compartment Excretion Rate-Limited Model 47
-Transport and Metabolic Rate-Limited Model 48

-Transport Rate-Limited and Simultaneous First-Order Elimination Model 49
-Clearance Aspects of Hepatic Elimination 53
-Purpose of the Investigation 57

CHAPTER III - EXPERIMENTAL 58

Materials and Equipment 58
-Iopanoic Acid Identification 59
-Iopanoic Acid Solution 59
-Taurocholate Solutions 60

Assay Method 60
-Fluorescent Excitation Analysis (FEA)-Principle 60
-FEA Equipment 61
-Calibration Procedures 62
-Assay of Blood 64
-Assay of Bile 64
-Assay of Urine 64

Protocol 65
-Surgical Preparation of the Dogs 65
-Drug Administration 65
-Bile Salt Replacement 66
-Blood Sampling 66
-Bile and Urine Collection 67

Statistical Analysis 68

CHAPTER IV - RESULTS AND DISCUSSION 70

-Multiple Infusion Experiment of Dog King, October 15, 1973 70
-The Influence of Michaelis Constant, Km 87
-Plateau Infusion Experiment of Dog King, October 29, 1973 107
-Effect of Taurocholate on Iopanoic Acid Tm and Vd 112
-Individual Analysis 112
-Group Analysis 123
-Proposal for Experimentation 140

REFERENCES 146

CHAPTER I

INTRODUCTION

Iopanoic acid (Telepaque) has been used for over twenty years as an oral x-ray contrast agent for the visualization of the gallbladder. Since its introduction by Sterling-Winthrop Research Institute in 1951, it has become the drug of choice for oral cholecystography, with more than 40 million doses having been administered (1).

Cholecystography - Definition and Use - Cholecysttography is the roentgenographic examination of the gallbladder with the aid of an x-ray contrast medium in an attempt to detect gallstones or other abnormalities of the gallbladder. It is estimated that 15 million Americans have gallstones (2). According to the National Center of Health Statistics, approximately one-third of a million Americans require cholecystectomies each year. Hospitalization and medical expense is estimated at approximately a half-billion dollars. Mortality ascribed to gallstone disease is around 6,000 annually.

Abel and Rowntree (3) of John Hopkins University experimented with a series of phthalein derivatives in a

search for a "serviceable hypodermic purgative." In 1909, Abel and Rowntree observed that tetrachlorophenolphthalein (I), when injected, has the same purgative action as did phenolphthalein itself; however, tetrachlorophenolphthalein had the additional advantage of being almost entirely excreted by the liver. The enhanced excretion by the liver was conceived by Evarts Graham (4) of the Washington University School of Medicine (St. Louis, Mo.) in 1922 to be due to the addition of the chlorine atoms to the molecule. This led to the concept of replacing the chlorine with halogen atoms of greater radio-opacity in order to obtain an x-ray shadow of the gallbladder and to the development of cholecystography. The Mallinckrodt Laboratories, working in cooperation with Graham (5, 6, 7), produced in 1924 sodium tetraiodophenolphthalein which became commercially available as Iodeikon (II). Iodeikon became the accepted standard contrast medium for visualization of the gallbladder for a period of nearly twenty years.

Iodeikon was not free from untoward reactions; administered orally, the liquid dosage form was nauseating to the taste. If the patient was able to keep it down, diarrhea frequently resulted with decreased visualization. As a result, it was usually administered intravenously. Even though it was administered by slow intravenous

infusion, the incidence of nausea and vomiting still remained high (8). The additional serious side effect of shock and dehydration was reported to be by no means uncommon (9).

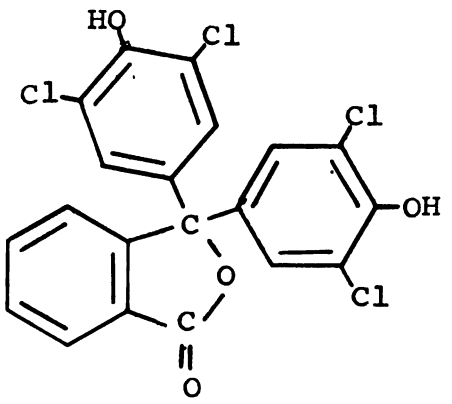

(I)

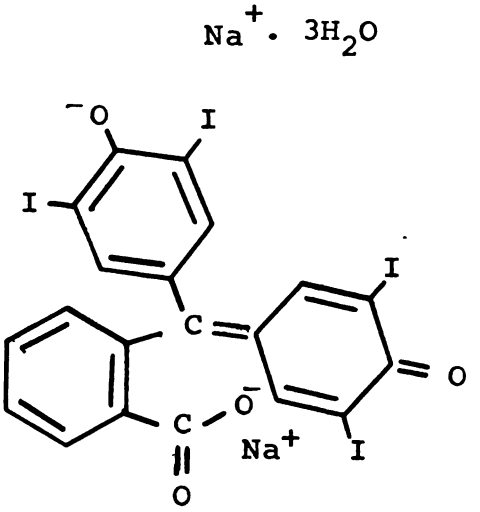

(II)

By the early 1940's, Iodeikon was replaced by Priodax (iodoalphionic acid) (III) because it could be administered in tablet form with greater convenience for both the radiologist and the patient. However, it provided no great reduction in nausea and vomiting. A majority of the patients still showed these untoward symptoms.

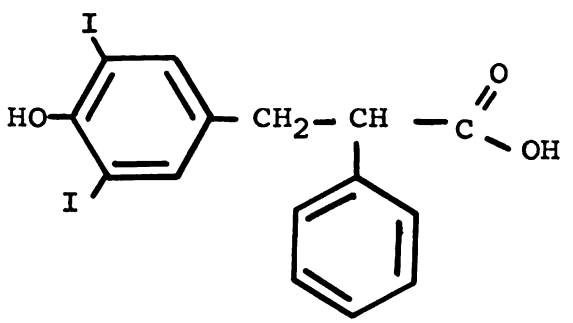

(III)

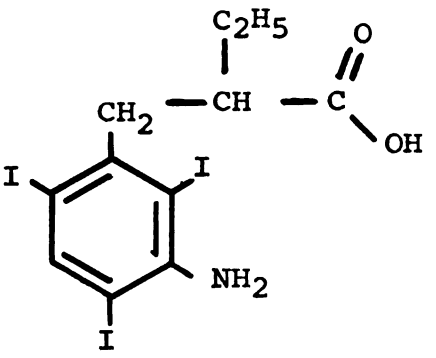

(IV)

Iopanoic Acid Synthesis - In 1949, while preparing a group of (amino-di-and tri-iodophenyl)-alkanoic acids, Archer et al. (10,11) of the Sterling-Winthrop Research Institute synthesized 3-(3-amino-2, 4, 6-triiodophenyl)-2-ethyl propiopic acid(IV).

Iopanoic Acid Cholecystographic Activity and Toxicity - Compound IV proved to be the most active cholecystographic agent of the series when tested in cats. This compound, later known as iopanoic acid and commercially as Telepaque gave a more intensive gallbladder visualization, at 100 mg/kg, than was obtained with Priodax at 200 mg/kg. In addition to this increased cholecystographic activity, the acute oral LD_{50} for iopanoic acid in mice was 16 gm/kg as compared with 3.8 gm/kg for Priodax (12). The acute I.V. LD_{50} in mice for iopanoic acid was 0.32 gm/kg (13).

By 1952, clinical trials (9, 14, 15, 16, 17, 18) had shown Telepaque to be significantly superior to Priodax in gallbladder visualization. Also, these clinical trials had shown that Telepaque, in 3 gm doses, resulted in fewer clinical side effects. Occasional visualization of the bile ducts was also reported (18, 19).

Despite the improvement iopanoic acid has brought to the field of cholecystography, it still has shortcomings. In approximately 15 percent of the patients (20, 21).

iopanoic acid fails to produce gallbladder opacification. Upon examination with a second dose, 10 to 20 per cent of these non-visualizations produce normal gallbladder opacification. Faint opacification in the first examination will cause questionable diagnosis, often requiring re-examination to confirm the diagnosis. Approximately 70 per cent of cases with faint opacification will prove to be normal on the second examination (21). Repeat examinations involve additional patient exposure to radiation, additional expense and time away from the job.

The clinical side effects of iopanoic acid are usually mild; however, they are quite frequent. Diarrhea, nausea, vomiting and dysuria occur in 40 per cent of cases (22). In addition, a few cases of coronary insufficiency and renal damage have been reported (23, 24, 25).

Iopanoic Acid Physical Properties - Iopanoic acid, molecular weight = 571, exists as cream-colored needles melting at 155.2-57 (10). The water solubility of the non-ionized form was calculated by Taketa et al. (26) to be 4.0 µg/ml. It is freely soluble in most organic solvents. The acid dissociation constant, K_a, of iopanoic acid is 2.5×10^{-5}M. The corresponding pKa is 4.6. The ultraviolet spectrum of iopanoic acid has molar absorptivities of E_{230} (38,000), and E_{310} (3,150) (27). It is known to

have two polymorphic forms (28) which will be discussed below.

Gastro-Intestinal Absorption of Iopanoic Acid.- Gastro-intestinal absorption of iopanoic acid is slow and irregular when compared to that of sodium iopanoate (29, 30). As an organic weak acid with a pKa of 4.6, one might predict, based upon the pH-partition theory (31, 32, 33), good absorption of the undissociated form from the acidic environment of the stomach were it not so insoluble. Since iopanoic acid solubility is only 4 ug/ml, one can expect precipitation of the free acid form when a concentrated alkaline solution is added to the acid environment of the stomach. However, experiments (26, 34) in dogs have demonstrated that the compound is better absorbed at higher pH's than at lower pH's.

One should expect no significant difference in the absorption rate of saturated solutions of iopanoic acid tablets when compared to a saturated solution made from freshly precipitated drug. However, Goldberger et al. (28) have demonstrated a significant difference in the absorption rate between the two saturated solutions. They suggested this difference in absorption may be due to a difference in solubility and dissolution rate of the solids. They concluded that freshly precipitate iopanoic acid apparently

exists in a different polymorphic form from that occurring in aged crystals. Therefore, there is good evidence that iopanoic acid is dissolution rate limited in its absorption.

In vivo experiments in unanesthetized dogs (28) have demonstrated increased rate and degree of absorption of iopanoic acid in the presence of bile. This increased absorption is similar to the absorption of the freshly precipitated iopanoic acid. It is postulated that the irregularity of Telepaque absorption may be due to the variation in the amount of bile present in the gut lumen. Reinke and Berk (35) have shown that nearly all of an iopanoic acid dose reaches the systemic circulation via the portal venous system rather than from the intestinal lymphatics.

In conclusion, literature data support the contention that iopanoic acid absorption is dissolution rate limited, differing between aged and freshly precipitated crystals, and occurs via the portal venous system.

Plasma Protein Binding - Lang and Lasser (36) studied iopanoic acid binding to human serum albumin using the equilibrium dialysis method. They concluded iopanoic acid is bound at a stronger binding site ($K_1 = 7 \times 10^5$, $n = 3$) and at a second, weaker site ($K_2 = 9 \times 10^2$, $n_2 \cong 40$). Studies with normal human serum indicated that albumin was

the sole binding protein. Lang and Lasser (36) concluded also that as clinically employed, the portion of circulating iopanoate bound to serum albumin must be at least 97 per cent.

Rinke and Berk (35) reported iopanoic acid binding to albumin of lymph. Using lymph and whole blood dialyzed against Tris-buffered I^{125} Telepaque, they found that the amount of I^{125} Telepaque in blood was 1.5 to 2 times higher than that in lymph. This ratio is similar to the albumin ratio of the two fluids. They also demonstrated that, although iopanoic acid is lipid soluble, it was not taken up measurably by chylomicrons.

Possible Mechanistic Aspects of Hepatic Uptake - McChesney and Hoppe (27) found, in the cat, that iopanoic acid has little tendency to accumulate in any tissue except the liver. Several groups of workers have been studying possible mechanisms for this apparent selective hepatic uptake of dyes and radiopaques.

A possible mechanism for selective hepatic uptake involves binding to hepatic cytoplasmic proteins or to liver cell membranes. Arias and associates (37) have established the existence of two hepatic cytoplasmic proteins, Y and Z. They have shown definite binding of bilirubin, BSP, flavaspidic acid, bunamiodyl and other

similar anions. Arias postulated that Y-and Z-proteins may have a general function relating to the uptake of many organic anions that are transferred from plasma into liver. Sokoloff, Berk, et al. (38) have extended Arias' binding studies to iopanoic acid and found that iopanoic acid did indeed bind to Y-and Z-proteins. It is interesting to note that they found that iothalamate, a urographic contrast agent, does not bind to Y-and Z-proteins.

Studies (39) using anions similar to iopanoic acid have demonstrated binding by hepatic plasma membranes in vitro. There is an apparent correlation with anions that compete for sulfabromophthalein (BSP) removal in vivo and anions that reduce BSP binding to isolated liver-cell membranes in vitro. Since iopanoic acid is known (40, 41) to retard BSP elimination in vivo, it is logical to surmise that iopanoic acid might also be bound to liver-cell membranes.

Another possibility for selective hepatic uptake could involve an active transport system that would work against a concentration gradient. Many problems exist in identifying such a system. In vivo competitive inhibition studies of iopanoic and iodipamide (42) could reflect completion at either an active transport step or at a protein binding step. Metabolic inhibitors could reflect

either inhibition at the active transport step or at the conjugation step.

Identification of the exact mechanism for selective hepatic uptake is still unknown. Some progress is being made; however, detailed studies reveal additional complexities. Kaplowitz and coworkers have recently shown that the Y-protein appears to be identical in properties to glutathione-S-aryl transferase which participates in the conjugation of BSP (43, 44), but of course does not function as a glucuronidating enzyme.

Glucuronidation and Biliary Excretion - Iopanoic acid is metabolized to the glucuronide (27, 45). McChesney and Hoppe (27) have shown this metabolite to be the ester glucuronide (V).

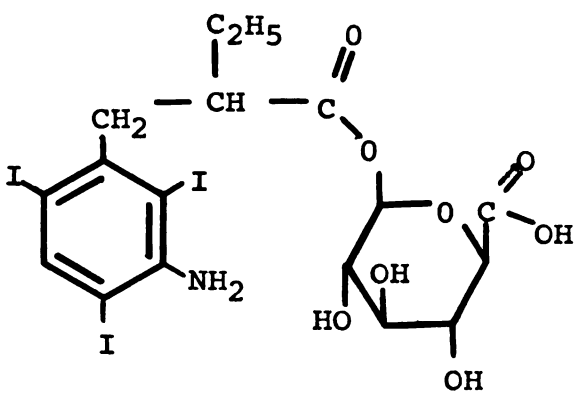

V

This glucuronide conjugate is found both in the bile and in the urine (46). In the cat, bile contains greater than 95 per cent of the conjugated form (27). Conjugation enhances biliary excretion by increasing both the molecular weight and water solubility of a compound. Millburn et al. (47) have shown an apparent molecular weight dependency for a diverse group of aromatic compounds. The larger the molecular weight, the more pronounced biliary elimination becomes. Smith (48) reported that with the exception of quaternary compounds, the extent of biliary excretion of foreign compounds and their metabolites having molecular weights less than about 300 is less than 5-10 per cent of dose administered in rats, guinea pigs, rabbits, and cats. These lower molecular weight compounds are usually excreted in the urine. Marked species variations in the extent of biliary excretion of anions can occur for compounds whose molecular weights range from 300 - 600. Millburn, et al. (47, 49) have proposed the molecular weight threshold for the rat, guinea pig and rabbit are of the order of 325 $\pm$ 50, 400 $\pm$ 50, 475 $\pm$ 50 respectively. The threshold values of other species have not been ascertained, but it was suggested that they almost certainly lie within the range of 300 to 500. Smith (47) reviewed the biliary excretion of organic compounds and their metabolites of molecular

weights greater than 500 in various species, including man. He concluded that the bile appears to be the dominant route for their elimination. Unfortunately, most of the reported studies have not considered the effect of drug concentration and the possibility of saturating a capacity limited process. Obviously many factors influence the excretion process; for example, pH-partition and protein-binding properties of a compound might be dominant in reducing urinary excretion. In such cases, the compound is available in the body for a longer period of time to undergo metabolism. The biliary excretion characteristics of the metabolites (particularly the higher molecular weight conjugates), may be predominantly controlled by their diffusivity or transport through canalicular wall. There is some evidence that the extent of reabsorption from the biliary tree is dependent upon the rate of bile flow. Mroszcyak (50) has reported a bile flow dependency on the biliary excretion of diethylstibestrol glucuronide. When bile flow rate was reduced, there was a compensurate increase in urinary excretion. Iopanoic acid glucuronide having a molecular weight of 747 is excreted via the bile in dogs to an extent of greater than 95 per cent (51). However, 30 per cent of a 3 gm dose is usually excreted via the urine in man.

Pharmacokinetics of Iopanoic Acid by Previous Workers - Literature search shows very little detailed pharmacokinetics analysis of iopanoic acid blood curves or rates of biliary excretion.

Holmdahl and Lodin (29) administered iopanoic acid and its sodium salt to two groups of 13 patients and reported average blood iodine levels over a period of 24 hours. One group received 4 gm of iodine as iopanoic acid and the other, 2.57 gm of iodine as the sodium salt of iopanoic acid. The peak level obtained from the free acid dose was about 50 per cent that of the sodium salt dose despite the higher total dose of the drug ingested.

Variations in the apparent absorption of iopanoic acid has been noted by the frequent literature reports of dense granules in the bowel on cholecystography (18, 52, 53, 54).

Fink et al. (53), in 1964, approximated the absorption of iopanoic acid to be 45 per cent. How they arrived at this figure is not explained beyond a statement that it was "the best that could be determined from the data available."

McChesney and Hoppe (27) administered a 3 gm oral dose of iopanoic acid to five human subjects and collected urine and feces specimens for a period of 132 hours. They found an average of 31.2 per cent of the dose in the urine as the

glucuronide conjugate and 4.7 per cent as free iopanoic acid. The feces contained 62 per cent of the dose. Our kinetic analysis of their excretion data shows a total mean urinary excretion rate constant = 0.03 hr^{-1} ($t_{\frac{1}{2}}$ = 22 hrs); a mean urinary conjugate excretion rate constant of 0.03 hr^{-1} ($t_{\frac{1}{2}}$ = 24 hrs), and a mean fecal excretion rate constant of 0.04 hr^{-1} ($t_{\frac{1}{2}}$ = 17 hrs).

Analysis of McChesney and Hoppe's data shows that urinary and fecal excretion rates appear to follow first order kinetics. The urinary and fecal half-lives are summarized below:

Subject	Total Urinary Half-Life (Hrs)	Total Fecal Half-Life (Hrs)
A	26	17
B	26	15
C	17	19
D	34	21
E	16	13

The difference in the values of the fecal versus urinary rate constant is probably caused by incomplete absorption, producing higher amounts of fecal excretion in the first 48 hours.

Schroder and Rooney (55) gave two gram doses of Telepaque to five human subjects, collecting 24-hour urine and fecal specimens. They found 12 per cent of the dose was excreted in five days via the urine and 77 per cent excreted via the feces. Our kinetic analysis of their data shows a mean excretion rate constant for both urine and feces of 0.04 hr^{-1} ($t_{\frac{1}{2}}$ = 17 hrs). There appears to be a significant difference in the percent of dose excreted via the urine when these results are compared with those of McChesney & Hoppe. Thirty-six percent of the 3 gm doses was excreted in the urine in the former study while 12 percent of the 2 gm dose was excreted in the latter study.

Oral 3 gm doses administered to four normal fasting human subjects by Perlman et al. (56) gave maximum blood concentrations of 100-150 mg/L at approximately 9 hours. Analysis of their blood curves yielded estimates of terminal half-lives ranging from 15 to 23 hours. In a four-day period, these subjects excreted an average of 6 percent of the dose in the urine and twenty percent in the feces for a total of 26 percent, thus indicating incomplete collection. Studies by these workers on other subjects given a light, fat-free meal four hours prior to the dose showed an average total excretion of 45 percent. Subjects given a fatty meal

prior to the dose excreted an average total of 51 percent. Compared to the data of McChesney and Hoppe and Schroder and Rooney, these workers apparently did not achieve complete urinary and/or fecal collections.

Two recent papers (57, 58) studied the pharmacokinetics of iopanoic acid infusions. Moss, Amberg and Jones (57) studied the effect of bile salt replacement on the biliary excretion of iopanoate in unanesthetized dogs and concluded that increasing the bile salt replacement level appeared to "set a hepatic transport maximum at a particular level." Dunn and Berk (58) in similar studies on anesthetized animals argued that no transport maximum was apparent. They concluded that Telepaque was limited in its liver uptake and biliary excretion only by the concentration gradient. In a subsequent paper on unanesthetized dogs, Berk et al. (59) also reported that bile salts stimulate iopanoic acid excretion. Thus, anesthesia appears to have a profound effect on the mechanism responsible for biliary excretion.

The Dog as an Experimental Model for Cholecystographic Investigation - The dog has been used as an experimental animal since the beginning of cholecystography. In 1923 Evarts Graham and his associate, Warren Cole, (4), gave six dogs I.V. injections of the sodium salt of tetraiodophenolphthalein. They obtained a faint gallbladder shadow

in only one dog and none at all in the other five animals. The dog which gave a shadow was the one dog which had accidentally been given no food the day before. Realizing that a fasting period was critical, they were able to obtain gallbladder shadows in about every instance thereafter.

The dog represents a good experimental animal for use in investigative cholecystography since its gallbladder is large enough to permit adequate x-ray contrast when filled with a radio-contrast agent. Like man, the dog is able to conjugate iopanoic acid to the ester glucuronide which in both species is normally concentrated within the gallbladder.

CHAPTER II

THEORETICAL ASPECTS OF SATURATED CAPACITY-LIMITED SYSTEMS

After an intravenous bolus injection, one usually expects a drug to be eliminated from the body by first-order processes such that the blood data can be described by a series of exponentials. In some instances, as the concentration is increased, a capacity-limited kinetic behavior is seen, ultimately resulting in zero-order elimination. Nelson et al. (60) administered iopanoic acid to unanesthetized dogs by I.V. bolus injections during the study of the effect of phenobarbital on the drug's elimination. Close examination of their data revealed the possibility of zero-order kinetics. After a short distribution phase, the blood curves appeared linear with time down to a concentration of 30 mg of iodine per liter (mg I/L).*

At the same time, data from diphenylhydantoin infusion experiments in unanesthetized dogs by Blum et al.(61) was being reviewed. It also did not appear to fit the expected

---

*Expressed in terms of mg of iodine in the iopanoic acid molecule. To convert to mg of drug, multiply by a factor of 1.5.

kinetics of zero-order input and first-order output. When plotted on linear paper, their infusion data had noticeable portions of linearity. These observations led us to conceive a non-linear system such as an enzyme having Michaelis-Menten kinetics. The system apparently is saturated above a threshold blood concentration. Infusing the drug into the animal at rates exceeding the maximum rate of elimination results in linear slopes when the threshold concentration is exceeded.

This realization led us back to the original bromosulfophthalein (BSP) infusion studies of Wheeler et al. (62, 63). Using a set of three infusion rates, Wheeler was able to determine the transport maximum, Tm*, of BSP. Figure 2.1 is a plot of plasma concentration versus time redrawn from his original publication (63). As noted, each of the three infusion rates produced linear segments having different slopes. Wheeler was able to obtain estimates of Tm by plotting the so-called "hepatic removal rate," (R_H), in mg per minute against the corresponding plasma slopes, $\frac{\Delta p}{\Delta t}$, as shown in Fig. 2.2, also redrawn from this same paper (63). The plot is based upon the following equation:

---

*The transport maximum, Tm, is the equivalent to the maximum velocity constant, Vm. The latter will be used for the theoretical discussion of our models.

FIGURE 2.1 The plot of plasma BSP concentration versus time redrawn from a Wheeler publication (63). The first infusion of 10.53 mg BSP/min was from 0-60 min. The second infusion of 1.83 mg BSP/min was from 60-120 min. The third infusion of 5.32 mg BSP/min was from 120-180 min. The corresponding plasma slopes were, 0.194, -0.038 and 0.051 mg %/min, respectively.

FIGURE 2.2 The plot of the "hepatic removal rates," R_H, versus the corresponding plasma slopes. The estimated Tm from this plot is 3.3 mg/min and the estimated "relative storage capacity," S, is 30 mg/mg %.

Fig. 2.1

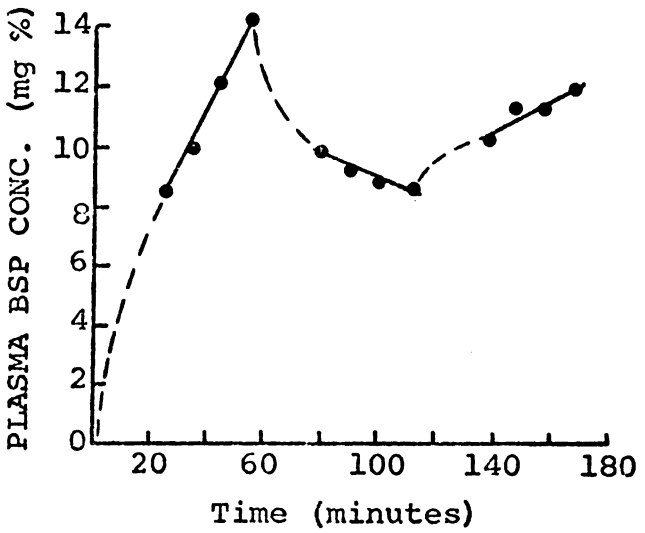
PLASMA BSP CONC. (mg %)
0
2
4
6
8
10
12
14
20
60
100
140
180
Time (minutes)

Fig. 2.2

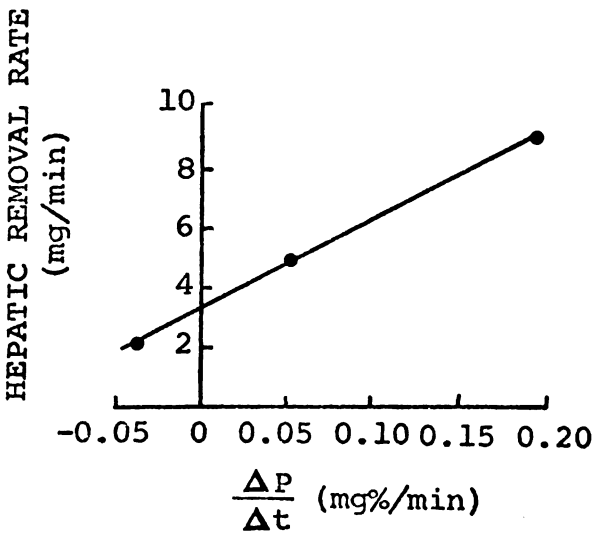
HEPATIC REMOVAL RATE (mg/min)
2
4
6
8
10
-0.05
0
0.05
0.10
0.15
0.20
ΔP/Δt (mg%/min)

$$R_H = Tm + S \times \frac{\Delta p}{\Delta t} \qquad (2.1)$$

where

R_H = hepatic removal rate, mg per minute, defined as indicated in Eq. 2.2.

Tm = excretory transport maximum, mg per minute.

S = "relative storage capacity," mg per mg per 100 ml.

$\frac{\Delta p}{\Delta t}$ = rate of change of plasma concentration, mg per 100 ml per minute.

The hepatic removal rate is calculated from the following equation:

$$R_H = I - PV \times \left(\frac{\Delta p}{\Delta t}\right) \qquad (2.2)$$

where

I = BSP infusion rate, mg per minute.

PV = plasma volume in hundreds of ml.

Plasma volume was measured by the use of I^{131}-labeled human serum albumin. Since it was necessary to determine each subject's plasma volume in order to use Wheeler's method, Eq. 2.1 had a somewhat limited application.

By substitution of Eq. 2.2 into Eq. 2.1 and by rearrangement, Eq. 2.3 is obtained:

$$I = Tm + (S + PV) \times \left(\frac{\Delta p}{\Delta t}\right) \qquad (2.3)$$

Examining Eq. 2.3, it becomes apparent that Wheeler's S, "relative storage capacity," term is a volume constant having the same units as the plasma volume. It also

becomes apparent from Eq. 2.3 that it is not necessary to measure the plasma volume to determine Tm. Rather than plotting R_H versus $\frac{\Delta p}{\Delta t}$ to obtain an estimate of Tm from Y-axis intercept and S from the slope, one can plot the infusion rate, I, against $\frac{\Delta p}{\Delta t}$. The Y-axis intercept is Tm, but the slope is equal to (S + PV). The apparent volume term, (S + PV), should probably be referred to as the apparent volume of distribution, Vd. These relationships are shown in the following equations:

$$I = Tm + Vd \times \left(\frac{\Delta p}{\Delta t}\right) \qquad (2.4)$$

$$\frac{\Delta p}{\Delta t} = \frac{I - Tm}{Vd} \qquad (2.5)$$

Wheeler's model is applicable only to those drugs having a central compartment limited to the actual plasma volume and a peripheral compartment limited by definition to only the liver. By using either Eq. 2.4 or 2.5, estimates of both Tm and Vd can be obtained for drugs undergoing saturation kinetics even when distributed in more than one location compartment. At distribution equilibrium, Vd is the sum of the various body compartments. Segre in 1972 (64) used Wheeler's model, but also overlooked this simplification. Others have attempted physiological or non-kinetic interpretations of Wheeler's data (65).

<u>One Compartment Model</u> - The simple one compartment

model for a zero-order input and a Michaelis-Menten output can be shown as:

Model A

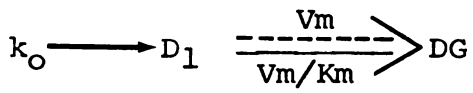

$$\frac{dD_1}{dt} = k_o - \left(\frac{Vm}{Km + C_1}\right) C_1 \qquad (2.6)$$

$$V_1\left(\frac{dC_1}{dt}\right) = k_o - \left(\frac{Vm}{Km + C_1}\right) C_1 \qquad (2.7)$$

$$\frac{dC_1}{dt} = \frac{k_o}{V_1} - \left(\frac{Vm/V_1}{Km + C_1}\right) C_1 \qquad (2.8)$$

where

k_o = the infusion rate, in mg per minute.

$D_1 = C_1V_1$ = the amount in mg of drug in the body compartment.

Vm = Tm = the maximum velocity or transport maximum in mg per minute of the capacity-limited step.

Km = Michaelis constant in mg per liter.

V_1 = apparent volume of distribution in liters.

Throughout this chapter, the capacity-limited Michaelis-Menton step will be presumed to be at complete saturation. In other words, when the concentration of the drug is much larger than the Michaelis constant, ($C_1 >> Km$), then the Michaelis-Menten output will approach a value equal to Vm.

This results in Eq. 2.9.

$$\left(\frac{Vm/V_1}{Km + C_1}\right) C_1 = Vm/V_1 \qquad (2.9)$$

When $C_1 >> Km$, Model A can then be written as:

Model B

$$k_o \longrightarrow D_1 \xrightarrow{Vm} DG$$

Thus, Eq. 2.8 will become:

$$\frac{dC_1}{dt} = \frac{k_o - Vm}{V_1} \qquad (2.10)$$

Figure 2.3 is the analog computer-generated blood concentration-time curve for a one compartment model with a zero-order input greater than the saturated, zero-order output. The infusion is cut off after 200 minutes, allowing the blood concentration to drop.

Each different infusion rate, k_o, will produce a different linear upslope. The upslopes and the downslope (when $k_o = 0$) can be plotted against their corresponding infusion rate, k_o. Figure 2.4 is an example of such a plot An estimate of Vm can be obtained from the X-axis intercept* and the V_1 can be obtained from the reciprocal of the slope. In this case, $V_D = V_1$.

---

*If $\frac{dC}{dt} = 0$, then $0 = \frac{k_o - Vm}{Vd}$ and k_o is then equal to Vm.

FIGURE 2.3 The analog computer simulation for C_1 versus time of Model B where Vm = 8 mg/min, Vd = 8.4 L and k_o = 12 mg/min. The time that the infusion was ended, T_1 = 200 min. The upslope $\frac{dC_1}{dt} = \frac{k_o - Vm}{V_1}$ and the downslope, $\frac{dC_1}{dt} = \frac{-Vm}{V_1}$.

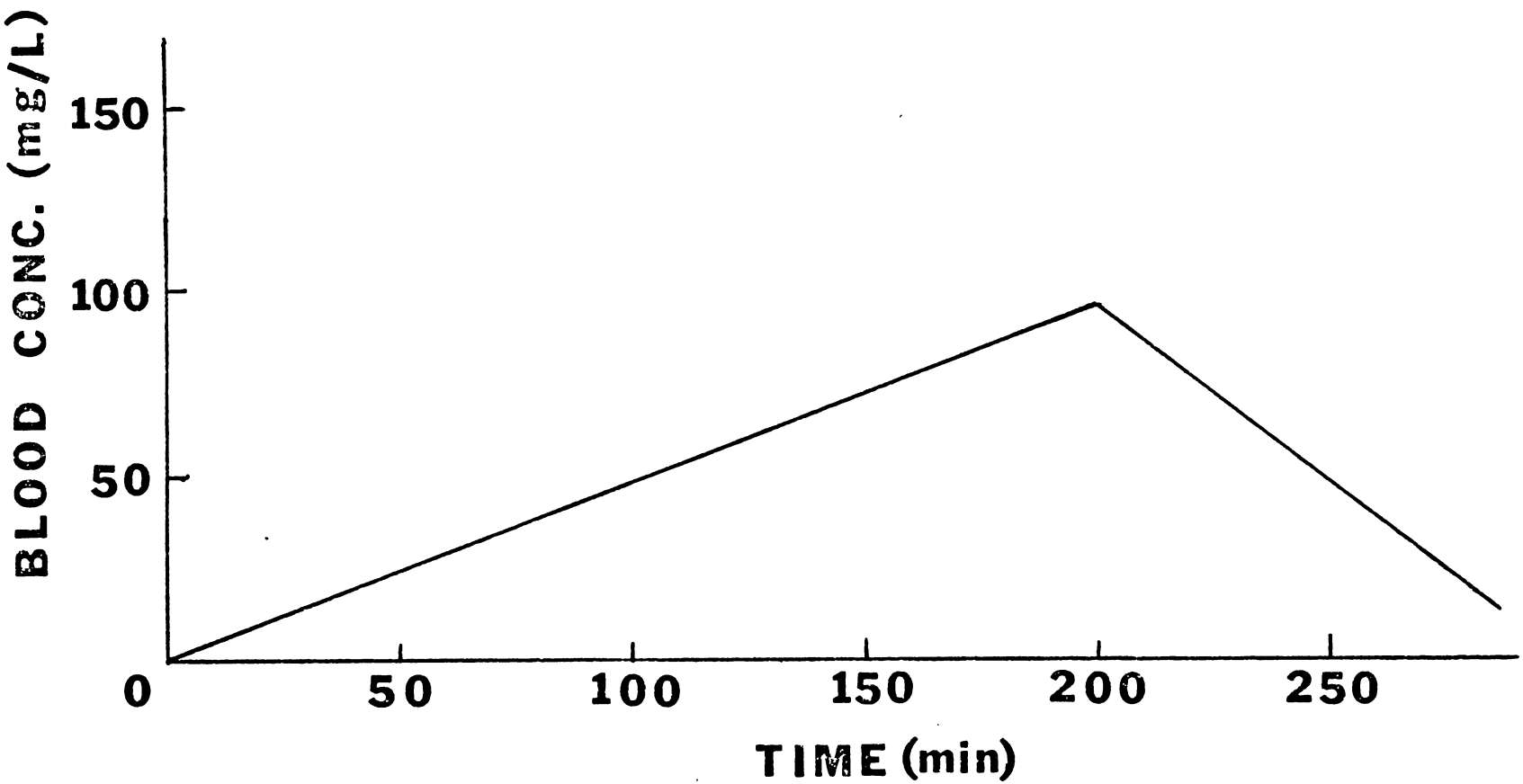
BLOOD CONC. (mg/L)
150
100
50
0
50
100
150
200
250
TIME (min)

FIGURE 2.4 The blood slope - infusion rate plot of Model B. The data points represent the blood slopes of two infusion rates and of the downslope. The X-axis intercept = Vm and the slope = $\frac{1}{V_1}$.

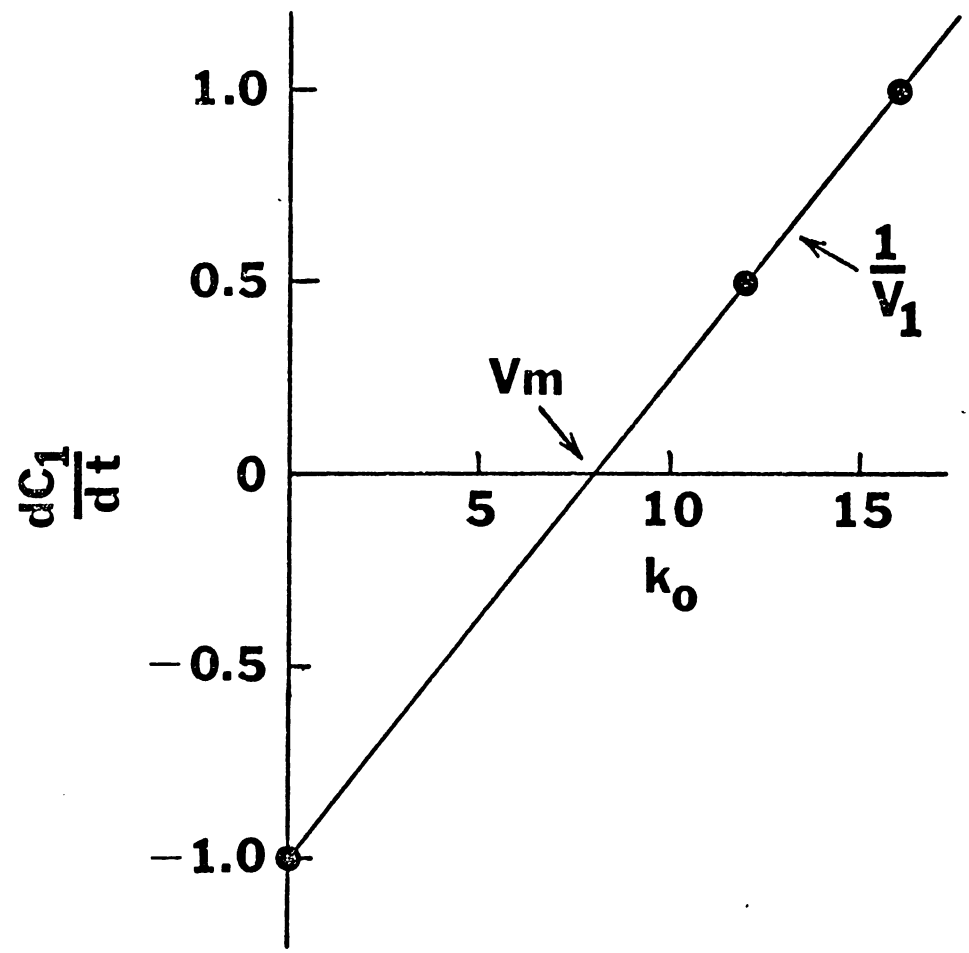
1.0
0.5
0
−0.5
−1.0
5
10
15
k_o
Vm
$\frac{1}{V_1}$
$\frac{dC_1}{dt}$

Two Compartment Models - A number of models can be proposed which could represent a drug distributing between two compartments in which transport, metabolism, or excretion is taking place in only one of the compartments.

Two Compartment - Metabolic Rate-Limited Model -

Model C

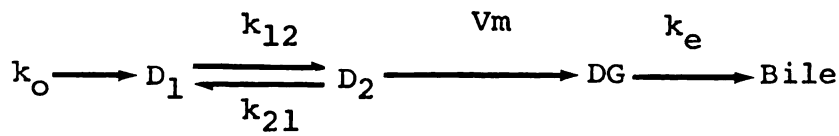

where

$D_1 = C_1V_1$ = amount in mg of drug in the central compartment.

$D_2 = C_2V_2$ = amount in mg of drug in the peripheral compartment (liver) where metabolism occurs.

V_1, V_2 = volume of distribution of the drug within compartments, in liters.

k_{12}, k_{21} = microscopic rate constants in $min.^{-1}$ into and out of the peripheral compartment.

DG = amount in mg of metabolite in the liver compartment.

The differential equations for the rate of change with respect to time of amounts of the drug or its metabolites in each compartment of Model C are:

$$\frac{dD_1}{dt} = k_o - k_{12}D_1 + k_{21}D_2 \qquad (2.11)$$

$$\frac{dD_2}{dt} = k_{12}D_1 - k_{21}D_2 - Vm \qquad (2.12)$$

$$\frac{dDG}{dt} = Vm - ke(DG) \tag{2.13}$$

$$\frac{d\ Bile}{dt} = ke(DG) \tag{2.14}$$

Equations 2.11 and 2.12 can be transformed into the Laplace domain as shown in the following equations:

$$\bar{D}_1(s) = \frac{k_o}{s} - k_{12}\bar{D}_1 + k_{21}\bar{D}_2 \tag{2.15}$$

$$\bar{D}_2(s) = k_{12}\bar{D}_1 - k_{21}\bar{D}_2 - \frac{Vm}{s} \tag{2.16}$$

Solving the Laplace equations for $\bar{D}_1$, the following equation is obtained:

$$\bar{D}_1 = \frac{k_o(s + k_{21}) - Vmk_{21}}{s^2(s + k_{12} + k_{21})} \tag{2.17}$$

Taking the anti-Laplace of Eq. 2.17 and rearranging results in Eq. 2.18 and Eq. 2.19:

$$D_1 = \left(\frac{(k_o - Vm)k_{21}}{k_{12} + k_{21}}\right)t + \frac{k_o k_{12} + Vmk_{21}}{(k_{12} + k_{21})^2}\left[1 - e^{-(k_{12} + k_{21})t}\right] \tag{2.18}$$

$$C_1 = \left(\frac{k_o - Vm}{V_1\left(1 + \frac{k_{12}}{k_{21}}\right)}\right)t + \frac{k_o k_{12} + Vmk_{21}}{V_1(k_{12} + k_{21})^2}\left[1 - e^{-(k_{12} + k_{21})t}\right] \tag{2.19}$$

A plot of C_1 versus t will show a convex ascending curve which will converge to a straight line when the exponential term on the right side of Eq. 2.19 becomes zero,

at which time the system is at distribution equilibrium. Figure 2.5 is an analog computer generated curve of Eq. 2.19. Note the presence of linear segments both on the upslope and on the downslope. Extrapolation of the two linear segments to zero time and post-infusion zero time, respectively, permits one to estimate the sum of the microscopic rate constants k_{12} and k_{21}, by the procedure of feathering. This is indicated in the insert to Fig. 2.5 where the log-linear slope is equal to $-\frac{k_{12} + k_{21}}{2.303}$. If k_{12} and k_{21} have larger values, the rate at which distribution equilibrium is approached is much faster and the non-linear components become less pronounced. This can be seen from Eq. 2.19 where the exponential term converges to zero faster when k_{12} and k_{21} are larger. Therefore, as k_{12} and k_{21} become larger, the blood curve in Fig. 2.5 approaches that in Fig. 2.3.

The non-linear portion of Fig. 2.5, denoted as A, could partially also reflect pre-saturation in those models in which saturation of the capacity-limited step is not instantaneous. Wheeler's data, reproduced in Fig. 2.1, appears to fit a two compartment model since it indicates the existence of the non-linear distribution phases. It should be stressed, however, that the two compartment model requires saturation to be achieved which

FIGURE 2.5 The analog computer simulation for C_1 versus time of Model C where Vm = 8 mg/mm, V_1 = 2.8 L, V_2 = 5.6 L, k_{12} = 0.069 min^{-1}, k_{21} = 0.035 min^{-1}, k_o = 12 mg/min, T = 200 min. The linear upslope, $\frac{dC_1}{dt} = \frac{k_o - Vm.}{V_1 + V_2}$

The linear post-infusion downslope, $\frac{dC}{dt} = \frac{-Vm}{V_1 + V_2}$

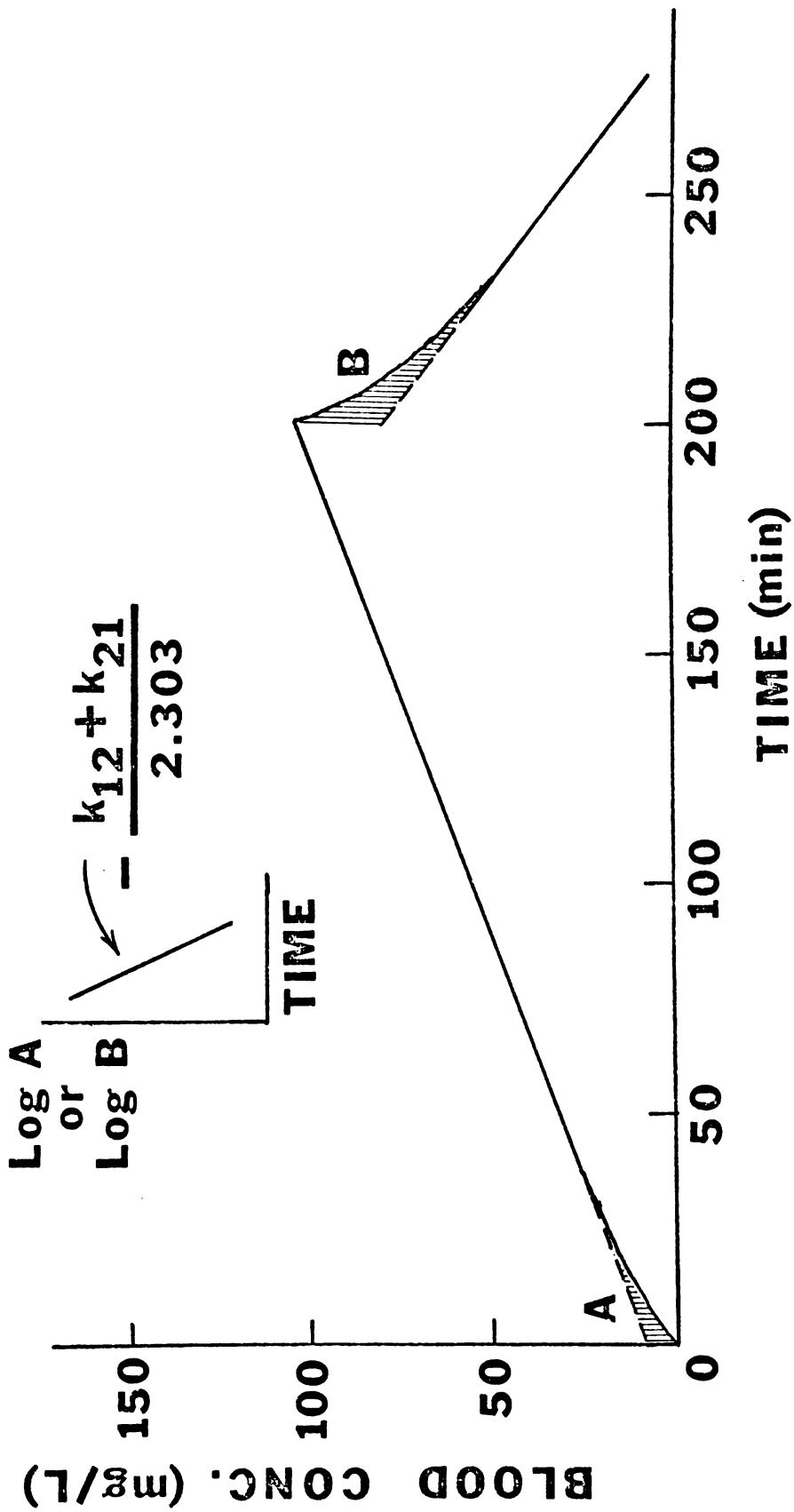
BLOOD CONC. (mg/L)
150
100
50
0
50
100
150
200
250
TIME (min)
A
B
Log A
or
Log B
TIME
$-\frac{k_{12}+k_{21}}{2.303}$

only takes place when C >> Km. Obviously, the smaller the Km value, the lower the concentration necessary to achieve saturation. Also, the Michaelis-Menten (M-M) equation reduces to apparent first-order kinetics when C << Km. In such cases the apparent first-order rate constant is equal to $\frac{Vm/Vd}{Km}$. If Km is sufficiently small, the apparent first-order constant, $\frac{(Vm/Vd)}{Km}$, may become large and therefore not rate-limiting. At intermediate concentrations between pure saturation and pure first-order the system also may not be rate-limited by the M-M step. Equation 2.14 represents the excretion rate of the metabolite in the bile where k_e represents the first-order rate constant for excretion. If the value of k_e is much smaller than the pseudo-first-order M-M step $\frac{Vm/Vd}{Km + C}$, k_e will become rate-limiting.

Therefore, it becomes possible for a decay curve of a drug in the blood to exhibit an abrupt break from a zero-order decay to a log linear decay. This abrupt break in the decay curve will represent the blood concentration at which the biological system is at the threshold of saturation. Above this threshold, the biological system's kinetics will be controlled by the maximum velocity (Vm or Tm) of the enzymatic or active transport step. Below this

threshold, the kinetics will be controlled by the overall interaction of the pseudo-first-order behavior of the enzymatic/active transport step and the first-order behaviors of the other rate determining steps. Iopanoic acid in dogs appears to be an example of saturation kinetics as described above.

Biliary Excretion - Integration of Eq. 2.13 results in Eq. 2.20.

$$DG = \frac{Vm}{k_e} (1 - e^{-k_e t}) \qquad (2.20)$$

Appropriate substitution into Eq. 2.14 will result in Eq. 2.21.

$$\frac{d\ Bile}{dt} = Vm(1 - e^{-k_e t}) \qquad (2.21)$$

Figure 2.6 is a schematic representation of Eq. 2.21. It should be emphasized that the infusion would have to be continued for a period of at least 4 to 5 half-lives relative to the value of k_e to reach Vm or to what is more commonly referred to as Tm, the transport maximum.

The Two Compartment Volume Constant - It was mentioned earlier that Wheeler's data is compatible with a two compartment model and that his volume terms, S and PV, can be combined to form a single volume constant, Vd. Note also the upslope in Fig. 2.5 as derived from Eq. 2.19

FIGURE 2.6 The schematic representation of Eq. 2.21 from Model C drawn on semi-log paper. The feathered portion has a slope = - ke/2.303. The plateau level represents the excretion rate at maximum capacity (Vm).

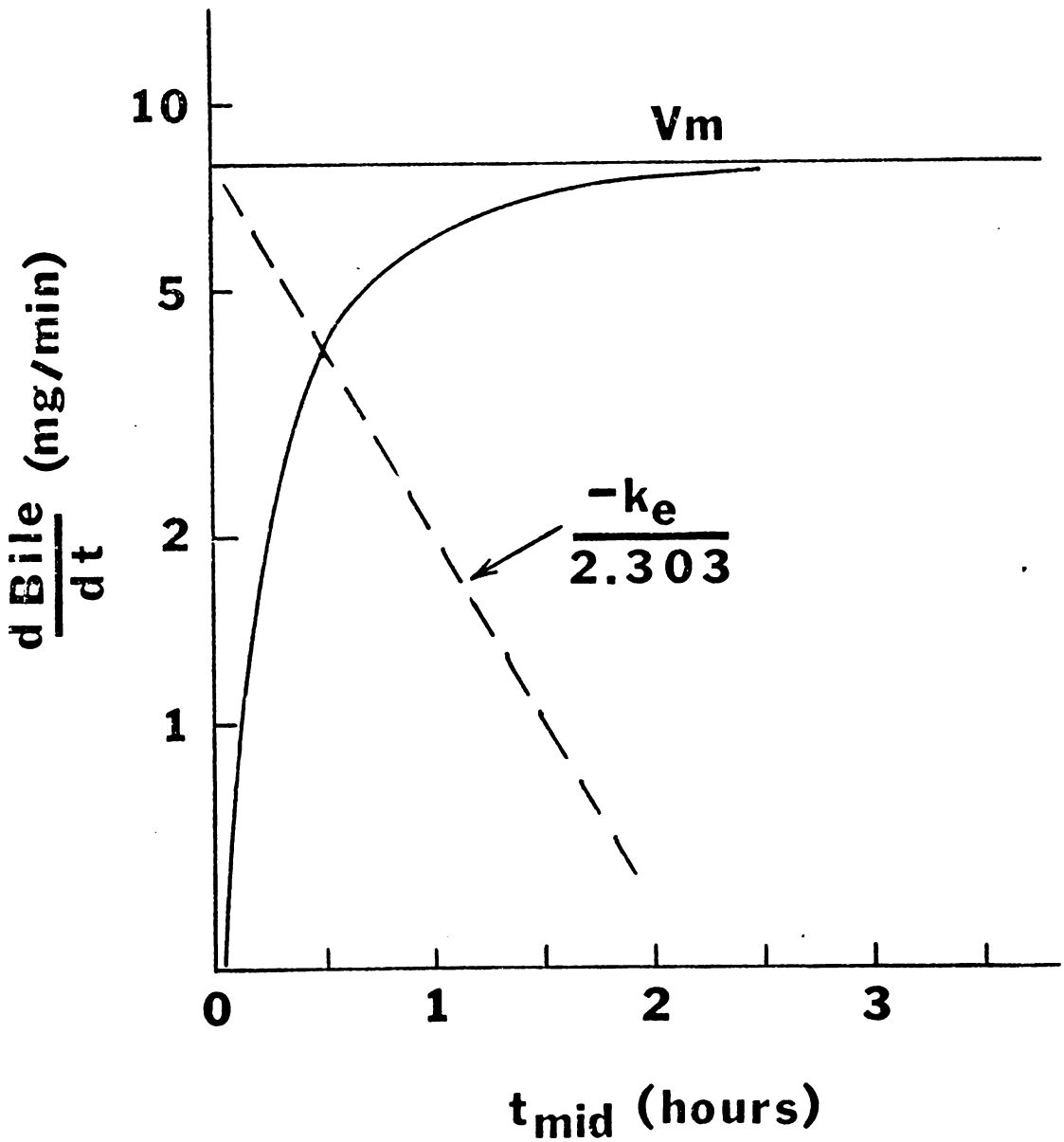
10
5
2
1
0
1
2
3
Vm
$\frac{-k_e}{2.303}$
$\frac{d\,Bile}{dt}$ (mg/min)
t_{mid} (hours)

reduces to Eq. 2.22 when its exponential term becomes zero.

$$C_1 = \left(\frac{k_o - Vm}{V_1\left(1 + \frac{k_{12}}{k_{21}}\right)}\right) t + \frac{k_o k_{12} + Vm\, k_{21}}{V_1(k_{12} + k_{21})^2} \qquad (2.22)$$

The differential equation for the linear slope then becomes:

$$\frac{dC_1}{dt} = \frac{k_o - Vm}{V_1\left(1 + \frac{k_{12}}{k_{21}}\right)} = \frac{k_o - Vm}{Vd} \qquad (2.23)$$

Thus, at distribution equilibrium, Vd is equal to $V_1\left(1 + \frac{k_{12}}{k_{21}}\right)$ for this particular model.

The Two Compartment Post-Infusion Period - When the infusion is terminated, the system must re-establish equilibrium, causing a rapid, non-linear drop in blood concentration. The integrated equation describing the post-infusion decay of the drug is as follows:

$$D_1 = D_1' e^{-(k_{12} + k_{21})t^*} - \left(\frac{Vm\, k_{21}}{k_{12} + k_{21}}\right) t^* + \frac{(D_1' + D_2')(k_{12} + k_{21})k_{21} + Vm\, k_{21}}{(k_{12} + k_{21})^2}\left[1 - e^{-(k_{12} + k_{21})t^*}\right] \qquad (2.24)$$

where

D_1' = amount in mg of drug in the central compartment when in infusion ended.

D_2' = amount in mg of drug in the peripheral compartment (liver when infusion ended).

$t^* = t - T$ = the time in minutes post-infusion, corrected for the infusion period of T minutes.

when $e^{-(k_{12} + k_{21})t^*} \longrightarrow 0$, the system reaches distribution equilibrium and the integrated concentration equation becomes:

$$C_1 = \frac{-Vm}{V_1\left(1 + \frac{k_{12}}{k_{21}}\right)} t^* + \frac{(D_1' + D_2')(k_{12} + k_{21})k_{21} + Vmk_{21}}{V_1(k_{12} + k_{21})^2} \qquad (2.25)$$

Once distribution equilibrium has been reestablished, the linear slope becomes equal to:

$$\frac{dC_1}{dt} = \frac{-Vm}{V_1\left(1 + \frac{k_{12}}{k_{21}}\right)} \qquad (2.26)$$

In Model C, the apparent volume constant at distribution equilibrium therefore has the following equivalents:

$$V_1\left(1 + \frac{k_{12}}{k_{21}}\right) = V_1 + V_2 \qquad (2.27)$$

$$V_1\left(1 + \frac{k_{12}}{k_{21}}\right) = Vd \qquad (2.28)$$

As with any multi-compartment model at distribution equilibrium, the two compartment model behaves as a single compartment system.

Estimation of Vm - A plot of the linear portions of the upslopes and the downslopes against their corresponding infusion rates is illustrated in Fig. 2.7. In Fig. 2.7 as in Fig. 2.4, the X-axis intercept results in an estimate of the value of Vm. Likewise, the apparent volume of

FIGURE 2.7 The blood slope - infusion rate plot of Model C. The data points represent the linear blood slopes of two infusion rates and of the downslope. The X-axis intercept = Vm and the slope = $\frac{1}{V_1+V_2}$.

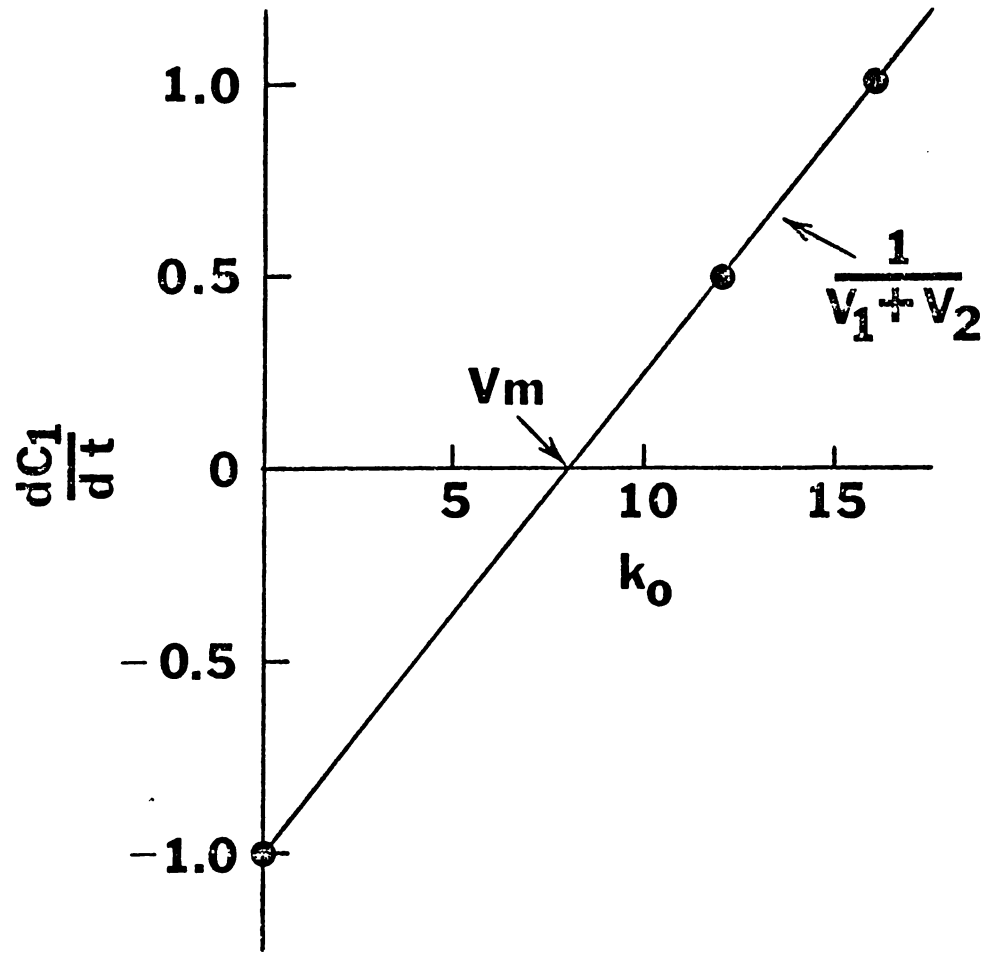
1.0
0.5
0
−0.5
−1.0
5
10
15
k_o
Vm
$\frac{dC_1}{dt}$
$\frac{1}{V_1+V_2}$

distribution (Vd) is obtained in both cases from the reciprocal of the slope. The only difference between the two plots is the definition of Vd. In the one compartment model, Vd is equal to V_1; in the two compartment model, Vd is equal to $V_1 + V_2$. If there were additional compartments, Vd would simply be the sum of all compartments at distribution equilibrium.

The subsequent models D through F will all have basically the same shape of blood curves as shown in Fig. 2.5 and will all have the same type of plots correlating the linear slopes with infusion rates as shown in Fig. 2.7. The following is a series of alternative theoretical two compartment models and their corresponding mathematical treatment.

Two Compartment-Transport Rate-Limited Model -

Model D

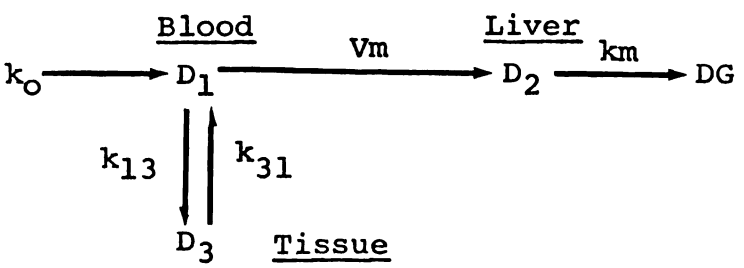

where $D_1 = C_1V_1$ = amount in mg of drug in the central compartment

$D_3 = C_3V_3$ = amount in mg of drug in a non-metabolizing peripheral compartment

V_1, V_3 = volume of distribution of the drug in the compartments in liters

k_{13}, k_{31} = microscopic rate constants in reciprocal time, into and out of the peripheral compartment

Vm = the maximum rate of uptake (transport) into the liver compartment. This presumes a saturable process functioning at maximum velocity

k_m = the pseudo first order rate constant for the formation of the metabolite, DG.

The differential equations representing the distribution compartments are:

$$\frac{dD_1}{dt} = k_o - Vm - k_{13} D_1 + k_{31} D_3 \qquad (2.29)$$

$$\frac{dD_3}{dt} = k_{13} D_1 - k_{31} D_3 \qquad (2.30)$$

Converting to Laplace domain, we have:

$$\bar{D}_1(s) = \frac{k_o - Vm}{s} - k_{13} \bar{D}_1 + k_{31} \bar{D}_3 \qquad (2.31)$$

$$\bar{D}_3(s) = k_{13} \bar{D}_1 - k_{31} \bar{D}_3 \qquad (2.32)$$

Solving for D_1, we obtain

$$D_1 = \left(\frac{(k_o - Vm)k_{31}}{k_{13} + k_{31}}\right) t + \frac{k_{13}(k_o - Vm)}{(k_{13} + k_{31})^2} \left[1 - e^{-(k_{13} + k_{31})t}\right] \qquad (2.33)$$

or

$$C_1 = \left(\frac{k_o - Vm}{V_1\left(1 + \frac{k_{13}}{k_{31}}\right)}\right) t + \frac{k_{13}(k_o - Vm)}{V_1(k_{13} + k_{31})^2}\left[1 - e^{-(k_{13} + k_{31})t}\right] \tag{2.34}$$

Differentiation of Eq. 2.34 results in:

$$\frac{dC_1}{dt} = \frac{k_o - Vm}{V_1\left(1 + \frac{k_{13}}{k_{31}}\right)} + \frac{(k_o - Vm)k_{13}}{V_1(k_{13} + k_{31})} e^{-(k_{13} + k_{31})t} \tag{2.35}$$

when $e^{-(k_{13} + k_{31})t} \longrightarrow 0$

then $$\frac{dC_1}{dt} = \frac{k_o - Vm}{V_1\left(1 + \frac{k_{13}}{k_{31}}\right)} \tag{2.36}$$

Substitution of Vd for the denominator as in Eq. 2.28 we obtain:

$$\frac{dC_1}{dt} = \frac{k_o - Vm}{Vd} \tag{2.37}$$

Post-Infusion down slope:

At the termination of the infusion at T min, the Eq. 2.31 and 2.32 become:

$$\bar{D}_1(s) - D_1' = k_{31}\bar{D}_3 - k_{13}\bar{D}_1 - \frac{Vm}{s} \tag{2.38}$$

$$\bar{D}_3(s) - D_3' = k_{13}\bar{D}_1 - k_{31}\bar{D}_3 \tag{2.39}$$

Solving for $\bar{D}_1$, we have:

$$\bar{D}_1 = \frac{D_1'(s) - Vm + k_{31}D_1' - k_{31}\left(\frac{Vm}{s}\right) + k_{31}D_3'}{s(s + k_{13} + k_{31})} \tag{2.40}$$

The anti-Laplace yields:

$$D_1 = \frac{k_{31}(D_1' + D_3') - Vm}{k_{13} + k_{31}} + \frac{Vm\,k_{31}}{(k_{13} + k_{31})^2} - \left(\frac{Vm\,k_{31}}{k_{13} + k_{31}}\right) t^*$$

$$+ \left[D_1' - \frac{k_{31}(D_1' + D_3') - Vm}{k_{13} + k_{31}} - \frac{Vm\,k_{31}}{(k_{13} + k_{31})^2}\right] e^{-(k_{13} + k_{31})t^*} \qquad (2.41)$$

Where $t^* = t - T$ = the post infusion time

Let: $$B = \frac{k_{31}(D_1 + D_3) - Vm}{k_{13} + k_{31}} + \frac{Vm\,k_{31}}{(k_{13} + k_{31})^2} \qquad (2.42)$$

so that Eq. 2.20 becomes

$$D_1 = B - \frac{Vm\,k_{31}}{k_{13} + k_{31}}\, t^* + (D_1' - B)\, e^{-(k_{13} + k_{31})\, t^*} \qquad (2.43)$$

or

$$C_1 = \frac{B}{V_1} - \frac{Vm}{V_1\left(1 + \frac{k_{13}}{k_{31}}\right)}\, t^* + \frac{(D_1' - B)}{V_1}\, e^{-(k_{13} + k_{31})t^*} \qquad (2.44)$$

Differentiation leads to

$$\frac{dC_1}{dt} = -\frac{Vm}{V_1\left(1 + \frac{k_{13}}{k_{31}}\right)} - \frac{(D_1' - B)(k_{13} + k_{31})}{V_1}\, e^{-(k_{13} + k_{31})t^*} \qquad (2.45)$$

Finally distribution equilibrium is reestablished when

$$e^{-(k_{13} + k_{31})t^*} \longrightarrow 0$$

then

$$\frac{dC_1}{dt} = \frac{-Vm}{V_1\left(1 + \frac{k_{13}}{k_{31}}\right)} \qquad (2.46)$$

or

$$\frac{dC_1}{dt} = \frac{-Vm}{Vd} \qquad (2.47)$$

Two Compartment Excretion Rate-Limited -

Model E

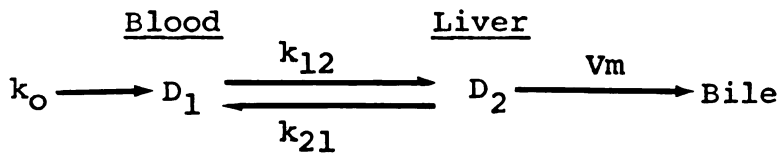

Where the terms are defined as in Model C, except that

Vm = the maximum rate of excretion presumed to be taking place by a saturable process functioning at maximum velocity.

The differential equations representing the distribution compartments are:

$$\frac{dD_1}{dt} = k_o - k_{12} D_1 + k_{21} D_2 \qquad (2.48)$$

$$\frac{dD_2}{dt} = k_{12} D_1 - k_{21} D_2 - Vm \qquad (2.49)$$

These equations are identical to those of Model C, where:

$$\frac{dC_1}{dt} = \frac{k_o - Vm}{V_1\left(1 + \frac{k_{12}}{k_{21}}\right)} + \frac{k_o k_{12} + Vm\, k_{21}}{V_1(k_{12} + k_{21})} e^{-(k_{12} + k_{21})t} \qquad (2.50)$$

when at distribution equilibrium

$$e^{-(k_{12} + k_{21})t} \longrightarrow 0$$

then

$$\frac{dC_1}{dt} = \frac{k_o - Vm}{V_1\left(1 + \frac{k_{12}}{k_{21}}\right)} \qquad (2.51)$$

and thus

$$\frac{dC_1}{dt} = \frac{k_o - Vm}{Vd} \qquad (2.23)$$

The downslope equations are also identical to those of Model C. Thus, the linear downslope at distribution equilibrium is:

$$\frac{dC_1}{dt} = \frac{-Vm}{V_1\left(1 + \frac{k_{12}}{k_{21}}\right)} \qquad (2.26)$$

and

$$\frac{dC_1}{dt} = \frac{-Vm}{Vd} \qquad (2.47)$$

This Model E does differ from Model B when biliary excretion rate curves are examined. Since saturation is presumed to occur instantaneously, the bile should exhibit saturation without a delay.

Transport and Metabolic-Rate-Limited Model -

Model F

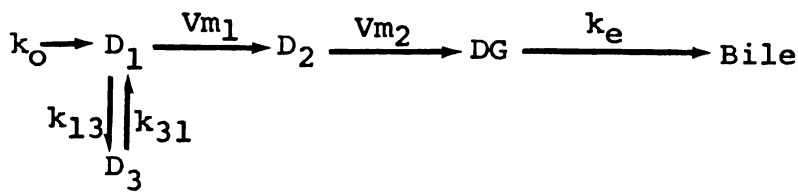

This model is identical to Model D, except

Vm_1 = the maximum rate of uptake (transport) into the liver compartment. This presumes a saturated process functioning at maximum velocity.

Vm_2 = the maximum rate of metabolism of D to DG. This presumes a saturable process functioning at maximum velocity.

The differential equations representing the rate of change of D_1 and D_3 with respect to time are:

$$\frac{dD_1}{dt} = k_o - Vm_1 - k_{13}D_1 + k_{31}D_3 \qquad (2.52)$$

$$\frac{dD_3}{dt} = k_{13}D_1 - k_{31}D_3 \qquad (2.30)$$

In this case all equations describing the blood compartment are identical to those of Model D. However, if $Vm_1 >> Vm_2$ the species within compartment two will accumulate independently:

$$\frac{dC_2}{dt} = \frac{Vm_1 - Vm_2}{V_2} \qquad (2.53)$$

Also the bile will become a reflection of Vm_2 and not of Vm_1:

$$\frac{d\ Bile}{dt} = Vm_2(1 - e^{-k_e t}) \qquad (2.54)$$

If $Vm_2 >> Vm_1$, then the bile would reflect Vm_1 since more drug cannot leave compartment two faster than it is entering.

Transport Rate-Limited and Simultaneous First Order Elimination Model -

Model G

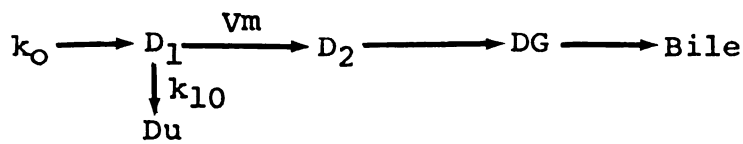

This model is in effect an extension of Model B with parallel zero order and first order processes occuring from the central compartment.

k_{10} = first order rate constant for excretion of D_1.

Du = the amount of drug excreted in mg. The differential equation for D_1 with respect to time is:

$$\frac{dD_1}{dt} = k_o - Vm - k_{10}D_1 \qquad (2.55)$$

On integration we have

$$D_1 = \frac{k_o - Vm(1 - e^{-k_{10}t})}{k_{10}} \qquad (2.56)$$

The differential equation representing the excretion process is

$$\frac{dDu}{dt} = k_{10}D_1 \qquad (2.57)$$

Substitution for D_1 from Eq. 2.56 and integrating results in:

$$\frac{dDu}{dt} = k_o - Vm \quad (1 - e^{-k_{10}t}) \qquad (2.58)$$

Since Vm is in the coefficient of Eq. 2.55 and 2.58, the system represented by this model will appear similar to a model with a zero input and first-order output, eventually reaching steady state. The urinary excretion rate, $\frac{dDu}{dt}$, will approach the value of k_o - Vm. Thus, changing

FIGURE 2.8 The schematic representation of the steady state urinary excretion levels of Model G where Vm = 5 mg/min. Figure 2.8 (a) shows a steady state excretion level of 10 mg/min when infused at a rate of 15 mg/min. Figure 2.8 (b) shows a steady state excretion level of 25 mg/min when the infusion rate is doubled.

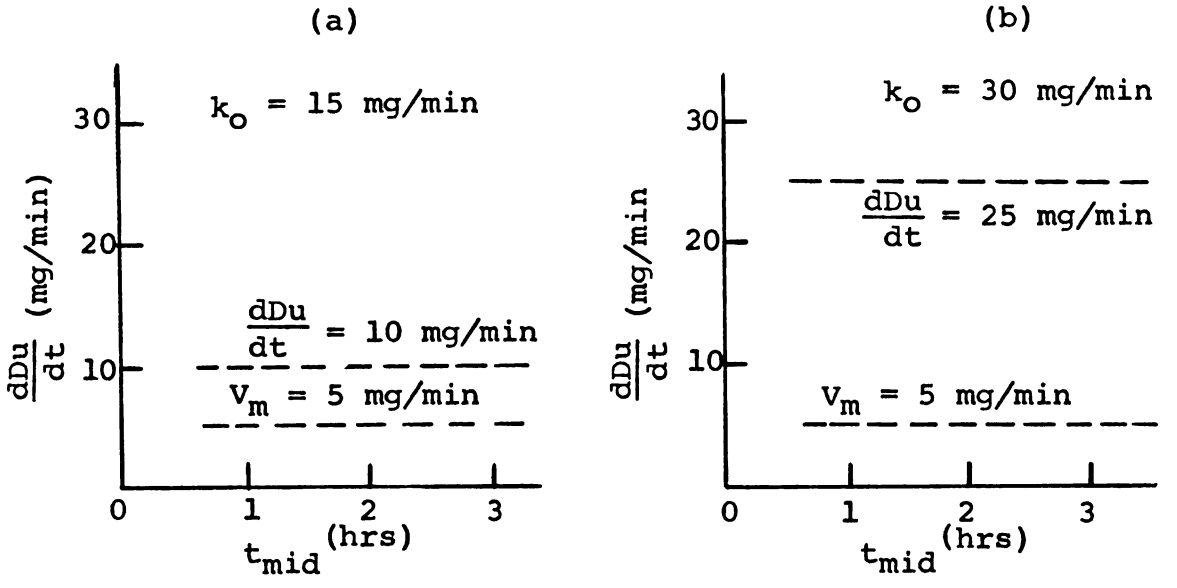
(a)
k_o = 15 mg/min
30
20
10
$\frac{dDu}{dt}$ (mg/min)
$\frac{dDu}{dt}$ = 10 mg/min
V_m = 5 mg/min
0
1
2
3
t_{mid} (hrs)
(b)
k_o = 30 mg/min
30
20
10
$\frac{dDu}{dt}$ (mg/min
$\frac{dDu}{dt}$ = 25 mg/min
V_m = 5 mg/min
0
1
2
3
t_{mid} (hrs)

the infusion rate will not give a linearly proportional change in the steady state excretion levels. This can be seen by the example in Fig. 2.8. In this example with a parallel first-order route of urinary excretion, the Vm of the saturated step is set at 5 mg/min. An initial infusion of 15 mg/min. will produce a urinary steady state excretion level of 10 mg/min. as shown in Fig. 2.8a. Doubling the infusion rate does not double the steady state excretion level. As shown in Fig. 2.8b, instead of 20 mg/min., in this example, the excretion level is 25 mg/min. There would also be a corresponding disproportionate jump in the steady state blood levels of such a system.

In dealing with capacity-limited systems, there are several implications involved with the concept of clearance that need to be discussed.

Clearance Aspects of Hepatic Elimination - The clearance of hepatic elimination is dependent upon hepatic blood flow and the capacity of the liver to eliminate the drug (66). This is defined by Eq. 2.59

$$\dot{V}_{Cl} = \dot{V}_B \left(\frac{a}{\dot{V}_B + a} \right) \qquad (2.59)$$

where

$\dot{V}_{Cl}$ = clearance, in volume per unit time.

$\dot{V}_B$ = hepatic blood flow, in volume per unit time.

$$\left(\frac{a}{\dot{V}_B + a}\right) = \text{extraction ratio}$$

a = the clearance capacity of the organ in units of volume per unit time

The clearance capacity term, a, represents, in effect, the Michaelis-Menten contribution which has the following alternate definitions:

$$a = \left(\frac{Vm}{Km + C_E}\right) K_p \qquad \text{for drugs cleared by capacity-limited processes} \qquad (2.60)$$

$$a = k_m K_p V_E = \left(\frac{Vm}{Km}\right) K_p \qquad \text{for drugs cleared by first-order processes.} \qquad (2.61)$$

$$a = \frac{Vm}{C_o} \qquad \text{for drugs cleared by saturated processes} \qquad (2.62)$$

where

k_m = first order rate constant for drug elimination, in time^{-1}.

K_p = apparent partition coefficient between the eliminating organ and the emergent venous blood.

$$K_p = \frac{C_E}{C_o}$$

C_E = the concentration in the eliminating organ, in amount per unit volume.

C_o = the concentration in the emergent venous blood in amount per unit volume, assumed to be in equilibrium with the tissue.

V_E = volume of the eliminating organ (liver).

Vm = maximum velocity constant, in amount per unit time.

Km = Michaelis constant, in amount per unit volume.

Due to the non-linear Michaelis-Menten term, introduced in Eq. 2.60, there is no analytical solution to the differential equations for the capacity limited flow model. However, using the CSMP digital computer program, Rowland (66) was able to generate data for this system and has examined the influence of various parameters on the clearance of such a system.

According to Eq. 2.59, the clearance of the organ becomes independent of hepatic blood flow if $\dot{V}_B >> a$. Any increase in flow would be compensated by a commensurate decrease in the mean extraction ratio. In such cases, substitution of Eq. 2.61 into Eq. 2.59 results in:

$$\dot{V}_{Cl} = K_p V_E k_m \qquad (2.63)$$

If, however, the clearing capacity (a) of the organ far exceeds organ blood flow, the clearance approaches blood flow. Thus, any change in blood flow would be expected to change the clearance of the drug. Such drugs are said to have perfusion rate-limited clearance characteristics.

Under saturated conditions where $C_E >> Km$, Eq. 2.60 reduces to Eq. 2.62. Hepatic blood flow, $\dot{V}_B$, is usually

much greater than Vm/C_o under almost all physiological conditions. Therefore, substitution for a, from Eq. 2.62 into Eq. 2.59 results in

$$\dot{V}_{Cl} = \dot{V}_B \left(\frac{Vm/Co}{\dot{V}_B + Vm/C_o} \right) = \frac{Vm}{C_o} \qquad (2.64)$$

Let us presume that a drug is infused at a rate greater than Vm. This will produce a rise in the concentration of the drug, C_o, in the blood emerging from the clearing organ. Based on Eq. 2.64, the clearance will correspondingly decrease.

Clearance in first-order systems is independent of concentration and is defined in terms of volume per unit time. However, application of this definition to saturated, capacity-limited systems (with no significant parallel first-order elimination) loses meaning. In such systems, the clearance varies with concentration and no longer becomes a characteristic parameter of the particular drug. It may be more appropriate under these saturated conditions to relate the clearance of the drug to the actual amount cleared per unit time, Vm. We suggest that this term, Vm, be called the zero-order mass clearance constant with units of amount per unit time. It is virtually independent of drug concentration. For equivalent clarity, the clearance of a drug during first-order

kinetics could then be referred to as the first-order volume clearance constant, with, of course, units of volume per unit time.

Purpose of the Investigation - The experimental portion of this thesis will therefore focus on the development of supportive evidence for the mathematical concepts presented in this chapter. Explicitly, we will a) present evidence supporting the concept that iopanoic acid is eliminated by a saturated capacity-limited process, b) use iopanoic acid to evaluate a multiple infusion technique for estimating Vm and Vd, c) investigate the effect of bile salt administration on iopanoic acid Vm and Vd.

CHAPTER III

EXPERIMENTAL

Materials and Equipment - The following materials and equipment were used: Lambda Pump, serial 1300[1]; Lambda Pump Driver, Model 1301[1]; Multichannel Analyzer[2]; Lithium-drifted Silicon Crystal Detector and Cryogenic Container[3]; Am-241 Source[4]; Power Supply, TC908[5]; Single Channel Analyzer, TC 441[5]; Auto-ranging Ratemeter, TC595[5]; P.E. 190 Tubing[6]; P.E. 240 Tubing[6]; Medical Grade Hanafee Tubing, 0.065, #RPX045-H[7]; Lancer Analyzer Cups, 2ml, and Caps, 11405 and 11450[8]; Taurocholic Acid, crude, from ox bile (Sodium Salt), No. T-0750[9].

---

[1]Harvard Apparatus Co., Inc., Millis, Mass.

[2]Packard Instruments, Burlingame, Ca.

[3]KeVex Corp., Burlingame, Ca.

[4]New England Nuclear, Boston, Mass.

[5]Tennelec, Oak Ridge, Tenn.

[6]Clay-Adams Division of Beckton, Dickinson and Co., Parsippany, N. J.

[7]Beckton, Dickinson and Co., Rutherford, N. J.

[8]Sherwood Medical Industries Inc., St. Louis, Mo.

[9]Sigma Chemical Company, St. Louis, Mo.

Iopanoic Acid Identification - The iopanoic acid used in this study was provided by the Winthrop Laboratories. Routine analytical methods were used to confirm the identification and purity of the compound. A sample was subjected to elemental analysis. The results were as follows: calculated for $C_{11}H_{12}I_3NO_2$: C, 23.14; H, 2.12; I, 66.69; N, 2.45. Found: C, 23.22; H, 2.17; I, 67.02; N, 2.32.

The compound's melting point of 155-156° is in good agreement with the literature value of 155.2-57 (10). Its ultraviolet spectrum was also in agreement with the literature, having absorption maximum at 230 and 310 nM. The NMR spectrum (60 megacycles) conformed to the expected pattern: NMR (DMSO-d_6): δ0.87(t,3H,CH_3); 1.50 (quint,2H,CH_2); 3.2 (d,2H,Ar $\underline{CH_2}$); 8.1 (5,1H,aromatic). The mass spectrum of iopanoic acid (chemical ionization) had a major peak corresponding to (M + 1) = 572.

Iopanoic Acid Solution - Parenteral solutions of iopanoic acid were prepared in 1 liter batches in the following manner:

Ten grams of iopanoic acid powder were dissolved in 250 cc of 200 mM Na_2CO_3. The solution was then titrated to pH 9.5 using 1N HCl. Following dilution to 1,000 ml, the osmolarity of the solution was adjusted to 308 $\pm$ 10 milliosmoles using a Fiske osmometer. The solutions were stored

in refrigerators and used within a period of three weeks. The solutions were filtered through filter paper (Whatman #30) prior to each experiment.

Taurocholate Solutions - Parenteral solutions of 0.5% or 1.0% sodium taurocholate were prepared by dissolving 5 gm or 10 gm, respectively, of sodium taurocholate to a liter of normal saline.

Assay Method - Fluorescent excitation analysis was used for the determination of iodine concentration in blood, bile and urine samples.

Fluorescent Excitation Analysis (FEA)-Principle - The K-shell electrons of an atom may be ejected when that atom is bombarded by a photon beam of gamma-rays or x-rays having energies higher than the binding energy of the K-shell electrons (67).

An L-shell or M-shell electron will then fall into the K-shell vacancy. This K-shell capture process causes the atom to emit x-ray photons of different energies, the predominant being E_α and E_β , given by Eq. 1 and 2.

$$E_\alpha = BE[K] - BE[L] \qquad (3.1)$$

$$E_\beta = BE[K] - BE[M] \qquad (3.2)$$

These photons are called the K_α and K_β characteristic radiations are are unique to each element. The

incident beam also undergoes Compton scattering, producing secondary lower energy photons. Multiple Compton scattering produces a diffuse background of low-energy x-rays. The process of exciting stable elements to emit characteristic radiation is termed fluorescent excitation.

FEA Equipment - To detect the characteristic photons within the background produced by other scattering, a liquid nitrogen cooled lithium-drifted silicon detector, Si(Li), was used. The instrument used was a 80mm^2, 3mm deep Si(Li) detection (KeVex Corporation), having 250 eV resolution.

A 600 mCi Am-241 source with a 1 cm^2 area was used for excitation. This source was collimated and aligned perpendicularly to the collimated Si(Li) detector. This configuration of source-to-detector produced a well defined geometry having a sensitive region of the order of 1cm^3. Elements within this volume will emit their characteristic x-rays proportional to their concentration.

The resultant detected x-rayswere accumulated in a 1024 multi-channel analyzer (MCA) in time intervals long enough to yield satisfactory statistics. The lower the concentration measured, the longer the counting time. For example, our counting times ranged from 20 to 500 seconds for concentrations of 20 mg I/cc down to 2 ug I/cc.

Calibration Procedures - The instrument was calibrated using a series of samples of known iodine concentration. From calibration procedure, iodine concentration was related to the ratio of counts under K_α peak to the Compton peak by the following equation:

$$\left(\frac{NK_\alpha}{NC}\right)_{sample} = K^* \cdot C + \left(\frac{NK_\alpha}{NC}\right)_{H_2O} \qquad (3.3)$$

where

NK_α = integrated number of counts under the K_α peak.

NC = integrated number of counts under the Compton peak

K^* = proportionality constant in units of min per mg.

C = iodine concentration in mg per cc.

$\left(\frac{NK_\alpha}{NC}\right)_{H_2O}$ = Ratio of NK_α over NC for the blank (water)

The proportionality constant, K^*, and the water intercept value, $\left(\frac{NK_\alpha}{NC}\right)_{H_2O}$, are instrument constants for iodine-containing samples. Therefore, Eq. 3.3 can be rearranged for convenience to:

$$C = K \left(\frac{NK_\alpha}{NC}\right)_{sample} - \left(\frac{NK_\alpha}{NC}\right)_{H_2O} \qquad (3.4)$$

where

$$K = \frac{1}{K^{\star}} = \text{proportionality constant} = 7.8 \text{ mg/min}$$

$$\left(\frac{NK_{\alpha}}{NC}\right)_{H_2O} = \text{blank (water) constant} = 0.002003.$$

The instrument used had a side detector permitting horizontal collimation. Using this arrangement, the path length through the sample was fixed by the walls of the 2 ml sample container. Thus, the volume of the sample was not an assay variable as long as the sample volume was greater than 1 ml.

Table 3.1 is a summary of data indicative of the accuracy of iodine concentration determination using the FEA setup (67) described above.

TABLE 3.1

Accuracy of Iodine Concentration Determination

Iodine Concentration (mgI/cc)	Counting Time (sec)	Coefficient of variance (%)
9.3	10	0.87
	20	0.72
0.99	50	1.02
	100	0.50
0.035	200	1.70
	500	1.24
0.0029	500	2.15

Accuracy is improved with longer counting time. As can be seen in Table 3.1, the longer the counting time, the smaller the coefficient of variance becomes. Counting time was adjusted according to the concentration in order to permit no fewer than 2000 counts under the K_{α} channel.

Assay of Blood - Iodine determinations in blood are representative of the unconjugate iopanoic acid. Sadee (68) found the blood to contain essentially only the unconjugated form. To convert blood iodine concentration to iopanoic acid concentration, multiply by a correction factor of 1.5.

Assay of Bile - Iodine determinations in bile are representative of the conjugated form of iopanoic acid. Analysis of biliary data (27) from cats showed virtually only the conjugate in fresh bile. Using thin-layer chromatography fresh dog bile showed greater than 95% of the glucuronide. To convert from mg of iodine in the bile to mg of glucuronide, multiply by a correction factor of 2.03.

Assay of Urine - Iodine determinations in urine are also representative of the conjugated form of iopanoic acid. McChesney and Hoppe (27) analyzed human urine and found that the glucuronide was present to an extent of 86%. The correction factor of 2.03 can be used to calculate mg content of glucuronide in urine.

Protocol - Male mongrel dogs weighing between 23 - 32 kg were used. All dogs were in good health. Laboratory blood tests were performed periodically to monitor the dog's health. All four animals maintained normal CBC, normal total bilirubin and normal SGOT. All experiments were begun several months after surgery.

Surgical Preparation of the Dogs - The four dogs used in these studies were surgically prepared for bile collection. This was achieved by cholecystectomy, ligation of the accessory pancreatic duct, and insertion of a modified Thomas Cannula into the second portion of the duodeum opposite the ampulla of Vater (69).

Drug Administration - The parenteral solutions of iopanoic acid were removed from the refrigerator and allowed to warm to room temperature prior to infusion. The solutions were infused through 0.065 catheters that had been placed in the inferior vena cava via one rear leg vein. The Seldinger technique (70) was used for insertion of the catheter. This technique involved a venous puncture with a needle and stilette. The stilette was removed and a wire leader inserted through the needle. The needle was withdrawn and a catheter threaded on to the leader into the vein. Finally the wire leader was withdrawn.

Separate Harvard Lambda pumps were used, one for the iopanoate infusion, the other for the taurocholate infusion. Both infusion lines were joined by means of a three-way connector necessitating only one infusion line into the vena cava. There was no visible precipitation where the two solutions converged.

Bile Salt Replacement - Taurocholate solutions were infused at rates calculated to deliver either 7.07 or 35.5 μM/min sodium taurocholate.

The taurocholate infusions were started as soon as possible, generally at least 2 hrs before the first iopanoic acid infusion was begun. This assured that the bile flow was well stabilized and that the taurocholate in the body was at steady state based on previous studies of Nelson (60) and Moss (57). Bile samples were collected for 4 to 6 control periods of 15 minutes each in order to monitor control bile flow. The essentially uniform bile flow produced by taurocholate infusions, minimized kinetic variations caused by changes in bile production.

Blood Sampling - Blood samples were obtained from the femoral vein opposite that used for the infusions by means of an indwelling catheter. The 0.065 catheter was inserted using the Seldinger technique (70). Blood samples of 1.5 ml were collected in heparinized plastic vials at intervals

ranging from one to five minutes depending upon the speed and duration of the infusion. Frequent samples (q 2-3 min) were obtained for short rapid infusions, while less frequent blood samples (q 4-5 min) were obtained for long, slow infusions. This assured at least 8 samples for determination of a valid linear slope for each infusion. The average number of blood samples per linear slope was over 14.

Bile and Urine Collection - To collect bile, a cork was removed from the Thomas Cannula and a polyethylene tubing, P.E. 190, was inserted 5-6 cm into the common bile duct through the open duodenal cannula. A surgical headlamp was used to facilitate this cannulation. The polyethylene tubing was adjusted so as to permit uniform bile flow. The bile was allowed to flow by gravity into graduated collection tubes that were changed generally at 15-minute intervals. The volume of each bile collection was recorded and a 1½ cc sample of each collection was used for assay purposes. The remaining bile of each collection was pooled and used as a source for the isolation of the conjugate. At the end of the experiment, the tubing was removed and a fresh cork placed in the Thomas Cannula.

To collect urine, a polyethylene tubing, P.E. 240, was used. A 10 cm segment at the tip of the tubing was perforated to allow increased ease of urine withdraw. The tubing was inserted, with aid of K-Y Jelly, into the bladder through the urethra. The external end of the tubing was fitted with a three-way stopcock permitting periodic urine collection with a 60 cc plastic disposable syringe. A 10-20 cm saline flush was occasionally used following a urine collection in those cases in which incomplete urine collection was suspected. The total volume per collection was recorded, and a 1½ cc sample of each collection was kept for assay purposes.

Statistical Analysis - Statistical analysis was performed on the linear blood slopes utilizing a least mean squares method without weights. The linearity of these blood slopes was verified statistically in several ways. The least mean squares program itself provided the slope ($\frac{dC}{dt} = b$), the correlation coefficient(r), the coefficient of determination (r^2), the t value for r, the error of variance of y, ($S^2x \cdot y$), and the sum of squares of x, (Σx^2). The standard deviation of the slope, Sb, was calculated from the equation:

$$Sb = \sqrt{\frac{S^2y \cdot x}{\Sigma x}}$$

The 95% confidence interval was calculated from the equation:

$$95\% \text{ confidence interval} = \pm Sb \cdot t_{0.05}$$

The value $t_{0.05}$ was obtained from statistical tables for percentiles of the t distribution (two tailed) based upon the degrees of freedom. The coefficient of variance was calculated from the equation:

$$\text{coefficient of variance} = \frac{Sb}{b} \times 100\%$$

Statistical analysis of the linear relationship between the infusion rates and the experimentally determined blood slopes was performed in a similar fashion.

CHAPTER IV

RESULTS AND DISCUSSION

After it was discovered that DPH and iopanoate infusions appeared to yield linear curves above a critical rate of infusion, experiments were undertaken to explain this phenomenon more fully. These experiments revealed that rates of infusion of greater than 14 mg of sodium iopanoate per minute (equivalent to 9-10 mg I/minute) caused a linear increase in blood iodine concentrations. In addition, the experiments revealed that as long as the blood level was above a saturation threshold level of approximately 30 mg I/L of whole blood, the post infusion elimination curve of iopanoate was also linear with time. Therefore, multiple infusions above this level were chosen as a method to investigate the relationship between infusion rate and the resultant linear slopes of the blood curve.

Multiple Infusion Experiment of Dog King, October 15, 1973 - A male mongrel dog named King (31.5 kg) was infused with sodium iopanoate at varying rates via a hind leg vein

catheter with a concomitant infusion of 35.5 μM/min. of sodium taurocholate.

Fig. 4.1 illustrates the blood concentration-time plot for a series of three different zero order infusion rates plus two post-infusion downslopes. Note the apparent linearity of the blood slopes above the 30 mg I/L threshold concentration. Table 4.1 contains the actual blood concentration-time data measured during the period up to 256 minutes.

During the initial infusion period, when the concentration of the drug was below 30 mg I/L, a non-linear upslope was observed. This is believed to be due to a combination of the influence of non-equilibrium distribution and of a pre-saturated capacity-limited step. If iopanoic acid is eliminated by a parallel first order process to a significant extent, the linear slope should not be detected. Therefore, we can conclude that a parallel first order process does not exist to a significant extent within the concentration range studied.

The lack of a non-linear component in Fig. 4.1 immediately after the infusion was stopped is particularly interesting. The mathematical analysis of the two compartment models presented in Chapter II supports the contention that the post-infusion non-linear component (the

FIGURE 4.1 The blood concentration time plot of the multiple infusion experiment of dog King, October 15, 1973. The data for this plot is given in Table 4.1. The blood concentration is in units of mg of iodine per liter. The first infusion was at 11.0 mg I/min for 72 min. The second infusion of 13.8 mg I/min was begun at 112 min and was ended at 152 min. The third infusion of 18.4 mg I/min was begun at 224 min and ended at 256 min.

TABLE 4.1

King - High Taurocholate (Oct. 15, 1973)

Time (min)	Whole Blood Conc. (mgI/L)		Time (min)	Whole Blood Conc. (mgI/L)	
0	0		132	43.2	
4	6.2		136	45.7	
8	11.7		140	48.3	N=7
12	17.9		144	49.9	
16	20.8		148	51.7	
20	22.5		152	54.7	
24	25.3		156	49.6	
28	28.2		160	46.5	
32	31.3		164	41.0	
36	32.4		168	36.6	N=7
40	34.2		172	36.2	
44	35.7		176	32.1	
48	37.9		176	29.4	
52	39.2	N=11	184	25.1	
56	40.5		188	23.3	
60	41.2		192	22.6	
64	42.6		196	20.5	
68	45.9		200	18.4	
72	46.5		204	18.1	
76	42.1		208	16.1	
80	38.6		212	15.7	
84	32.6	N=5	216	13.7	
88	31.9		220	10.6	
92	25.4		224	9.6	
96	23.6		228	16.1	
100	21.5		232	29.3	
104	20.0		236	37.0	
108	20.2		240	39.8	
112	17.9		244	48.9	
116	23.0		248	51.7	N=6
120	29.1		252	57.8	
124	37.0		256	62.4	

k_1 = 11.0 mgI/min

k_2 = 0

k_3 = 13.8 mgI/min

k_4 = 0

k_5 = 18.4 mgI/min

so-called " α-phase") is due to a redistribution process and relates to the sum of the forward and reverse microscopic constants. These were seen in the BSP (63) and DPH (61) infusion studies. In all the two compartment models reported in Chapter II, the immediate post-infusion period is defined by a constant plus and exponential term. The exponential hybrid rate constants involved, for example, in Eq. 2.23, represents the sum of the rate constants into and out of the peripheral compartment. The larger the magnitude of the rate constants, the faster the exponential term converges on zero. Thus, if the rates of transfer into and out of the second compartment are large enough, the " α-phase" will essentially vanish. This appears to be the case with iopanoic acid. The drug, therefore appears to act as if it is being distributed in a single compartment.

The linear segments above 30 mg I/L were statistically analyzed and the results are summarized in Table 4.2. Included are five linear segments obtained during three different rates of infusion and two post-infusion periods.

As illustrated in Fig. 4.2, the resultant slopes can be plotted versus their infusion rates according to Eq. 2.23 as introduced in Chapter II:

TABLE 4.2

King-High Taurocholate (Oct. 15, 1973)
Blood Slope Analysis

(1)	(2)	(3)	(4)	(5)	(6)	(7)	(8)	(9)
Infusion Rate	$\frac{dC}{dt}$ (mgI/L/min)	N	r	r^2	p (D.F.=N-2)	Sb (mgI/L/min)	$Sb \cdot t_{0.05}$ (mgI/L/min)	$\frac{Sb}{b}$ x 100%
11.0	0.384	11	0.00487	0.98977	<0.001	0.0130	±0.0294	3.4%
0.0	-0.968	5	-0.98231	0.96493	<0.005	0.1065	±0.3388	11%
13.8	0.606	7	0.99425	0.98853	<0.001	0.0292	±0.0750	4.8%
0.0	-0.933	7	-0.98735	0.97486	<0.001	0.0670	±0.1723	7.2%
18.4	1.313	6	0.99164	0.98335	<0.001	0.0854	±0.2371	6.5%

Infusion Rate - Blood Slope Analysis

(10)	(11)	(12)	(13)	(14)	(15)	(16)	(17)
b	N	r	r^2	p	Sb	$Sb \cdot t_{0.05}$	$\frac{Sb}{b}$ x 100%
0.120226	5	0.99830	0.99660	<0.001	0.0040	±0.0129	3.4%

$\frac{1}{Vd} = 0.120226$ Vd = 8.32L

$\frac{Tm}{Vd} = 0.9584$ Tm = 7.97 mgI/min

FIGURE 4.2 The blood slope-infusion rate plot of the multiple infusion experiment of dog King, October 15, 1973. The blood slopes, $\frac{dC}{dt}$, are plotted in mg of iodine per liter per min. along with their 95% confidence intervals against their corresponding infusion rates in mg of iodine per min. The data for this plot is given in Table 4.2. The estimated Tm = 7.97 mg I/min and the estimated Vd = 8.32 L.

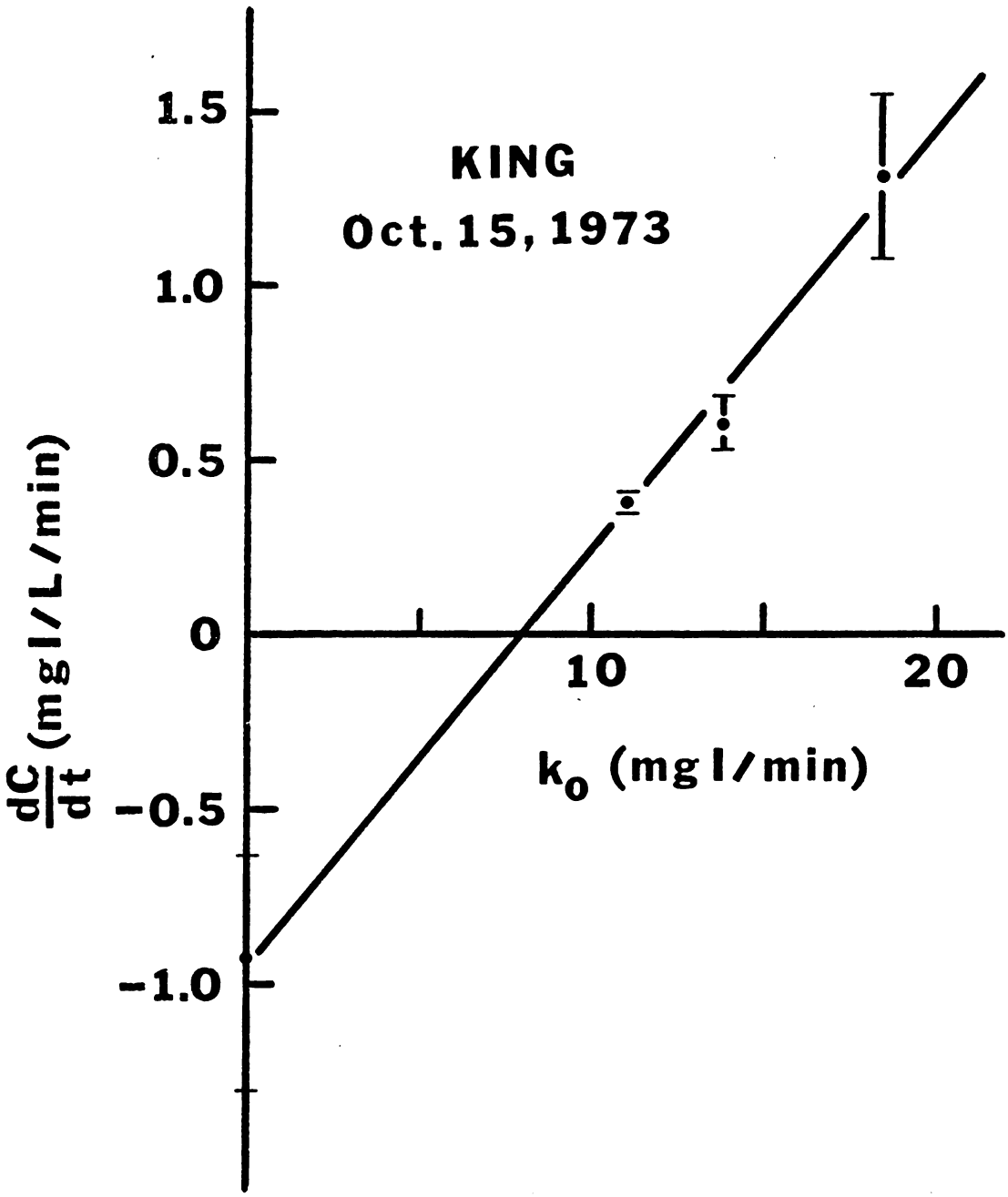
KING
Oct. 15, 1973
1.5
1.0
0.5
0
-0.5
-1.0
10
20
k_o (mg l/min)
$\frac{dC}{dt}$ (mg l/L/min)

$$\frac{dC}{dt} = \left(\frac{1}{Vd}\right)k_o - \frac{Vm}{Vd} \qquad (2.23)$$

Column 1 of Table 4.2 lists the infusion rates used in the experiment, Column 2 and Column 8, respectively, list the slope and its 95 percent confidence interval. The analysis of the blood slope - infusion rate data according to Eq. 2.23 is included in the lower half of Table 4.2. The resultant values for the slope (1/Vd), Y-axis intercept (Tm/Vd), the Vd, and Tm values are summarized at the bottom of the table.

The statistical data strongly support the contention that the segments are linear; the r^2 values are all greater than 0.96. Equally important, the coefficients of variance of the slope obtained during the infusion periods (Column 9, Table 4.2) were 3.4, 4.8 and 6.8 percent, respectively, while during the post-infusion periods, they were 7.2 and 11 percent, respectively.

Thus, the predicted values for Tm and Vd of dog King at the high taurocholate infusion rate were 7.97 mg I/min. and 8.32 L, respectively.

Figure 4.3 is a semi-log plot of the blood decay curve below the saturation threshold following the second infusion. As can be seen, the sub-threshold decay curve

FIGURE 4.3 The semi-logarithmic plot of the blood decay curve following the second infusion experiment of dog King, October 15, 1973. The data for this plot is given in Table 4.1. The first-order decay has an apparent half-life of 29 minutes.

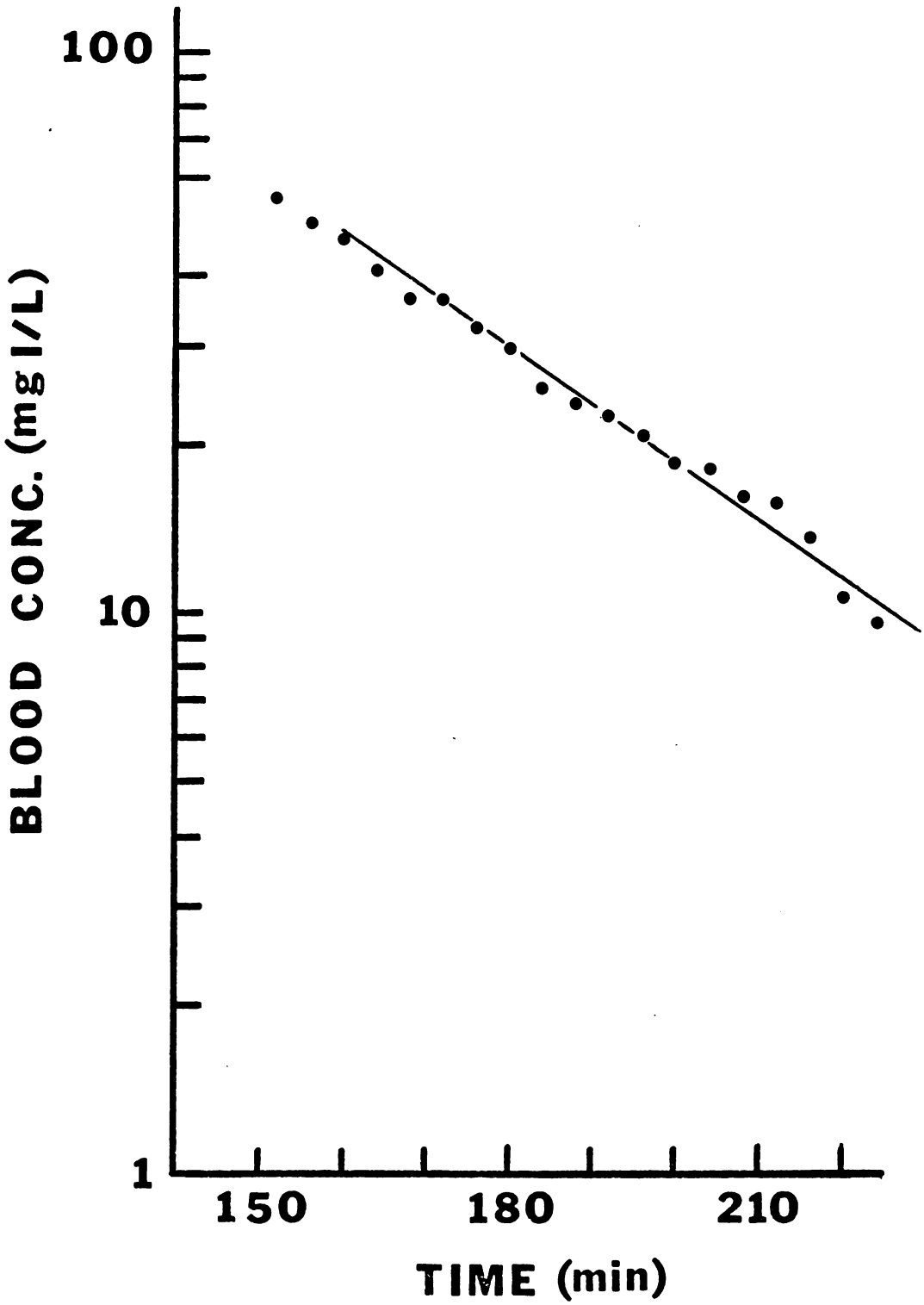
100
10
1
BLOOD CONC. (mg I/L)
150
180
210
TIME (min)

appears to obey pure first-order kinetics with a half-life of 29 minutes. Such an abrupt change from zero to first order is possible as was discussed earlier in Chapter II. If the first order processes in series with the capacity-limited step are faster than the non-saturated M-M process, one would expect to see a non-saturated capacity-limited segment immediately below a saturation phase with a convex descending curve which eventually becomes log-linear when $C << Km$. However, if the capacity-limited process is followed or preceded by one or more first order processes whose rate constants are much slower than the pseudo-first order rate constant of the capacity-limited process, then the rate-limited step below saturation will be something other than capacity-limited step. Such a system would exhibit a concave descending curve below a saturation phase when plotted on linear graph paper. This system would therefore appear to abruptly change from zero to first order kinetics.

At the time that blood samples were being obtained from King, bile was also collected. However, since the system dropped below threshold twice during the experiment, biliary excretion did not reach a plateau. The results of a subsequent study maintaining saturation throughout the experiment on dog Blackie is shown in Fig. 4.4. Figure 4.4

FIGURE 4.4 The semi-logarithmic plot of the combined biliary and urinary excretion rate data versus mid-point times of the multiple infusion experiment of dog Blackie, February 11, 1974. The feathered portion had an apparent half-life of 25 minutes. The excretion rate appeared to reach saturation of about 6.1 mg I/min.

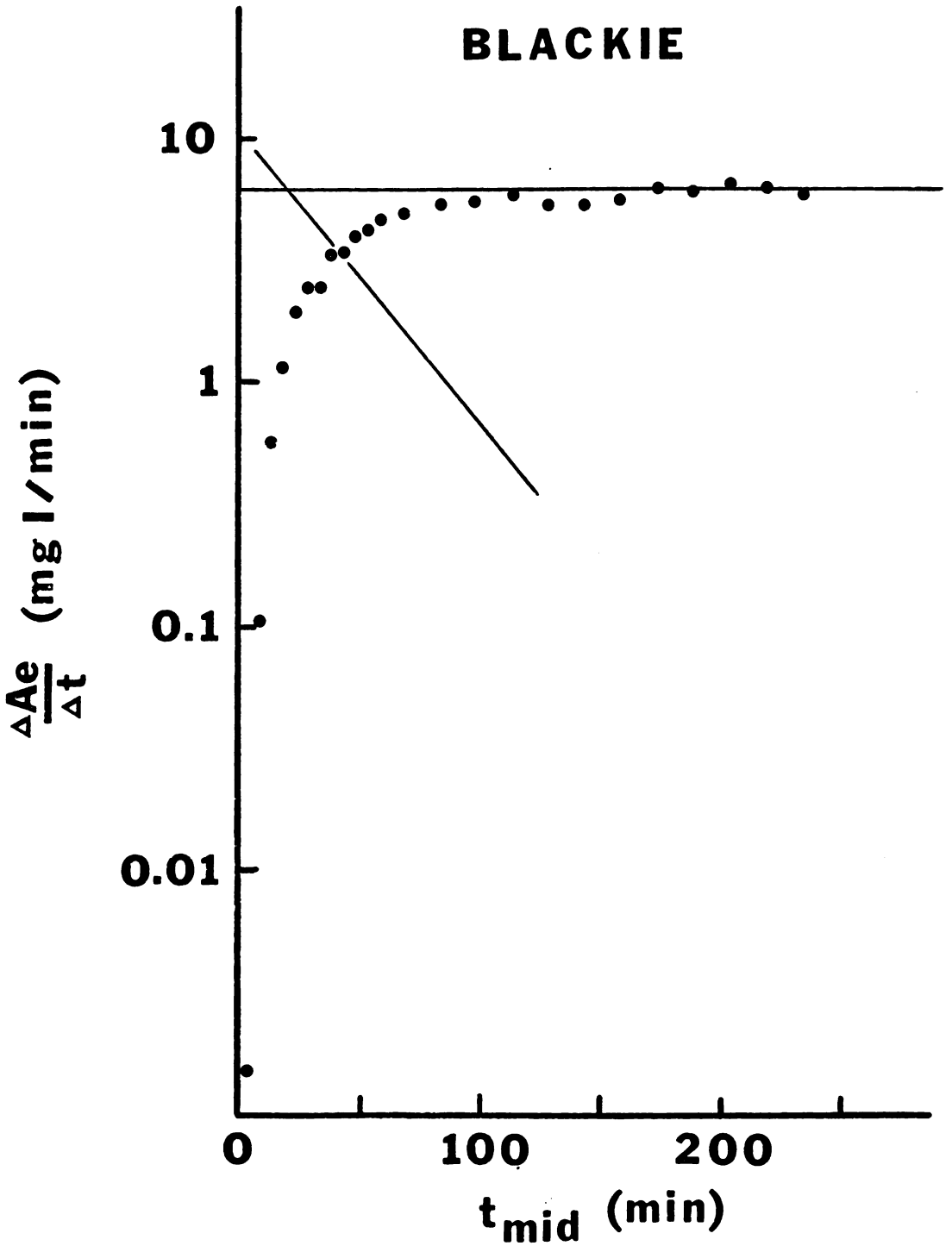
BLACKIE
10
1
0.1
0.01
$\frac{\Delta Ae}{\Delta t}$ (mg l/min)
0
100
200
t_{mid} (min)

is a plot of the dog's biliary and urinary excretion rate data versus mid-point times.

We elected to combine biliary and urinary excretion data since the combination reflects the total loss of the glucuronide from the body. The urinary excretion rate is usually a minor component (less than 10-20 percent) and is apparently inversely proportionate to bile flow rate.

Note the long time (>120 minutes) which is required before the curve becomes asymptotic. The transport maximum, Tm, estimated from the blood multi-infusion technique is 6.46 mg I/min. The excretion rate curve appears to plateau near or at the value of 6.1 mg I/min. Although the blood curve reaches saturation within twenty-five minutes, the excretion clearly takes greater than two hours. Feathering the excretion rate curve revealed an apparent mono-exponential decay process corresponding to a half-life of 25 minutes. This delay of saturation of the exretion rate compared to the blood indicates the existence of a first-order process subsequent to the capacity-limited step. This also indicates that the excretion of the iopanoate glucuronide into bile cannot be the capacity-limited step. Had it been, there would be very little, if any, delay of appearance of saturation between the

blood and excretion rate curves. The only expected delay would be the time for the cannulicular bile to reach the site of sampling - probably less than 10 minutes.

Thus, it is logical to surmise that the capacity-limited step is of either the conjugation step or perhaps an active or facilitated hepatic uptake step.

Note that in Fig. 4.4 the feathered log-linear slope appears to be mono-exponential. However this extrapolation is entirely dependent on the asymptotic value used for the calculations. If true, this mono-exponential behavior would indicate that there is a single first-order process subsequent to the capacity-limited step. If there were two first order processes subsequent to the capacity-limited step, one would theoretically see a bi-exponential curve. In the case of Model D, the biliary excretion rate equation would then be:

$$\frac{d\ Bile}{dt} = Vm(1 - Ae^{-k_m t} - Be^{-k_e t})$$

Obviously, if k_m or k_e differed by a large magnitude, the biliary excretion could appear to be mono-exponential. The analysis of the pre-asymptotic biliary excretion rate curve by itself does not afford sufficient evidence to identify the capacity-limited step.

A special experiment was undertaken in which the bile

collection was carried out to 900 minutes. The biliary excretion data obtained from this experiment of Wendall, February 26, 1974, are plotted in Fig. 4.5.

The excretion rate process was followed for over three decades of excretion rates. There is no doubt in this instance that the biliary excretion rate curve during the post-infusion period is poly-exponential. It appears to be represented by a tri-exponential equation. This would indicate a three-compartmental catenary model. However, further refinement of the experimental technique is needed before one can propose a specific model to interpret such results.

The Influence of Michaelis Constant, Km - It was noted earlier that Km must be small in order to have the results obtained from our experiments. In order to evaluate what contribution Km would have in the analysis of our data, a series of analog computer simulations were made of the following model:

Model H

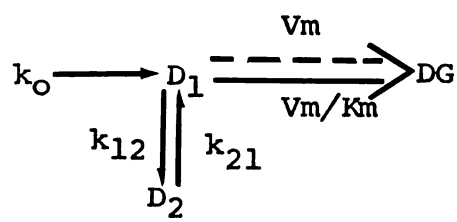

$$V_1\left(\frac{dC_1}{dt}\right) = k_o - k_{12}V_1C_1 + k_{21}V_2C_2 - \frac{VmC_1}{Km + C_1}$$

$$V_2\left(\frac{dC_2}{dt}\right) = k_{12}V_1C_1 - k_{21}V_2C_2$$

FIGURE 4.5 The semi-logarithmic plot of the biliary excretion rate data versus mid-point times following the end of the last infusion of the multiple infusion experiment of Wendall, February 26, 1974. The biliary excretion rate decay appears to be tri-exponential in nature. The corresponding half-lives are: $(t_{\frac{1}{2}})_{\alpha}$ = 17 min, $(t_{\frac{1}{2}})_{\beta}$ = 43.5 min and $(t_{\frac{1}{2}})_{\gamma}$ = 221 min.

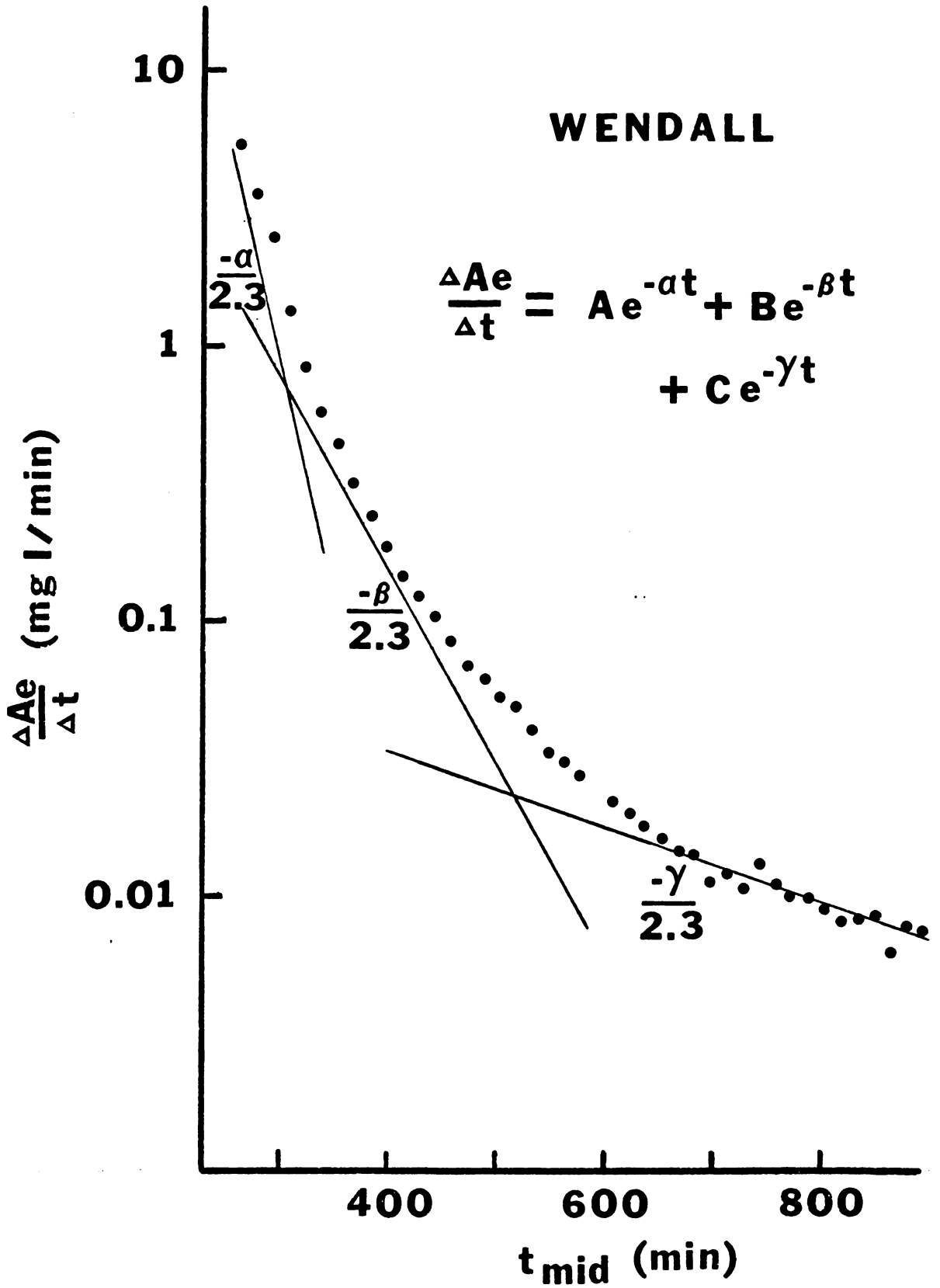
WENDALL
$\frac{\Delta Ae}{\Delta t} = Ae^{-\alpha t} + Be^{-\beta t} + Ce^{-\gamma t}$
$\frac{-\alpha}{2.3}$
$\frac{-\beta}{2.3}$
$\frac{-\gamma}{2.3}$
10
1
0.1
0.01
$\frac{\Delta Ae}{\Delta t}$ (mg l / min)
400
600
800
t_{mid} (min)

where

k_{12} = 0.10 min.$^{-1}$

k_{21} = 0.05 min.$^{-1}$

V_1 = 2.8 L

V_2 = 5.6 L

Km is either 50 mg/L, 12.5 mg/L or 1.25 mg/L

k_o is either 8, 10, 12, 14 or 16 mg/min.

Vm is held at 8 mg/min.

C_1 goes from 0 to 100 mg/L

Figure 4.6 is the analogue computer schematic of the above model.

In Figs. 4.7 through 4.12, note in all cases that the upslopes eventually appear to be linear. However, the downslopes appear to be more sensitive to the size of Km. Only at a very low Km (1.25 mg/L), Fig. 4.9 does the middle portion of the downslope approximate a straight line.

When the apparent linear slopes are plotted against their corresponding infusion rates, an apparent linear relationship exists. However, as can be seen in Fig. 4.13, only the plot of data from Km = 0 has an X-axis intercept of the true Tm. All five plots have the same slopes, indicating that Km does not affect the estimate of Vd. The X-axis intercept value, on the other hand, becomes

FIGURE 4.6 The analog computer program required for the fitting the two compartment model having a zero order infusion into and a Michaelis-Menton output from the central compartment.

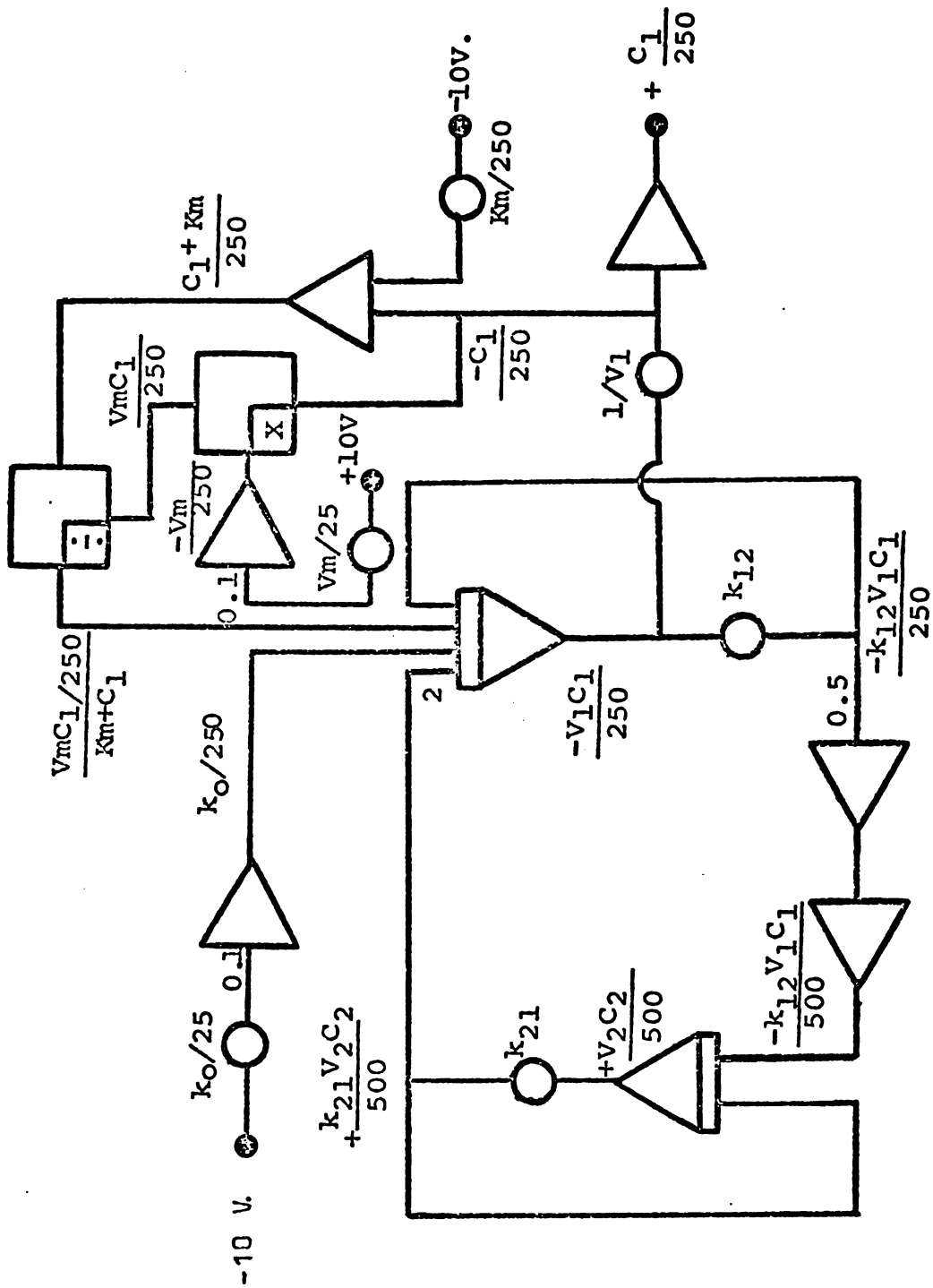
-10 V.
$k_o/25$
0.1
$k_o/250$
$\frac{k_{21}V_2C_2}{500}$
k_{21}
$+\frac{V_2C_2}{500}$
$-\frac{k_{12}V_1C_1}{500}$
0.5
$-\frac{k_{12}V_1C_1}{250}$
k_{12}
2
$-\frac{V_1C_1}{250}$
$\frac{VmC_1/250}{Km+C_1}$
÷
$-\frac{Vm}{250}$
0.1
$Vm/25$
+10V
x
$\frac{VmC_1}{250}$
$\frac{C_1+Km}{250}$
-10V.
$Km/250$
$-\frac{C_1}{250}$
$1/V_1$
$+\frac{C_1}{250}$

FIGURE 4.7 The analog computer simulation for C_1 versus time of Model H where Km = 50 mg/L and k_o = 12 mg/min. The apparent linear upslope $\frac{dC_1}{dt}$ = 0.88 mg/L/min.

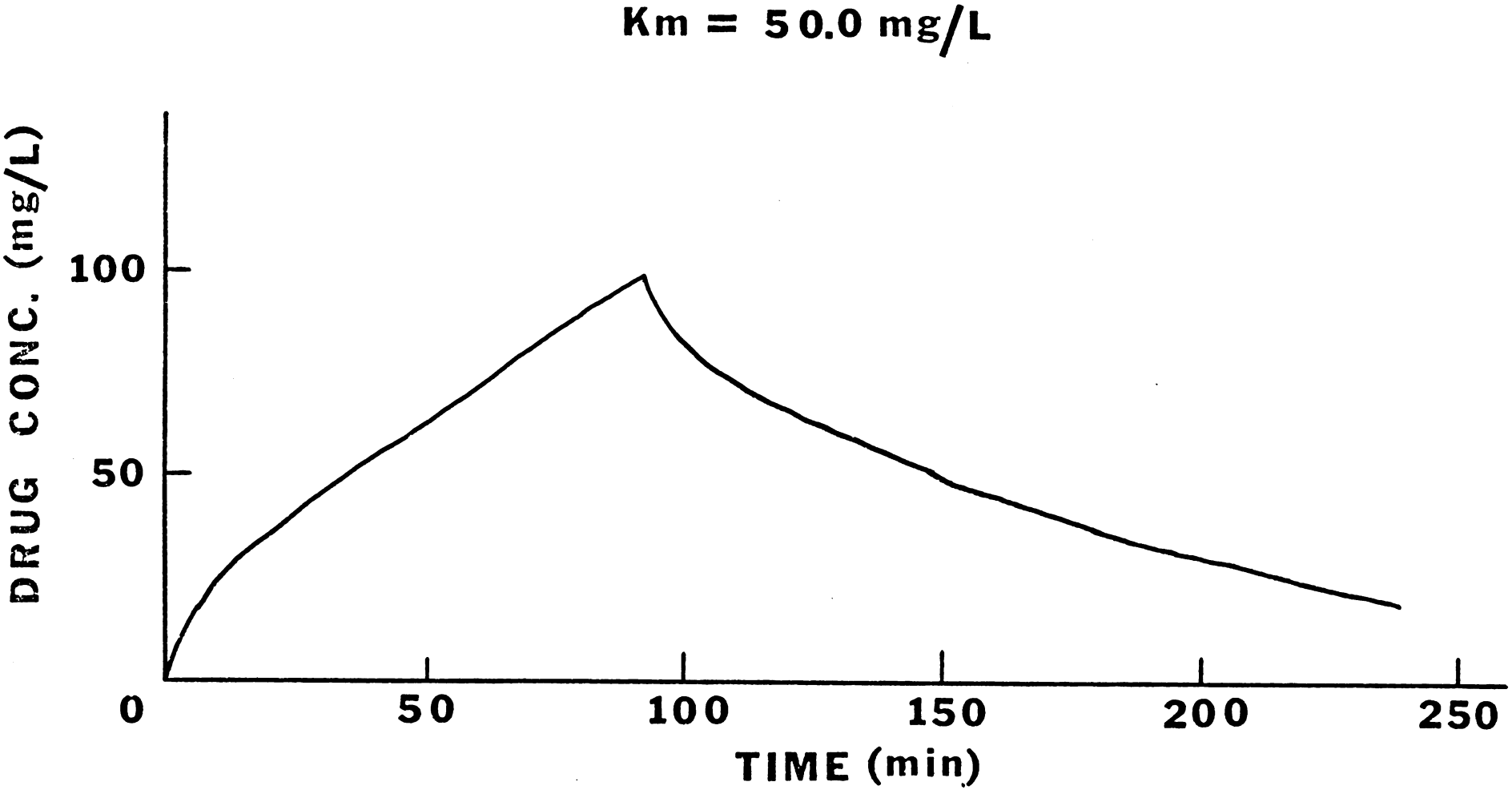
Km = 50.0 mg/L
DRUG CONC. (mg/L)
100
50
0
50
100
150
200
250
TIME (min)

FIGURE 4.8 The analog computer simulation for C_1 versus time of Model H where Km = 12.5 mg/L and k_o = 12 mg/min. The apparent linear upslope, $\frac{dC_1}{dt}$ = 0.54 mg/L/min.

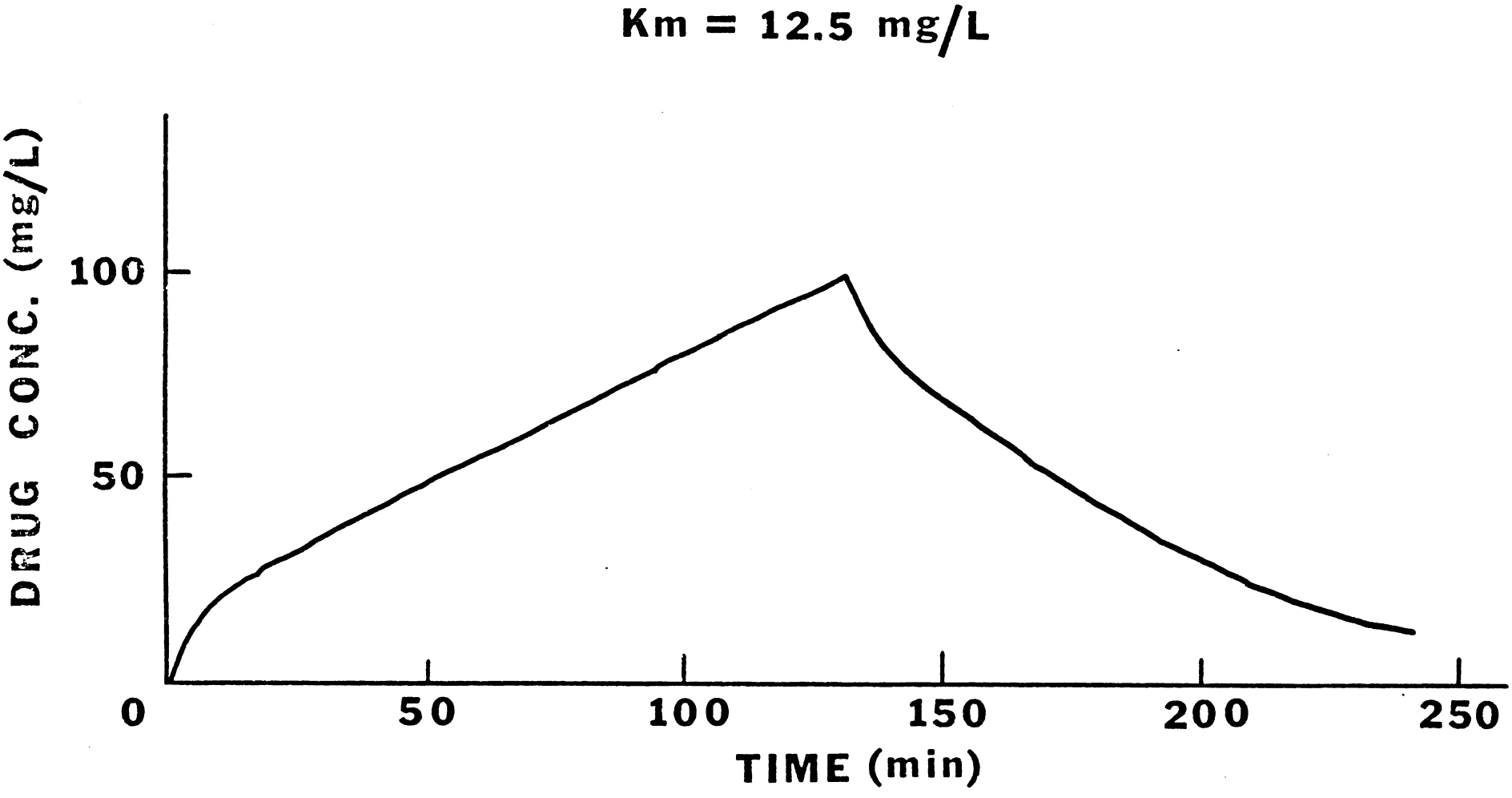
Km = 12.5 mg/L
DRUG CONC. (mg/L)
100
50
0
50
100
150
200
250
TIME (min)

FIGURE 4.9 The analog computer simulation for C_1 versus time of Model H where Km = 1.25 mg/L and k_o = 12 mg/min. The apparent linear upslope, $\frac{dC_1}{dt}$ = 0.52 mg/L/min. The apparent linear downslope, $\frac{dC_1}{dt}$ = -0.95 mg/L/min.

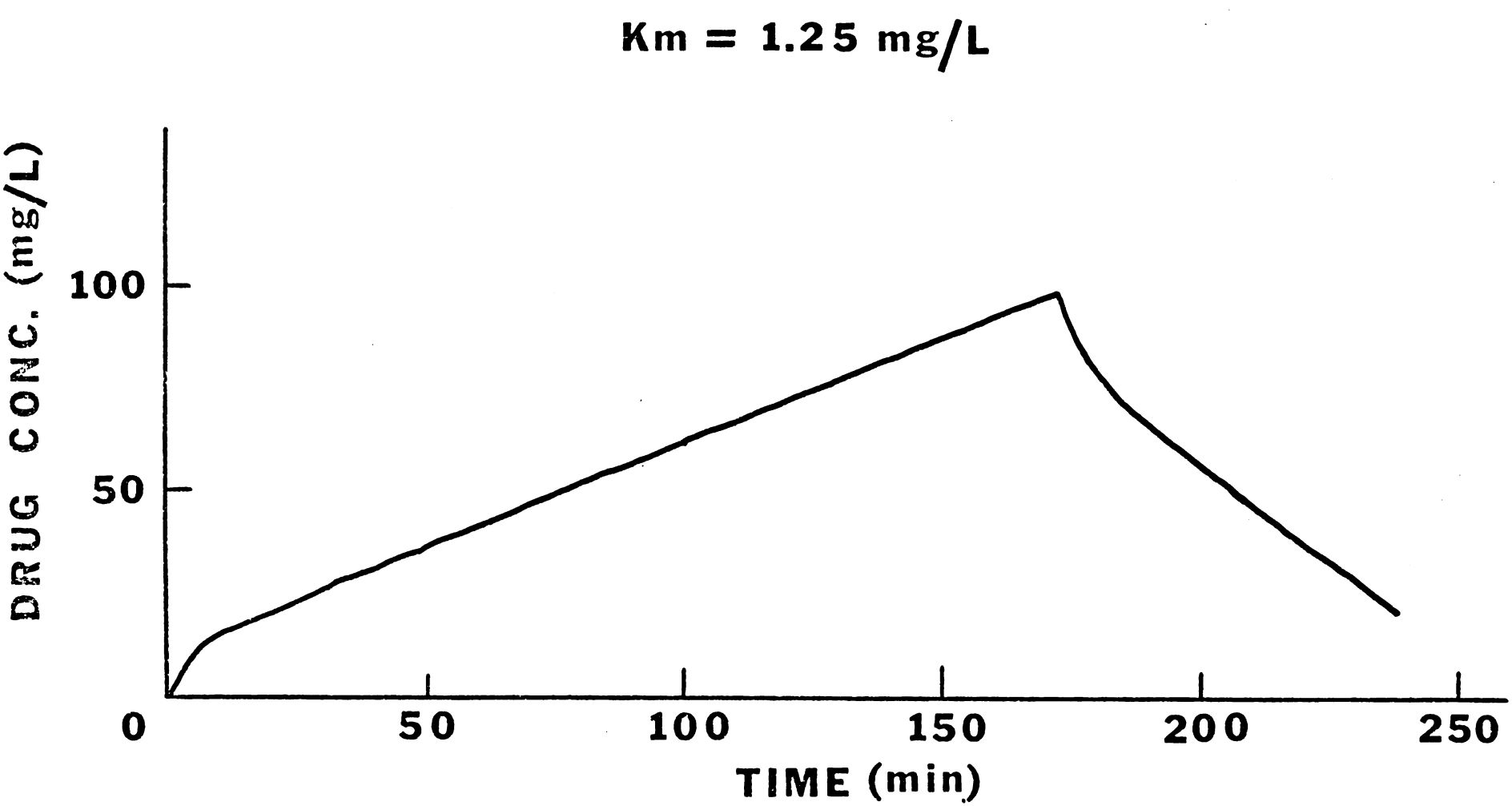
Km = 1.25 mg/L
DRUG CONC. (mg/L)
100
50
0
50
100
150
200
250
TIME (min)

FIGURE 4.10 The analog computer simulation for C_1 versus time of Model H where Km = 50 mg/L. The infusion rates are: k_1 = 14 mg/min, k_2 = 12 mg/min, k_3 = 10 mg/min, and k_4 = 8 mg/min. The corresponding slopes are 1.07, 0.88, 0.63 and 0.38 mg/L/min, respectively.

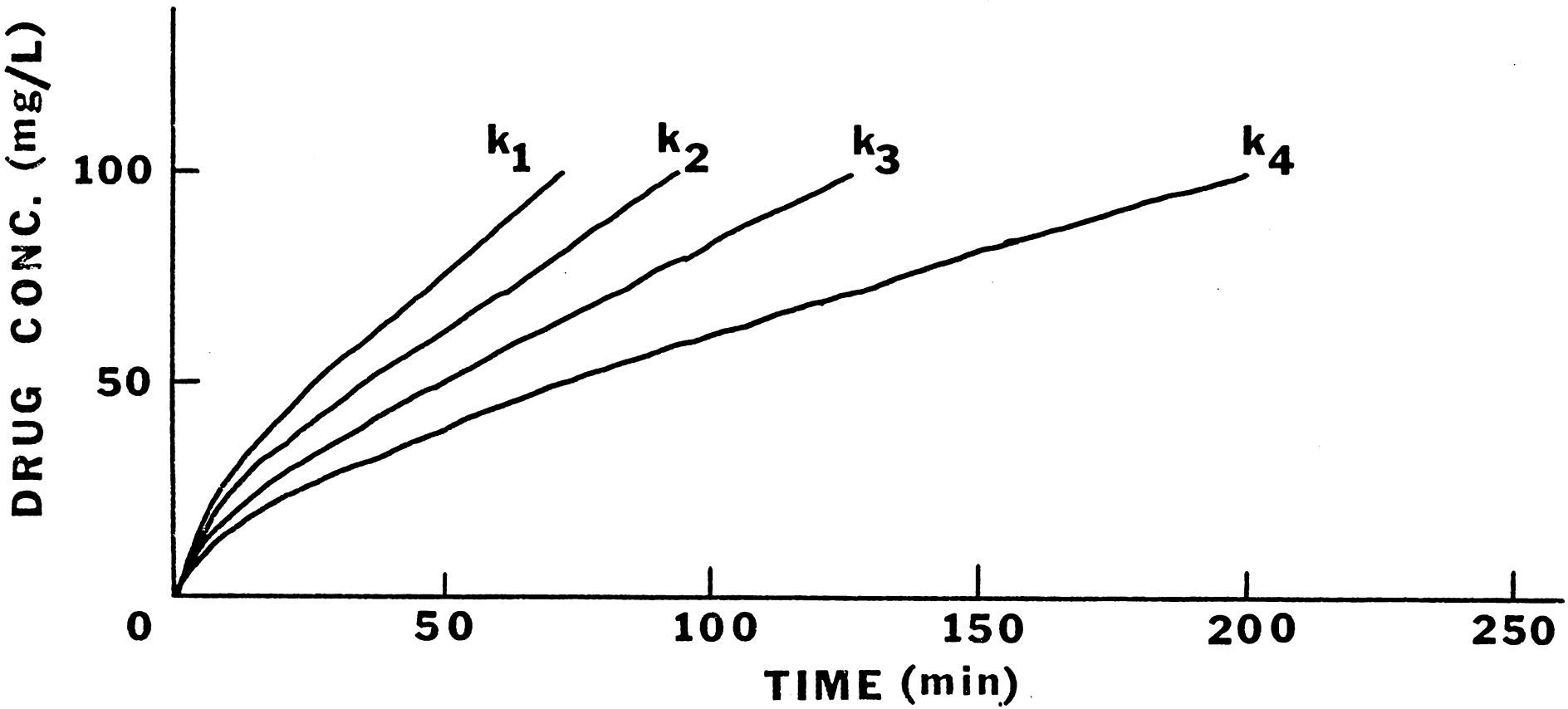
Km = 50.0 mg/L
DRUG CONC. (mg/L)
100
50
0
k1
k2
k3
k4
50
100
150
200
250
TIME (min)

FIGURE 4.11 The analog computer simulation for C_1 versus time of Model H where Km = 12.5 mg/L. The infusion rates are: k_1 = 10 mg/min, k_2 = 8 mg/min. and k_3 = 14 mg/min. The corresponding slopes are 0.38, 0.16, and 0.89 mg/L/min respectively.

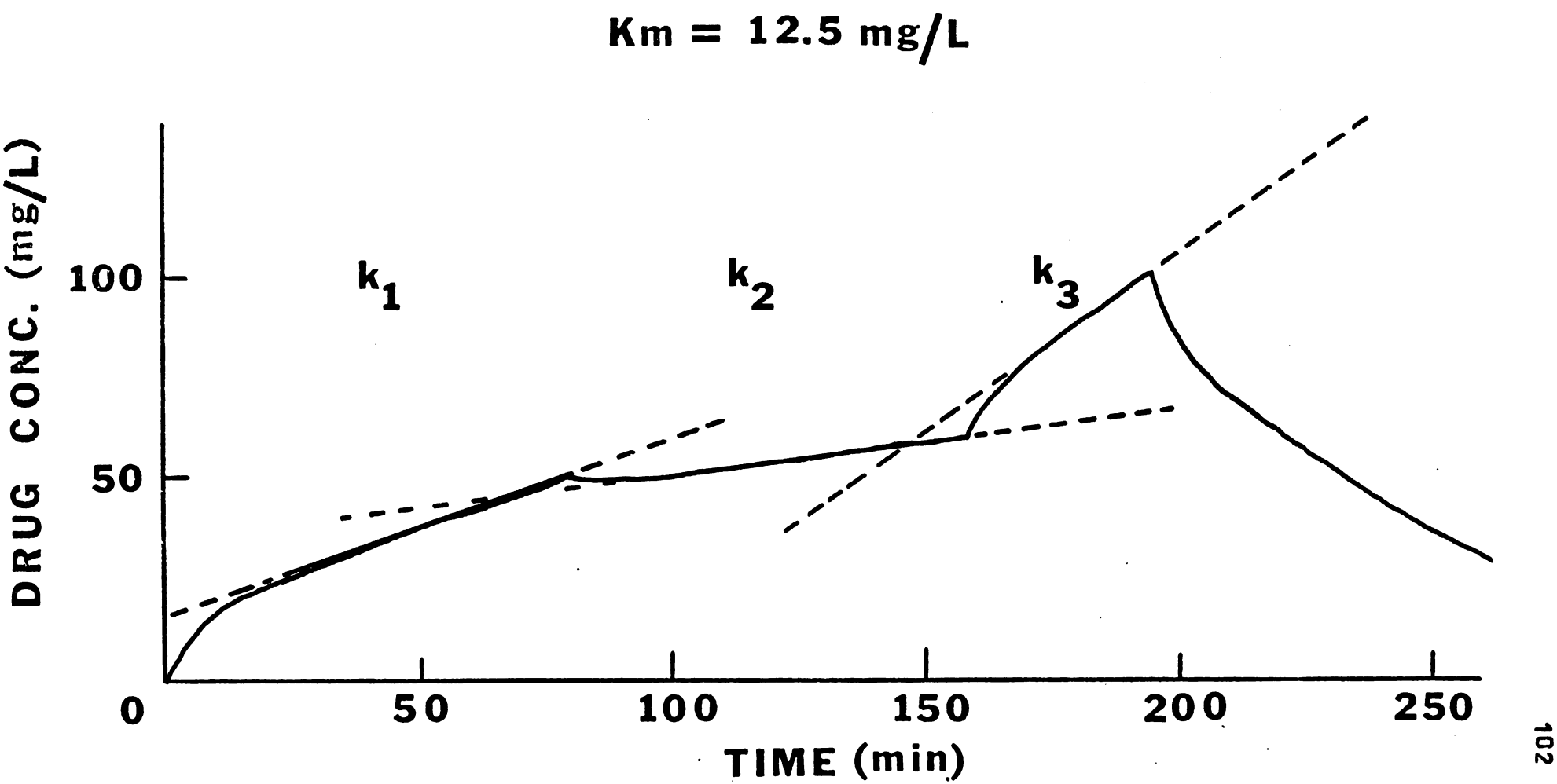
Km = 12.5 mg/L
DRUG CONC. (mg/L)
100
50
0
k1
k2
k3
50
100
150
200
250
TIME (min)

FIGURE 4.12 The analog computer simulation for C_1 versus time of Model H where Km = 1.25 mg/L. The infusion rates are: k_1 = 14 mg/min, k_2 = 8 mg/min, k_3 = 12 mg/min, k_4 = 16 mg/min and k_5 = 0. The corresponding slopes are 0.77, 0.03, 0.52, 1.07, and -0.96 mg/L/min, respectively.

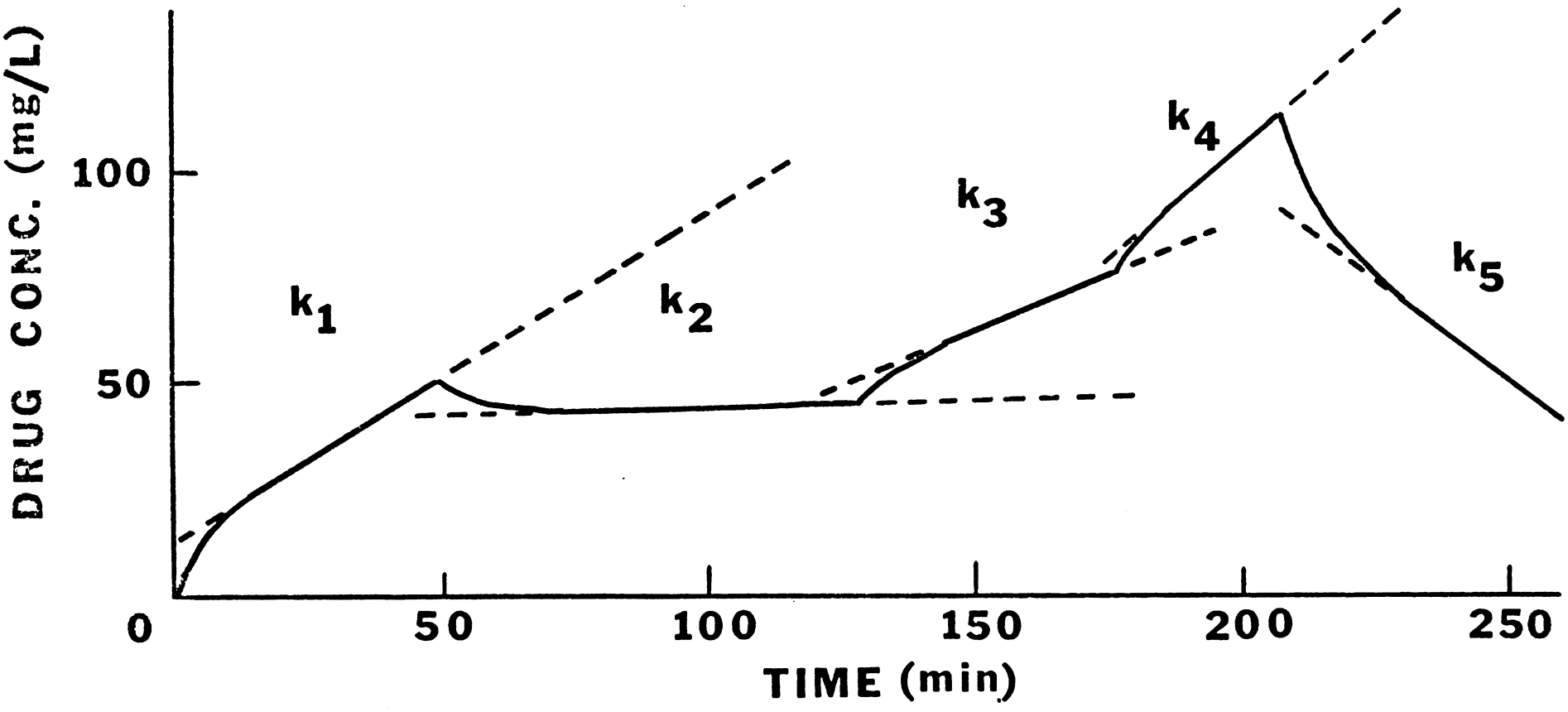
Km = 1.25 mg/L
DRUG CONC. (mg/L)
100
50
0
50
100
150
200
250
TIME (min)
k1
k2
k3
k4
k5

FIGURE 4.13 The plot of the apparent linear blood slopes versus their corresponding infusion rates of Model H where Km = 50 mg/L (Line A); Km = 12.5 mg/L (Line B); Km = 1.25 mg/L (Line C); and Km = 0 (Line D). The corresponding <u>apparent</u> maximum velocity constants, Vm, are: 4.8 mg/min, 6.8 mg/min, 7.7 mg/min, and 8.0 mg/min, respectively. The <u>true</u> maximum velocity constant Vm = 8.0 mg/min.

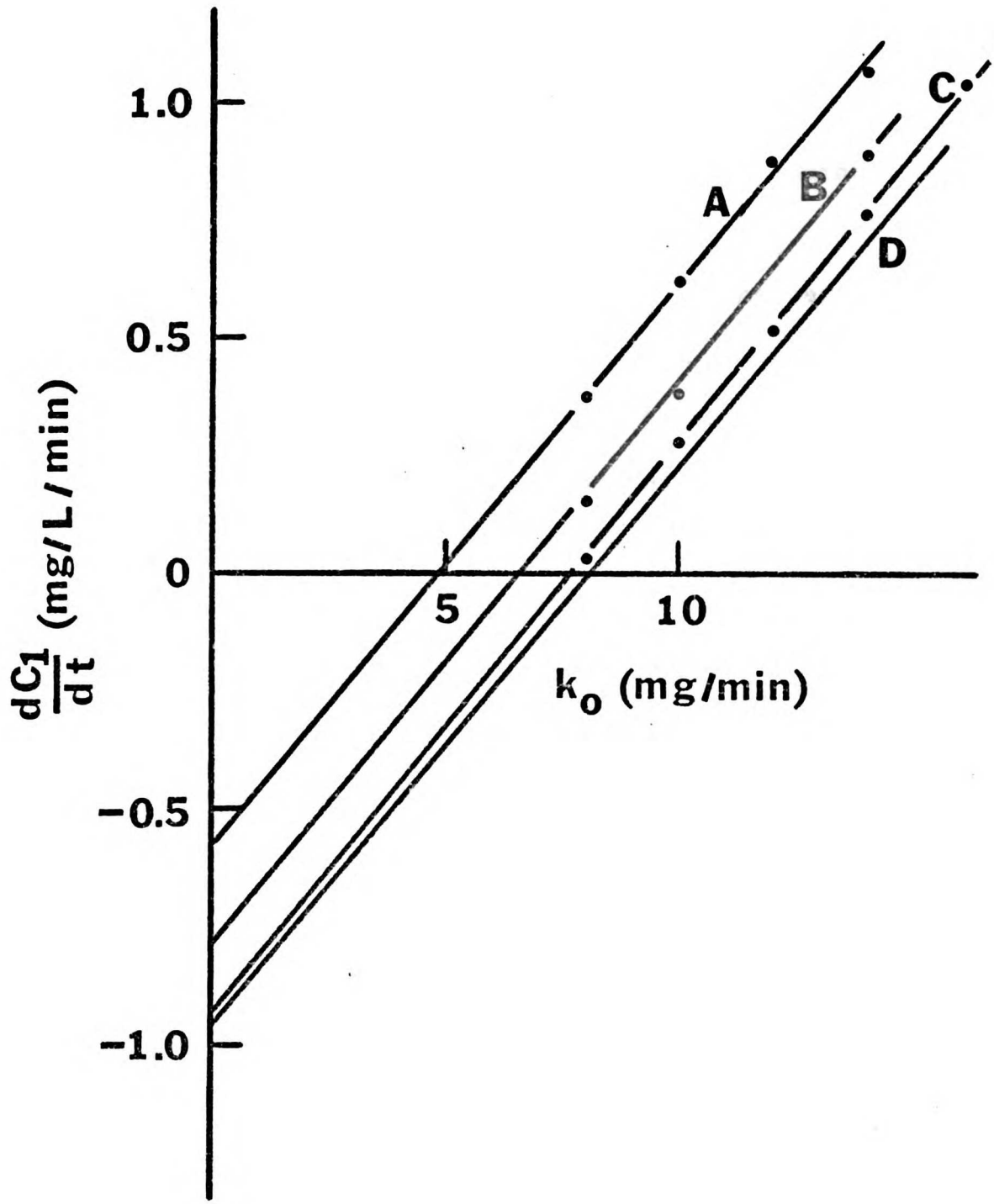
1.0
0.5
0
−0.5
−1.0
5
10
A
B
C
D
$\frac{dC_1}{dt}$ (mg/L/min)
k_o (mg/min)

increasingly smaller whenever Km is increased. Thus, our multi-infusion technique will yield estimates of the apparent Tm, not the theoretically true Tm. This apparent Tm, however, represents the maximum velocity of the system within a specific concentration range. This is the rate that would maintain the system at a constant blood level. It may or may not hold at a higher blood level depending on the magnitude of the Km.

In our iopanoic acid system, the downslope appears to be quite linear. Therefore, the Michaelis constant, Km, of our iopanoic acid system is likely to be quite small compared to the concentration range studied. As a result, our apparent Tm is probably close to the Tm representing complete saturation of the capacity-limited step.

Plateau Infusion Experiment of Dog King, October 29, 1973 - If we have actually defined the zero order mass clearance constant, Tm, by our method, then by infusing at this rate we should arrive at a horizontal slope even at two different levels of concentration. Figure 4.14 is the projected infusion plan carried out on King, October 29, 1973, based upon estimates obtained from his earlier experiment of October 15, 1973. Figure 4.15 shows the results of the study. As can be seen, the plateaus were achieved and maintained as predicted. This experiment

FIGURE 4.14 The projected infusion plan for dog King based upon estimates of Tm = 7.97 mg I/min and Vd = 8.32 L. The proposed infusion rates are: k_1 = 11.2 mg I/min, k_2 = 8.0 mg I/min, k_3 = 14.1 mg I/min, k_4 = 8.0 mg I/min, and k_5 = 0.

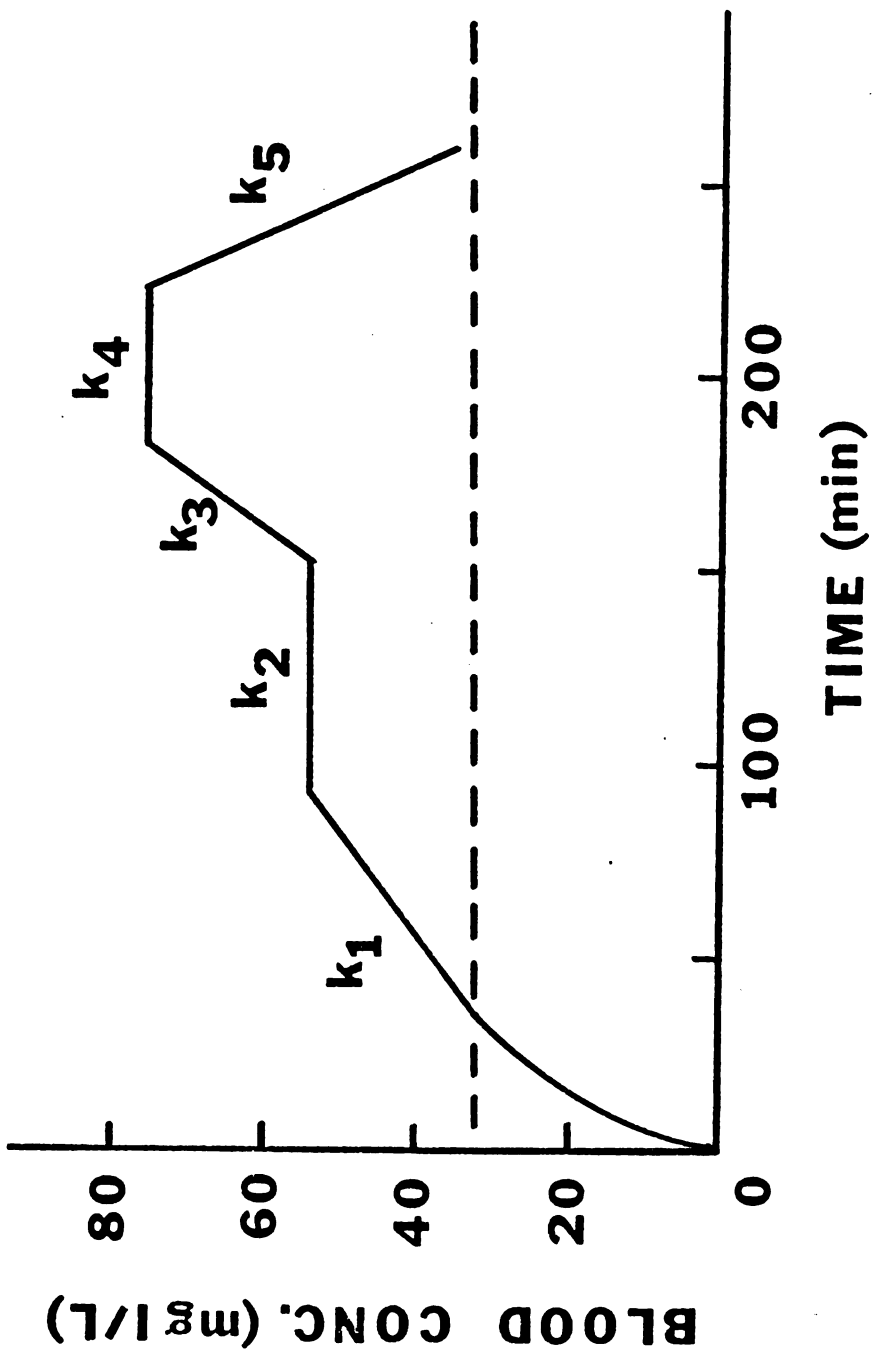
BLOOD CONC. (mg I/L)
80
60
40
20
0
100
200
TIME (min)
k1
k2
k3
k4
k5

FIGURE 4.15 The blood concentration - time plot of the multiple infusion experiment of dog King, October 29, 1973. The data for this plot is given in Table 4.3

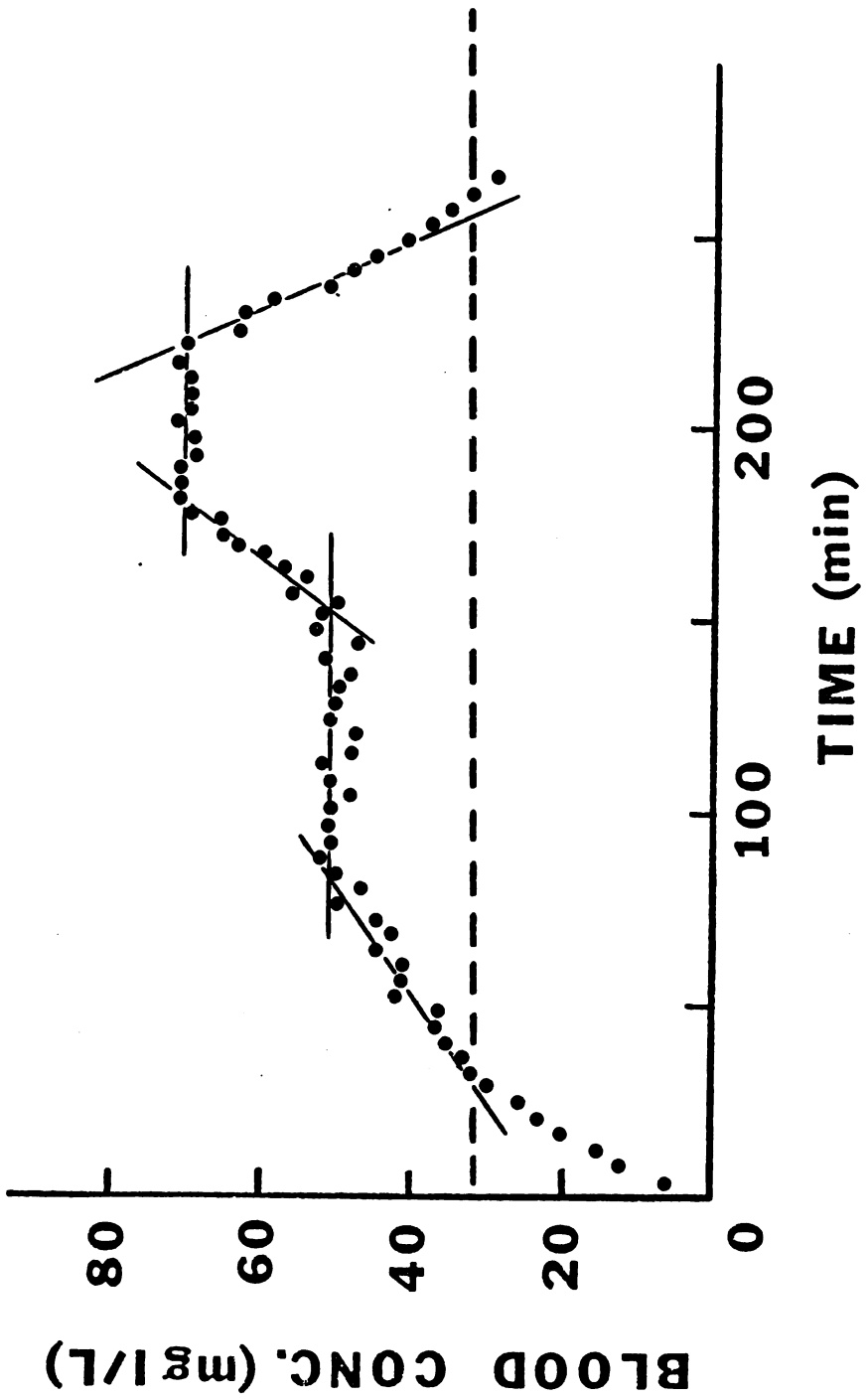
BLOOD CONC. (mg I/L)
80
60
40
20
0
100
200
TIME (min)

substantiates our theory and shows excellent reproducibility of Tm and Vd. Table 4.3 and Figure 4.16 represent an analysis of the October 29, 1973, experiment. As can be seen, Tm increased less than 2 percent and Vd increased less than 3 percent.

Effect of Taurocholate on Iopanoic Acid Tm and Vd - The multiple infusion technique was employed to determine Vm and Vd at two different taurocholate infusion rates in four dogs. The order of the high taurocholate infusion (35.5 μM/min), and the low taurocholate infusion (7.07 μM/min) were randomized in the four dogs.

Individual Analysis - Tables 4.3 to 4.10 contain the individual data analysis for each of the eight experiments. Blood slopes which appeared to be horizontal $\frac{dC}{dt} = 0$, did not yield meaningful statistical analysis due to the lack of regression. Their statistical analysis is limited to the statement that their slopes are not significantly different from zero. Linear regression analysis is also somewhat deceptive when dealing with near zero slopes. Visually, these near zero slopes appear to fit the data quite well. However, statistically, linear regression yields comparatively poor results. The statistical results of linear regression are dependent upon two general variables, 1) the tightness or goodness of fit and 2) the degree

TABLE 4.3

King-High Taurocholate (Oct. 29, 1973)
Blood Slope Analysis

(1) Infusion Rate	(2) $\frac{dC}{dt}$ (mgI/L/min)	(3) N	(4) r	(5) r^2	(6) p (D.F.=N-2)	(7) Sb (mgI/L/min)	(8) $Sb \cdot t_{0.05}$ (mgI/L/min)	(9) $\frac{Sb}{b} \times 100\%$
11.20	0.335	17	0.97243	0.94562	<0.001	0.0208	$\pm$0.0443	6.2%
8.06	0.0	-	-	-	-	-	-	-
14.10	0.722	11	0.97994	0.96028	<0.001	0.0489	$\pm$0.1106	6.8%
8.06	0.0	-	-	-	-	-	-	-
0.00	-0.947	8	-.98997	0.98004	<0.001	0.0552	$\pm$0.1351	5.8%

Infusion Rate - Blood Slope Analysis

(10) b	(11) N	(12) r	(13) r^2	(14) p	(15) Sb	(16) $Sb \cdot t_{0.05}$	(17) $\frac{Sb}{b} \times 100\%$
0.117249	5	0.99961	0.99922	<0.001	0.00190	$\pm$0.0060	1.6%

$\frac{1}{Vd} = 0.117249$ Vd = 8.53 L

$\frac{Tm}{Vd} = 0.9493$ Tm = 8.10 mg I/min

FIGURE 4.16 The blood slope - infusion rate plot of the multiple infusion experiment of dog King, October 29, 1973. The data for this plot is given in Table 4.2. The estimated Tm = 8.10 mg I/min and Vd = 8.53 L.

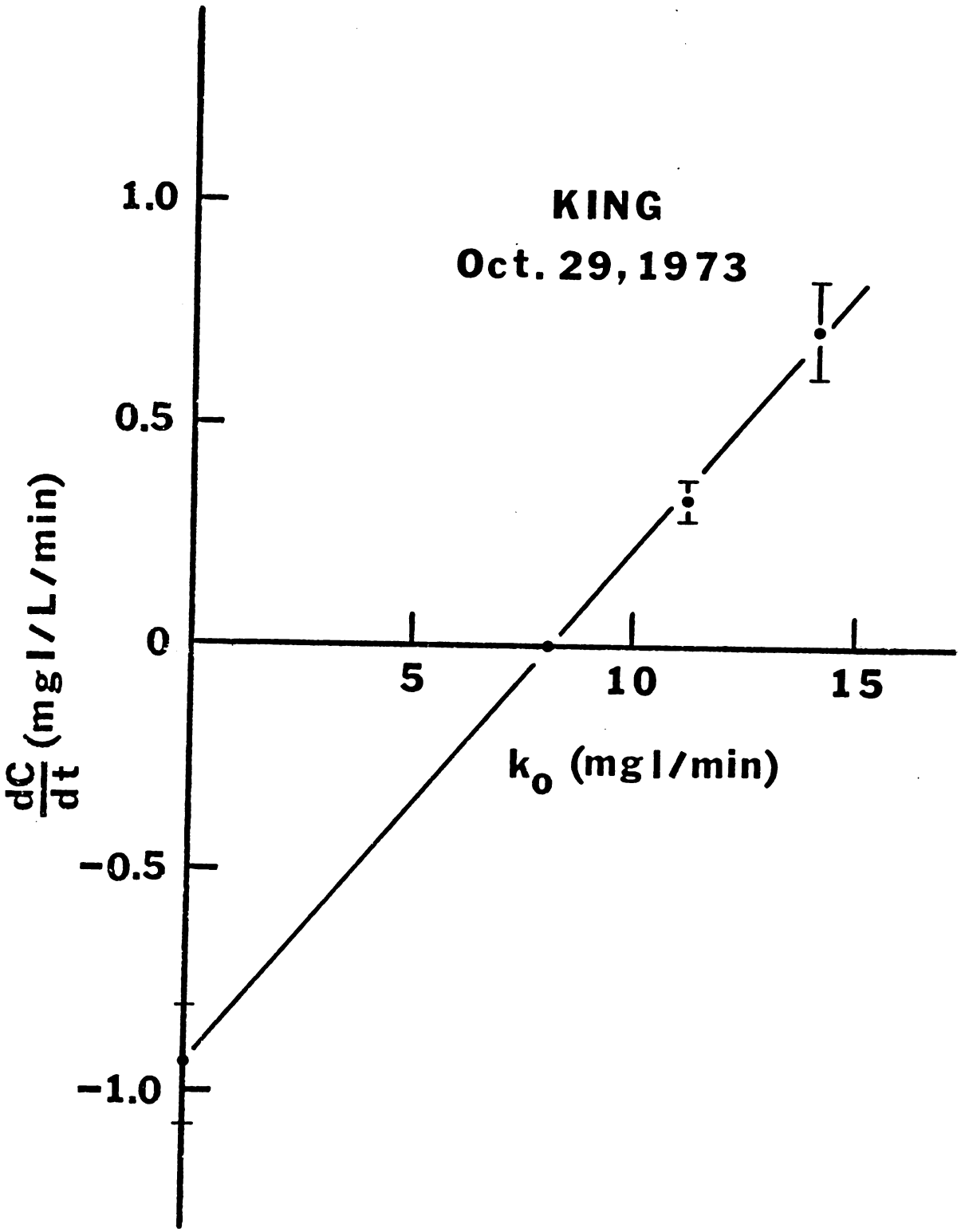
KING
Oct. 29, 1973
1.0
0.5
0
-0.5
-1.0
5
10
15
$\frac{dC}{dt}$ (mg l/L/min)
k_o (mg l/min)

TABLE 4.4

King-Low Taurocholate (Dec. 17, 1973)
Blood Slope Analysis

(1)	(2)	(3)	(4)	(5)	(6)	(7)	(8)	(9)
Infusion Rate	$\frac{dC}{dt}$ (mgI/L/min)	N	r	r^2	p (D.F.=N-2)	Sb (mgI/L/min)	$Sb \cdot t_{0.05}$ (mgI/L/min)	$\frac{Sb}{b}$ x 100%
11.21	0.473	13	0.98579	0.97178	<0.001	0.0243	$\pm$0.0535	5.1%
8.15	0.165	16	0.81616	0.66612	<0.001	0.0312	$\pm$0.0669	19%
8.15	0.211	32	0.84785	0.71885	<0.001	0.0241	$\pm$0.0492	11%
0.0	-0.697	23	0.98806	0.97626	<0.001	0.0237	$\pm$0.0493	3.4%

Infusion Rate - Blood Slope Analysis

(10)	(11)	(12)	(13)	(14)	(15)	(16)	(17)
b	N	r	r^2	p	Sb	$Sb \cdot t_{0.05}$	$\frac{Sb}{b}$ x 100%
0.105633	4	0.99863	0.99726	<0.005	0.00392	$\pm$0.0169	3.7%

$\frac{1}{Vd} = 0.105633$ Vd = 9.47L

$\frac{Tm}{Vd} = 0.6885$ Tm = 6.52 mg I/min

TABLE 4.5

Blackie-High Taurocholate (Dec. 3, 1973)
Blood Slope Analysis

(1) Infusion Rate	(2) $\frac{dC}{dt}$ (mgI/L/min)	(3) N	(4) r	(5) r^2	(6) p (D.F.=N-2)	(7) Sb (mgI/L/min)	(8) $Sb \cdot t_{0.05}$ (mgI/L/min)	(9) $\frac{Sb}{b} \times 100\%$
10.14	0.439	14	0.96038	0.92233	<0.001	0.0367	$\pm$0.0801	8.4%
7.49	0.172	14	0.89137	0.79454	<0.001	0.0252	$\pm$0.0550	15%
12.84	0.639	11	0.97570	0.95199	<0.001	0.0478	$\pm$0.1082	7.5%
0.0	-0.740	14	-0.99410	0.98823	<0.001	0.0233	$\pm$0.0508	3.2%

Infusion Rate - Blood Slope Analysis

(10) b	(11) N	(12) r	(13) r^2	(14) p	(15) Sb	(16) $Sb \cdot t_{0.05}$	(17) $\frac{Sb}{b} \times 100\%$
0.109725	4	0.99576	0.99154	<0.005	0.00717	$\pm$0.0308	6.5%

$\frac{1}{Vd} = 0.109725$ Vd = 9.11 L

$\frac{Tm}{Vd} = 0.7083$ Tm = 6.46 mg I/min

TABLE 4.6

Blackie - Low Taurocholate (Dec. 3, 1973)
Blood Slope Analysis

(1) Infusion rate (mgI/min)	(2) $\frac{dC}{dt}$ (mgI/L/min)	(3) N	(4) r	(5) r^2	(6) p (D.F.=N-2)	(7) Sb (mgI/L/min)	(8) $Sb \cdot t_{0.05}$ (mgI/L/min)	(9) $\frac{Sb}{b}$ x 100%
9.86	0.629	19	0.00637	0.99275	<0.001	0.0130	±0.0275	2.1%
7.27	0.356	16	0.94226	0.88787	<0.001	0.0339	±0.0726	9.5%
12.68	0.905	11	0.98112	0.96260	<0.001	0.0595	±0.1345	6.6%
7.67	0.388	11	0.94771	0.89815	<0.001	0.0436	±0.0986	11%
0.00	-0.520	18	-0.98446	0.96916	<0.001	0.0232	±0.0491	4.5¢

Infusion Rate - Blood Slope Analysis

(10) b	(11) N	(12) r	(13) r^2	(14) p	(15) Sb	(16) $Sb \cdot t_{0.05}$	(17) $\frac{Sb}{b}$ x 100%
0.113262	5	0.99734	0.99469	<0.001	0.00478	±0.0152	4.2%

$\frac{1}{Vd} = 0.113262$ Vd = 8.83 L

$\frac{Tm}{Vd} = 0.4884$ Tm = 4.31 mgI/min

TABLE 4.7

Oliver- High Taurocholate (Feb. 19, 1974)
Blood Slope Analysis

(1) Infusion Rate (mgI/min)	(2) $\frac{dC}{dt}$ (mgI/L/min)	(3) N	(4) r	(5) r^2	(6) p (D.F.=N-2)	(7) Sb (mgI/L/min)	(8) $Sb \cdot t_{0.05}$ (mgI/L/min)	(9) $\frac{Sb}{b} \times 100\%$
9.72	0.388	17	0.98874	0.97761	<0.001	0.0152	±0.0323	3.9%
4.40	-0.302	12	-0.97813	0.05674	<0.001	0.0203	±0.0453	6.7%
12.41	0.884	10	0.99191	0.98389	<0.001	0.0400	±0.0922	4.5%
7.15	0.0875	9	0.59594	0.35514	<0.100	0.0446	±0.1054	51%
0.00	-1.124	10	-0.98952	0.97915	<0.001	0.0580	±0.1337	5.2%

Infusion Rate - Blood Slope Analysis

(10) b	(11) N	(12) r	(13) r^2	(14) p	(15) Sb	(16) $Sb \cdot t_{0.05}$	(17) $\frac{Sb}{b} \times 100\%$
0.157291	5	0.99678	0.99357	<0.001	0.007306	±0.0232	4.6%

$\frac{1}{Vd} = 0.157291$ Vd = 6.36 L

$\frac{Tm}{Vd} = 1.0728$ Tm = 6.82 mgI/min

TABLE 4.8

Oliver-Low Taurocholate (Jan. 14, 1974)
Blood Slope Analysis

(1) Infusion Rate (mgI/min)	(2) $\frac{dC}{dt}$ (mgI/L/min)	(3) N	(4) r	(5) r^2	(6) p (D.F.=N-2)	(7) Sb (mgI/L/min)	(8) $Sb \cdot t_{0.05}$ (mgI/L/min)	(9) $\frac{Sb}{b} \times 100\%$
9.65	0.724	20	0.99385	0.98773	<0.001	0.0190	±0.0400	2.6%
4.29	0	--	--	--	--	--	--	--
12.38	1.236	11	0.97651	0.95357	<0.001	0.0909	±0.2056	7.4%
7.10	0.466	11	0.92726	0.85981	<0.001	0.0627	±0.1418	13%
0	-0.902	14	-0.99459	0.98921	<0.001	0.0272	±0.0593	3.0%

Infusion Rate - Blood Slope Analysis

(10) b	(11) N	(12) r	(13) r^2	(14) p	(15) Sb	(16) $Sb \cdot t_{0.05}$	(17) $\frac{Sb}{b} \times 100\%$
0.167830	5	0.99391	0.987857	<0.001	0.0107	±0.0342	6.4%

$\frac{1}{Vd} = 0.167830$ Vd = 5.96 L

$\frac{Tm}{Vd} = 0.8170$ Tm = 4.87 mg

TABLE 4.9

Wendall-High Taurocholate (Feb. 26, 1974)
Blood Slope Analysis

(1) Infusion rate (mgI/min)	(2) $\frac{dC}{dt}$ (mgI/L/min)	(3) N	(4) r	(5) r^2	(6) p (D.F.=N-2)	(7) Sb (mgI/L/min)	(8) $Sb \cdot t_{0.05}$ (mgI/L/min)	(9) $\frac{Sb}{b} \times 100\%$
10.70	0.383	13	0.99105	0.98218	<0.001	0.0156	$\pm$0.0343	4.1%
15.61	0.949	8	0.99373	0.98750	<0.001	0.0436	$\pm$0.1066	4.6%
9.27	0.186	16	0.92919	0.86339	<0.001	0.0198	$\pm$0.0425	11%
0.00	-1.168	14	-.99588	0.99178	<0.001	0.0307	$\pm$0.0669	2.6%

Infusion Rate - Blood Slope Analysis

(10) b	(11) N	(12) r	(13) r^2	(14) p	(15) Sb	(16) $Sb \cdot t_{0.05}$	(17) $\frac{Sb}{b} \times 100\%$
0.137316	4	0.99807	0.99614	<0.005	0.00604	$\pm$0.0260	4.4%

$\frac{1}{Vd} = 0.137316$ Vd = 7.28 L

$\frac{Tm}{Vd} = 1.1339$ Tm = 8.26 mgI/min

TABLE 4.10

Wendall-Low Taurocholate (April 1, 1974).
Blood Slope Analysis

(1) Infusion Rate (mgI/min)	(2) $\frac{dC}{dt}$ (mgI/L/min)	(3) N	(4) r	(5) r^2	(6) p (D.F.=N-2)	(7) Sb (mgI/L/min)	(8) $Sb \cdot t_{0.05}$ (mgI/L/min)	(9) $\frac{Sb}{b} \times 100\%$
9.61	0.419	13	0.99241	0.98488	<0.001	0.0156	±0.0344	3.7%
7.13	0.194	15	0.94082	0.88514	<0.001	0.0194	±0.0419	10%
12.33	0.873	12	0.97506	0.95074	<0.001	0.0628	±0.13997	7.2%
0.00	-0.666	19	-0.99838	0.99676	<0.001	0.00921	±0.0194	1.4%

Infusion Rate - Blood Slope Analysis

(10) b	(11) N	(12) r	(13) r^2	(14) p	(15) Sb	(16) $Sb \cdot t_{0.05}$	(17) $\frac{Sb}{b} \times 100\%$
0.121672	4	0.99681	0.00363	<0.005	0.00689	±0.0296	5.6%

$\frac{1}{Vd} = 0.121672$ Vd = 8.22 L

$\frac{Tm}{Vd} = 0.6792$ Tm = 5.58 mgI/min

of slope.

Blood slopes greater than 0.1 mgI/L/min were significantly different from zero ($p < 0.001$). Linear regression analysis of these slopes yielded r^2 values generally greater than 0.94. The coefficients of variation ranged from 1.4% to 19% with a mean of 6.8%.

As can be seen from the lower halves of Table 4.3 to 4.10, infusion rate-blood slope analysis also demonstrates excellent correlation. This can be visually seen in Figures 4.17 to 4.20. In these figures the blood slopes with their 95% confidence intervals are plotted against their corresponding infusion rates. In all four dogs, the Tm estimated for the low taurocholate infusion is consistently smaller than that for the high taurocholate infusion.

Group Analysis - Figure 4.21 illustrates the plot of the slopes of all four dogs at high TC (35.48 μM/min) against their corresponding infusion rates, weight corrected. As shown in Table 4.11, the apparent Tm obtained from this plot is 0.282 mg/min/kg. Multiplying this value times the average weight of 26.5 kg gives an apparent Tm of 7.49 mg/min at the high taurocholate infusion rate. As summarized in Table 4.12, averaging the individual apparent Tm's, weight corrected, of the four dogs at the high taurocholate

FIGURE 4.17 The blood slope - infusion rate plot for dog King. Low taurocholate infusion (A):Tm = 6.52 mg I/min, Vd = 9.47 L; High taurocholate infusion (B): Tm = 8.10 mg I/min, Vd = 8.53 L.

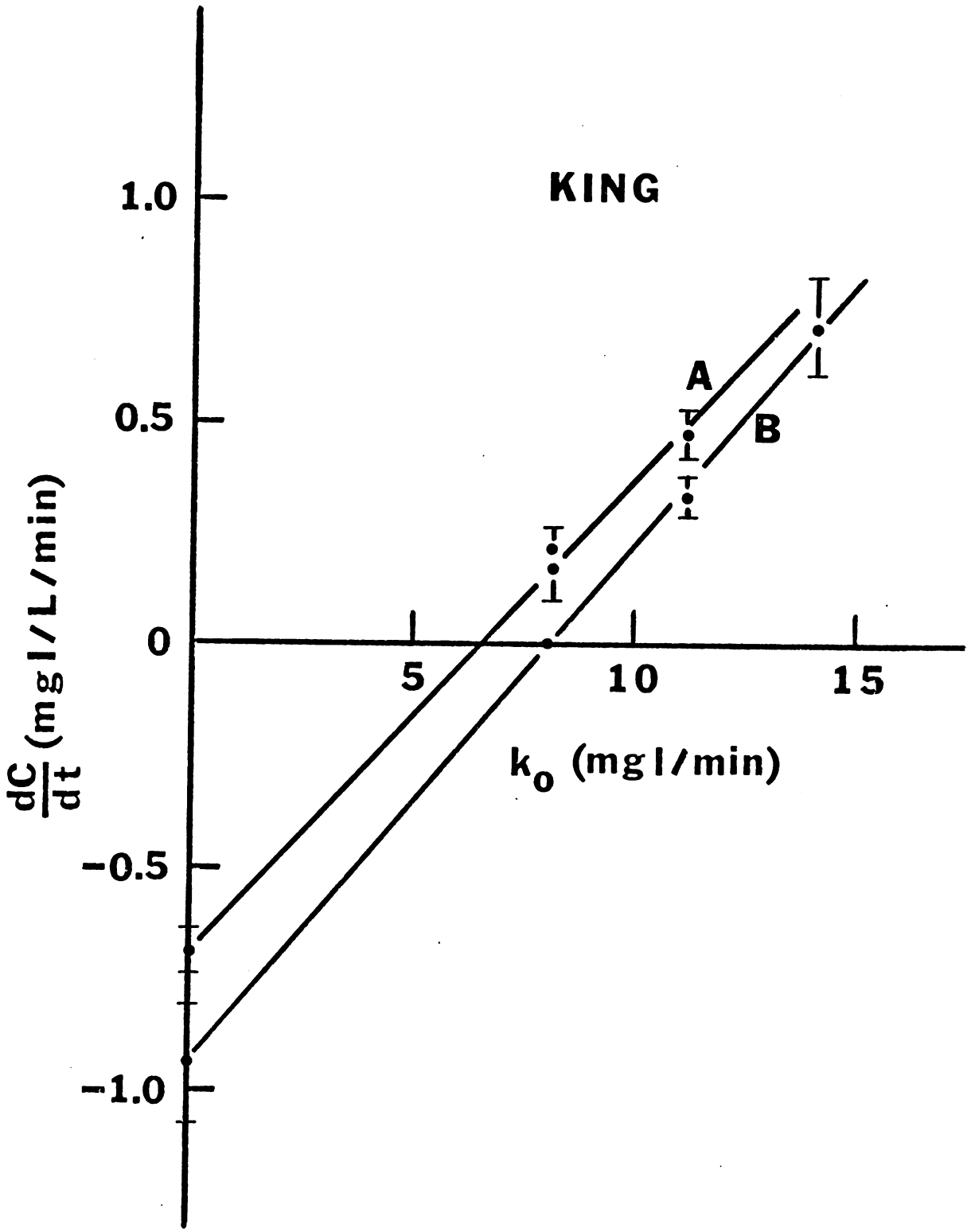
KING
1.0
0.5
0
-0.5
-1.0
5
10
15
A
B
$\frac{dC}{dt}$ (mg l/L/min)
k_o (mg l/min)

FIGURE 4.18 The blood slope - infusion rate plot for dog Blackie. Low taurocholate infusion (A): Tm = 4.31 mg I/min, Vd = 8.83 L; High taurocholate infusion (B): Tm = 6.46 mgI/min, Vd = 9.11 L.

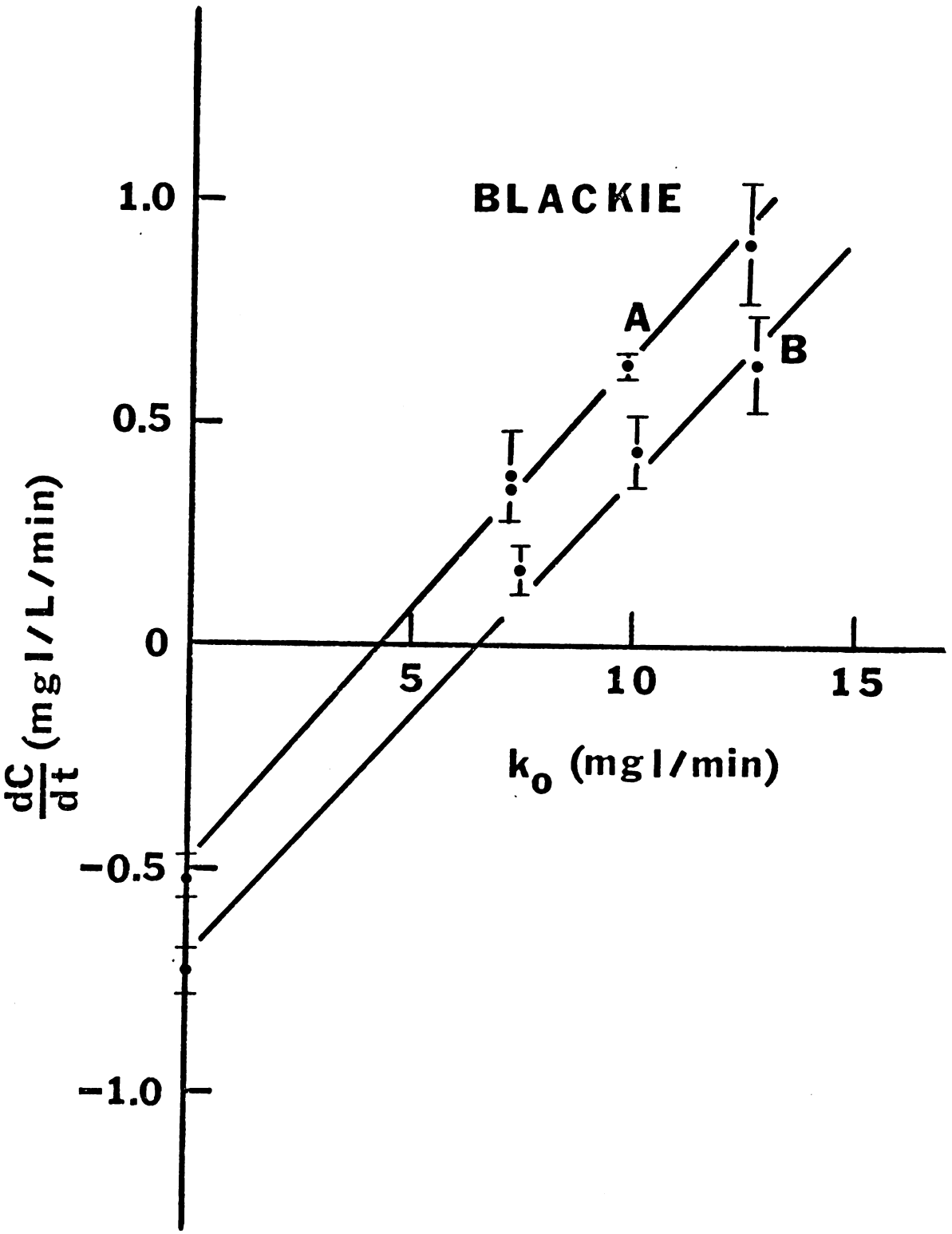
BLACKIE
A
B
1.0
0.5
0
-0.5
-1.0
5
10
15
$\frac{dC}{dt}$ (mgl/L/min)
k_o (mgl/min)

FIGURE 4.19 The blood slope - infusion rate plot for dog Oliver. Low taurocholate infusion (A): Tm = 4.87 mg I/min, Vd = 5.96 L; High taurocholate infusion (B): Tm = 6.82 mg I/min, Vd = 6.36 L.

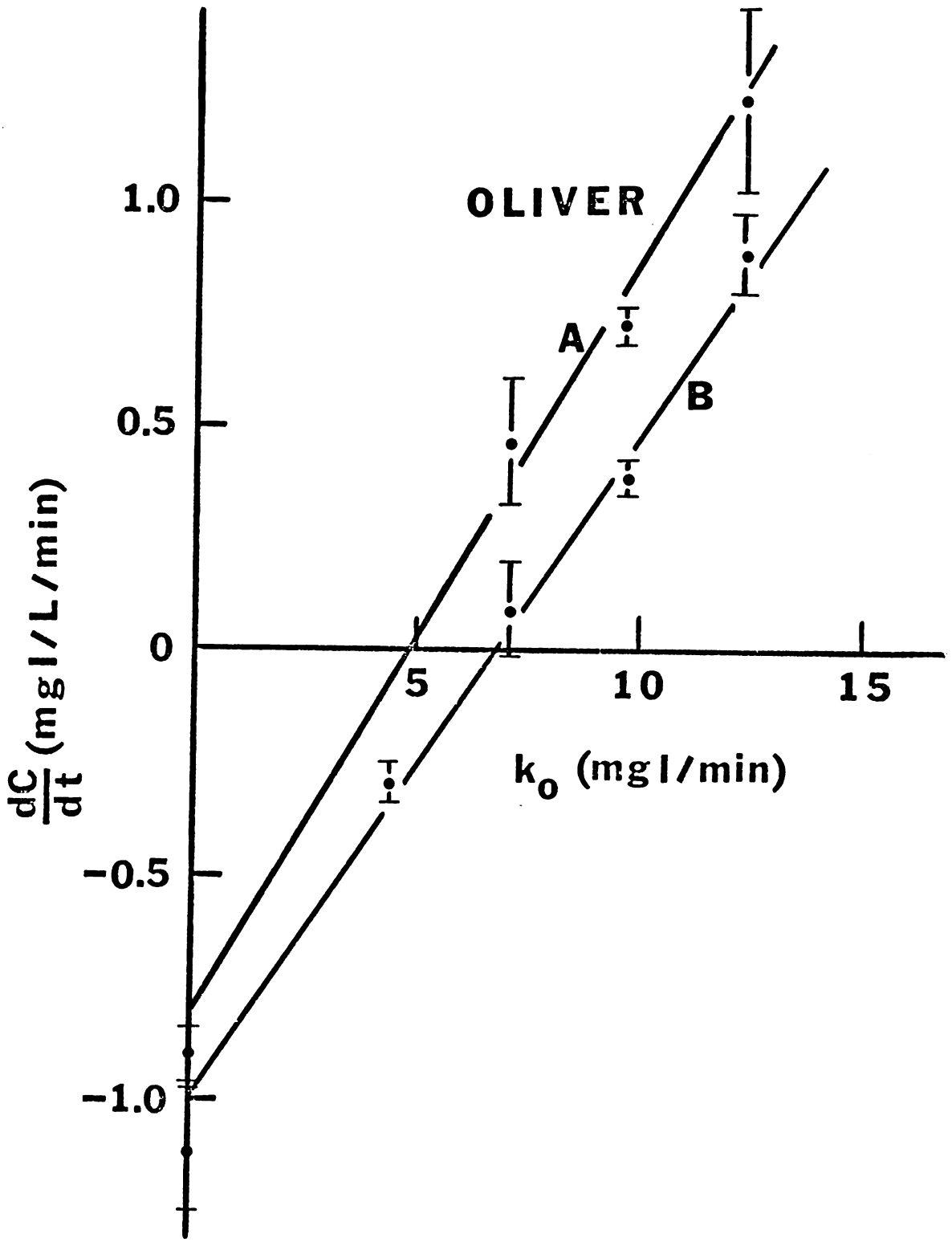
OLIVER
A
B
1.0
0.5
0
-0.5
-1.0
5
10
15
dC/dt (mgl/L/min)
k_o (mgl/min)

FIGURE 4.20 The blood slope - infusion rate plot for dog Wendall, low taurocholate infusion (A): Tm = 5.58 mg I/min, Vd = 8.22 L; High taurocholate infusion (B): Tm = 8.26 mg I/min, Vd = 7.28 L.

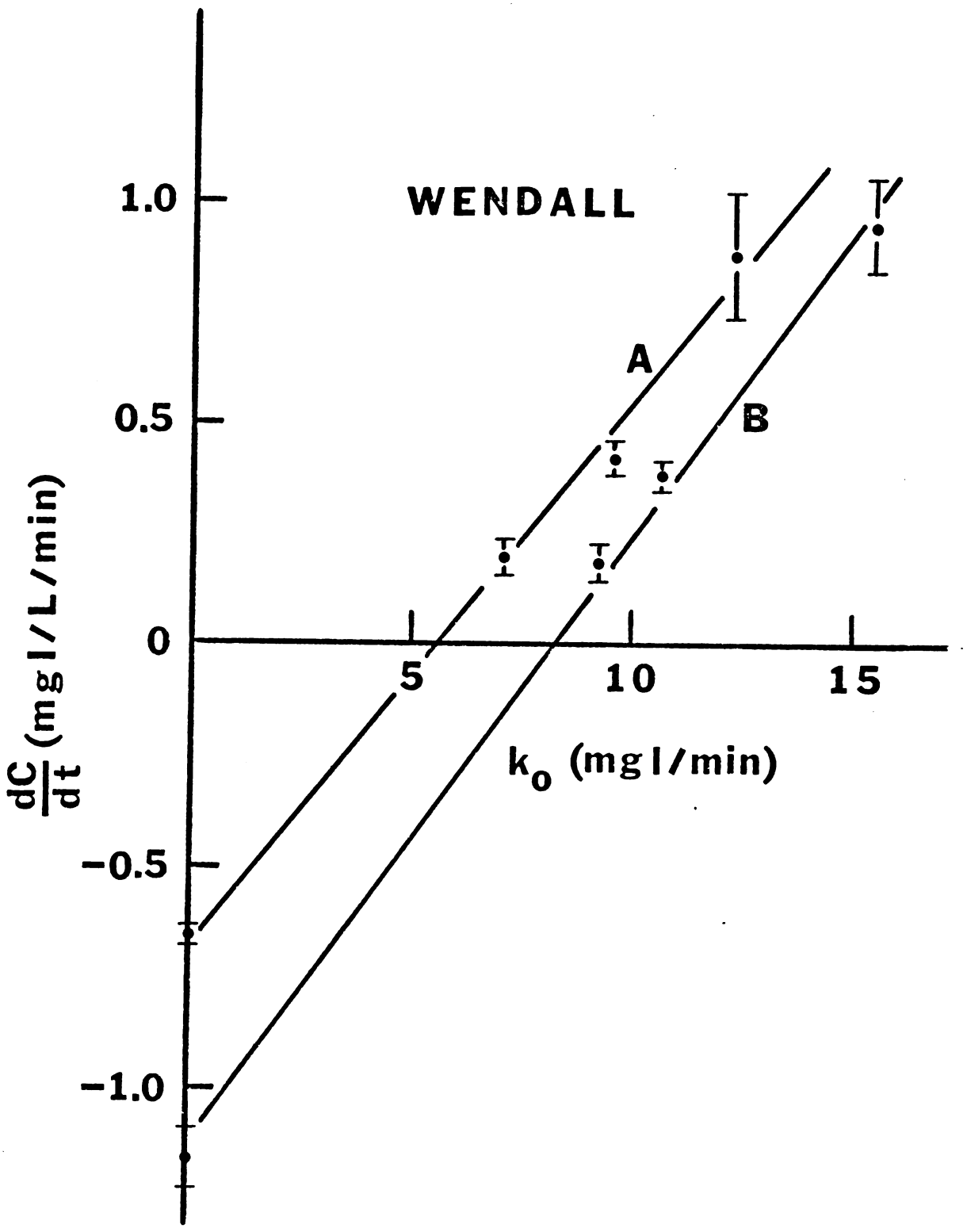
WENDALL
A
B
1.0
0.5
0
-0.5
-1.0
5
10
15
$\frac{dC}{dt}$ (mg l/L/min)
k_o (mg l/min)

FIGURE 4.21 The grouped blood slope - infusion rate (weight corrected) plot for all four dogs at the high taurocholate infusion rate. The estimated Tm = 0.282 mg I/min/Kg.

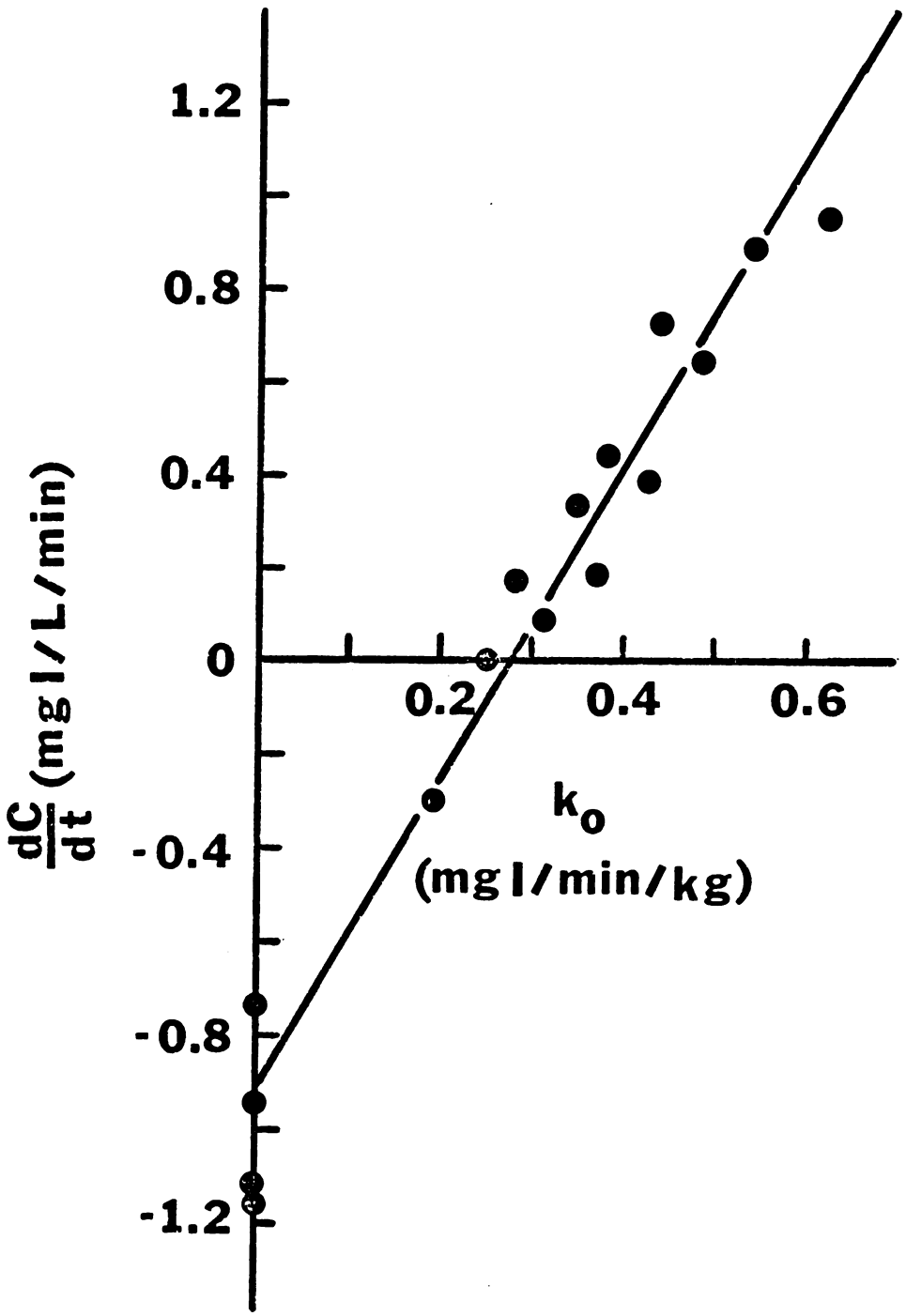
1.2
0.8
0.4
0
-0.4
-0.8
-1.2
0.2
0.4
0.6
$\frac{dC}{dt}$ (mg l/L/min)
k_o
(mg l/min/kg)

TABLE 4.11

GROUP ANALYSIS

Infusion Rates Weight Corrected of all Four Dogs vs Corresponding Blood Slopes

Taurocholate infusion rate (uM/min)	N	r	r^2	p	Sb (kg/L)	$Sb \cdot t_{0.05}$ (kg/L)	$\frac{Sb}{b} \times 100\%$
35.5	18	0.97931	0.95905	<0.001	0.172	± 0.364	5.2%
7.07	18	0.97087	0.94259	<0.001	0.201	± 0.425	6.2%

High Taurocholate

$\frac{1}{Vd} = 3.3264$ Vd = 0.301 L/kg

$\frac{Tm}{Vd} = 0.9378$ Tm = 0.282 mgI/min/kg

Low Taurocholate

$\frac{1}{Vd} = 3.2492$ Vd = 0.308 L/kg

$\frac{Tm}{Vd} = 0.6505$ Tm = 0.200 mgI/min/kg

TABLE 4.12

High Taurocholate Infusion

Dog	Tm (mgI/min)	Tm/kg (mgI/min/kg)	Vd (L)	Vd/kg (L/kg)
King	8.10	0.253	8.53	0.267
Blackie	6.46	0.244	9.11	0.344
Oliver	6.82	0.299	6.36	0.279
Wendall	8.26	0.330	7.28	0.291

Tm = 7.41 mgI/min
SD(σ) = 0.90 mgI/min

Vd = 7.82 L
S.D.(σ) = 1.24 L

Tm/kg = 0.282 mgI/min/kg
S.D.(σ) = 0.040 mgI/min/kg

Vd/kg = 0.295 L/kg
S.D.(σ) = 0.034 L/kg

infusion rate gives a mean of 0.282 ± 0.040 mg/min/kg (m ± S.D.). Averaging the apparent Tm's non-weight corrected, gives a mean of 7.41 ± 0.90 mg/min.

Figure 4.22 illustrates the plot of the slopes of the same four dogs at the low taurocholate infusion rate (7.07 μM/min) against their corresponding infusion rates, weight corrected. As shown in Table 4.11, apparent Tm obtained from this plot is 0.200 mg/min/kg. Multiplying this value times the average weight of 26.5 kg gives an apparent Tm of 5.31 mg/min at the low taurocholate infusion rate. As summarized in Table 4.13, averaging the individual apparent Tm's, weight corrected, of the four dogs at the low taurocholate infusion rate gives a mean of 0.203 ± 0.036 mg/min/kg. Averaging the apparent Tm's, non-weight corrected, gave a mean of 5.32 ± 0.95 mg/min. This represents a 40 percent increase in the apparent Tm for a five-fold increase in the taurocholic acid infusion rate. This difference is significant with a paired t-test ($p < 0.001$).

The high TC rate produced a mean Vd of 7.82 ± 1.24 L; the low TC rate produced a mean Vd of 8.12 ± 1.53 L. There was no significant difference in the apparent Vd of the two sets.

In our previous discussion we eliminated the excretion process as being responsible for the capacity-limited step.

FIGURE 4.22 The grouped blood slope - infusion rate (weight corrected) plot for all four dogs at the low taurocholate infusion rate. The estimated Tm = 0.200 mg I/ min,Kg.

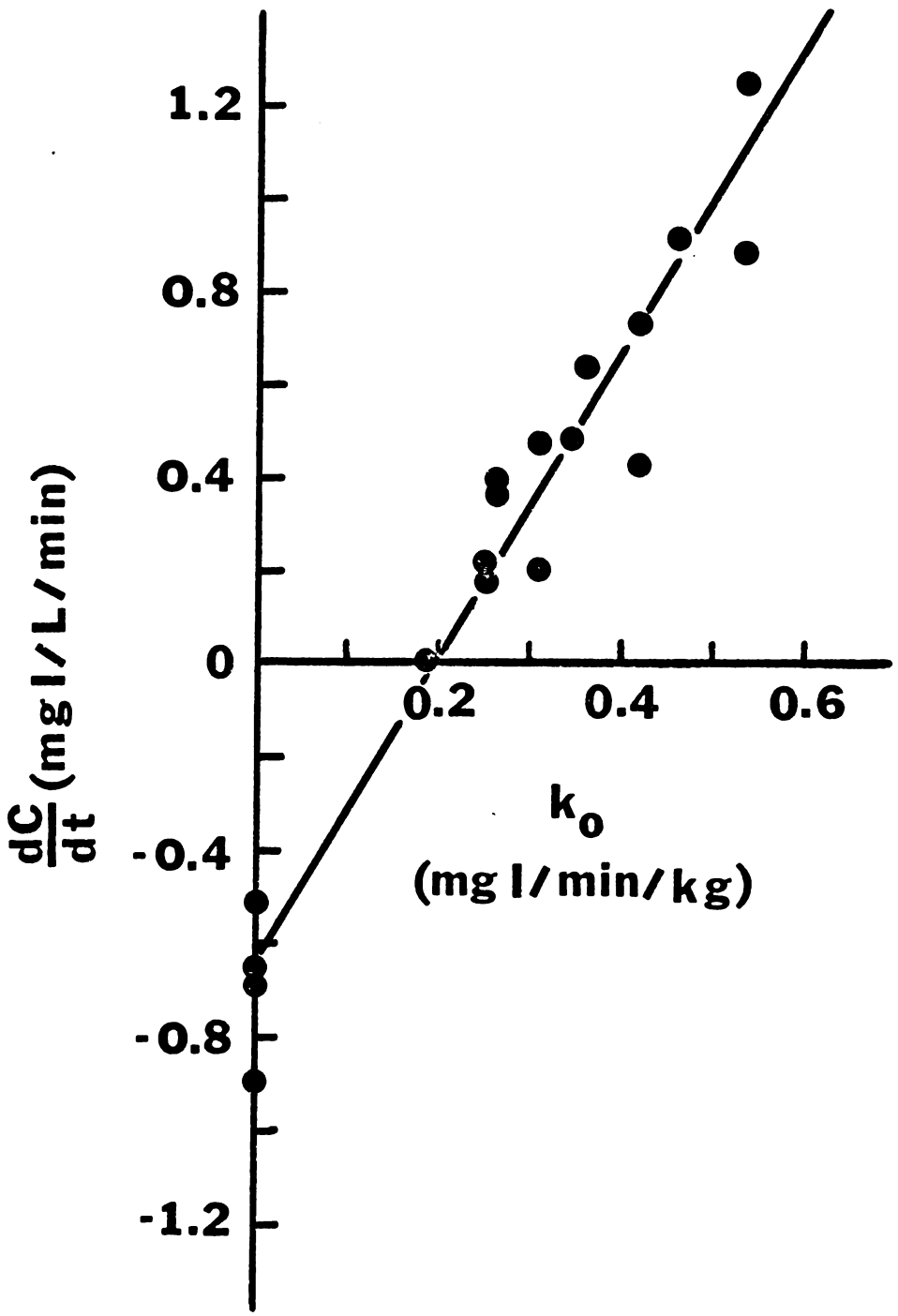
1.2
0.8
0.4
0
-0.4
-0.8
-1.2
0.2
0.4
0.6
dC/dt (mg l/L/min)
k_o
(mg l/min/kg)

TABLE 4.13

Low Taurocholate Infusion

Dog	Tm (mgI/min)	Tm/kg (mgI/min/kg)	Vd (L)	Vd/kg (L/kg)
King	6.52	0.201	9.47	0.291
Blackie	4.31	0.157	8.83	0.321
Oliver	4.87	0.212	5.96	0.259
Wendall	5.58	0.243	8.22	0.357

Tm = 5.32 mgI/min
S.D.(σ) = 0.95 mgI/min

Vd = 8.12 L
S.D.(σ) = 1.53 L

Tm/kg = 0.203 mgI/min/kg
S.D.(σ) = 0.036 mgI/min/kg

Vd/kg = 0.307 L/kg
S.D.(σ) = 0.042 L/kg

Therefore, the question arises as to how a change in the infusion rate of taurocholate can affect the Tm of a conjugation step or of an active/facilitated hepatic uptake step.

Proposal for Experimentation - Problems will exist in any attempt to delineate which of two steps is responsible for the capacity-limited step. Any metabolic inhibitor could theoretically inhibit either process. Any competitive inhibitor could theoretically inhibit both a common uptake process or conjugation of iopanoate even without being conjugated itself. One possibility does exist in that workers (71) have shown *in vitro* non-competitive irreversible inhibition of BSP conjugation by iopanoic acid. If further *in vitro* experiments show no inhibition of iopanoic acid conjugation by BSP, then it should be theoretically feasible to distinguish the two possibilities. *In vivo* experiments should exhibit competition of BSP and iopanoate on each other if they share a common capacity-limited uptake process. If, however, conjugation was responsible for the capacity-limited step, then *in vivo* experiments should show inhibition of BSP removal by iopanoic acid (Fig. 4.23), but not the reverse situation (Fig. 4.24)

More work in this area is needed in order to develop a specific liver function test - a test that could distinguish between a defect in uptake versus a defect in conjugation versus a defect in excretion.

FIGURE 4.23 The projected schematic of the apparent BSP's Tm versus iopanoic acid steady state blood concentrations from a series of experiments in which BSP's Tm is measured at different steady state levels of iopanoic acid . This assumes that iopanoic acid will inhibit BSP removal *in vivo*.

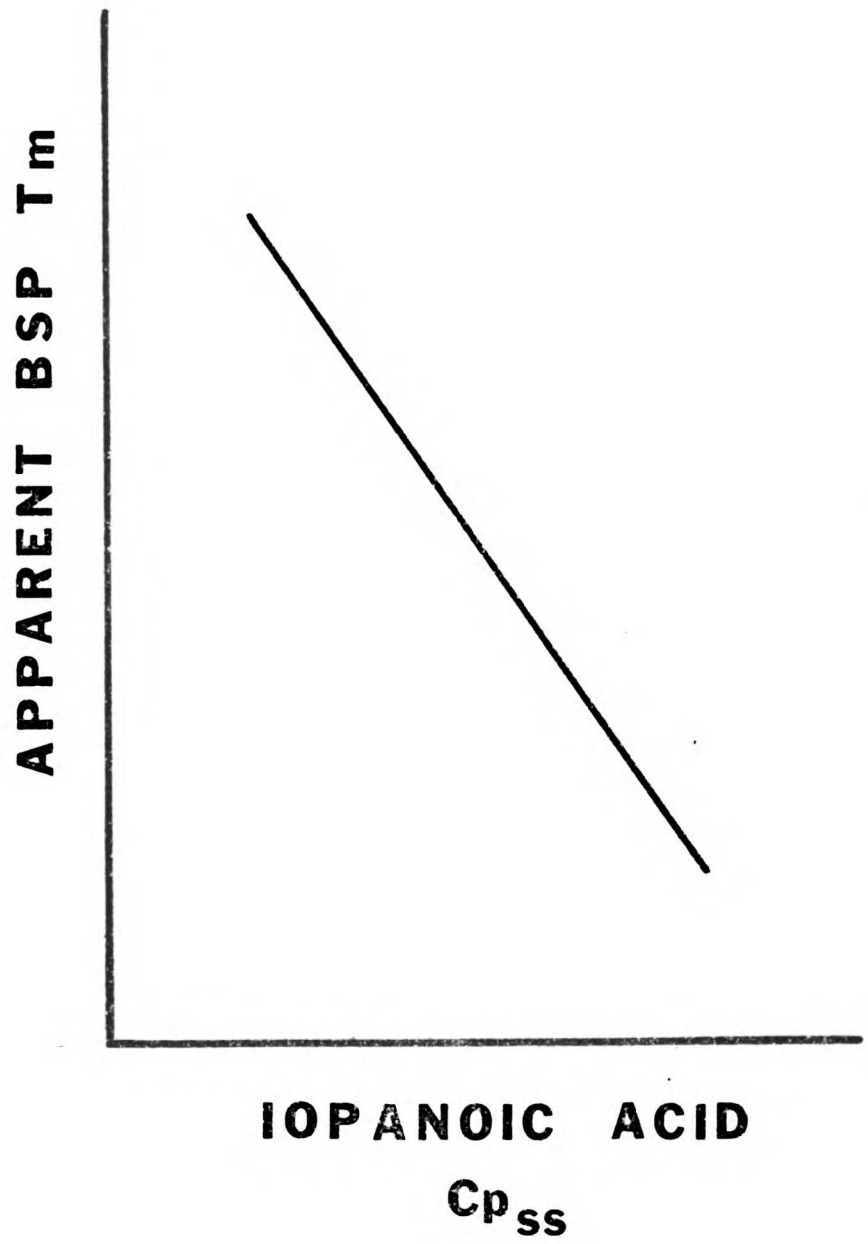
APPARENT BSP Tm
IOPANOIC ACID
Cp_{ss}

FIGURE 4.24 The projected schematic of the apparent iopanoic acid's Tm versus BSP steady state blood concentrations from a series of experiments in which iopanoic acid's Tm is measured at different steady state levels of BSP. This assumes that BSP does not inhibit iopanoic acid removal *in vivo*.

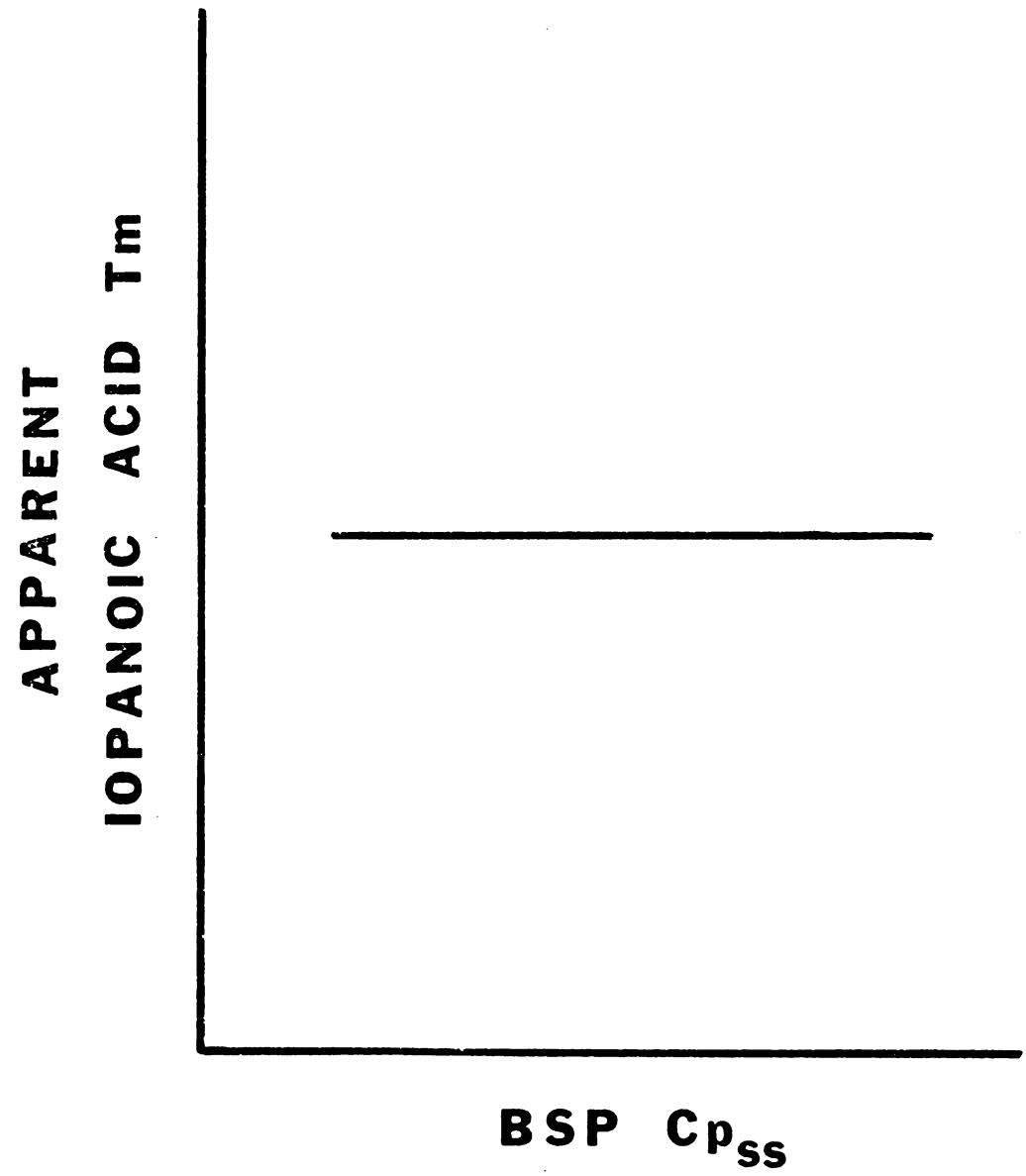
APPARENT
IOPANOIC ACID Tm
BSP Cp_{ss}

REFERENCES

1. R. N. Berk, P. M. Loeb, L. E. Goldberger, and J. Sokoloff. Oral Cholecystography with Iopanoic Acid. N. Engl. J. Med. 290: 204 (1974).

2. F. J. Ingelfinger. Digestive Disease as a National Problem, V. Gallstones. Gastroenterology. 55: 102-104 (1968).

3. J. J. Abel and L. G. Rowntree. On the Pharmacological Action of Some Phthaleins and Their Derivatives with Especial Reference to Their Behavior as Purgatives. I. J. Pharm. Exper. Therap. 1: 231 (1909).

4. E. A. Graham. The Story of the Development of Cholecystography. Am. J. Surgery. 13: 330 (1931).

5. E. A. Graham and W. H. Cole. Roentgenologic Examination of the Gallbladder. J.A.M.A. 82: 613 (1924).

6. E. A. Graham, W. H. Cole, and G. H. Copher. Visualization of the Gallbladder by the Sodium Salt of Tetrabromphenolphthalein. J.A.M.A. 82: 1777 (1924).

7. E. A. Graham, W. H. Cole, S. Moore, and G. H. Copher. Cholecystography: Oral Administration of Sodium Tetra-iodophenolphthalein. J.A.M.A. 85: 953 (1925).

8. J. O. Hoppe. The Evaluation of Iodinated Organic Compounds as Radiopaque Media. J. Am. Pharm. Assoc. 48: 368 (1959).

9. W. R. Christensen and M. C. Sosman. A Preliminary Report on Telepaque, A New Cholecytographic Medium. Am. J. Roentgenol.,66: 764 (1951).

10. T. R. Lewis and S. Archer. The Preparation of Some Iodinated Aminophenylalkanoic Acids. J. Am. Chem. Soc. 71: 3753 (1949).

11. S. Archer, J. O. Hoppe, and T. R. Lewis. The Preparation and Cholecystographic Properties of Some Aminotriiodophenylalkanoic Acids. J. Am. Pharm. Assoc. 40: 617 (1951).

12. J. O. Hoppe and S. Archer. Aryl Triiodo Alkanoic Acid Derivatives as Cholecystographic Media. Fed. Proc. 10: 310 (1951).

13. S. Archer and J. O. Hoppe. Acylated Triiodoaminophenylalkanoid Acids. Chem. Abs. 54: 1445 (1960).

14. E. F. Dunne, E. H. Jensen, and Robert C. Hughes. Preliminary Study of a New Cholecystographic Medium. Cleveland Clin. Quart. 18: 98 (1951).

15. R. H. Morgan and H. B. Stewart. Clinical Experience with Telepaque, a New Gallbladder Compound. Radiol. 58: 231 (1952).

16. E. F. Everett and L. G. Rigler. Cholecytography with Telepaque. Radiol. 58: 524 (1952).

17. F. M. Spencer. Experience with a New Cholecystographic Medium (Telepaque). Gastroenterology. 21: 535 (1952).

18. W. H. Shehadi. Telepaque A New Cholecystographic Medium with Improved Visualization of the Gallbladder and Visualization of the Bile Ducts. Am. J. Roentgenol. 68: 360 (1952).

19. L. Reynolds and H. Fulton. Oral Cholecystography with Iopanoic Acid (Telepaque. J.A.M.A. 159: 1358 (1955).

20. H. D. Rosenbaum. The Value of Re-Examination in Patients with Inadequate Visualization of the Gall-Bladder following a Single Dose of Telepaque. Am. J. Roentgenol. Radium Ther. Nucl. Med. 82: 1011 (1959).

21. R. N. Berk. The Consecutive Dose Phenomenon in Oral Cholecystography. Am. J. Roentgenol. Radium Ther. Nucl. Med. 110: 230 (1970).

22. W. W. White and H. W. Fisher. A Double Blind Study of Oragrafin and Telepaque. Am. J. Roentgenol. Radium Ther. Nucl. Med. 87: 745 (1962).

23. J. E. Wennberg, R. Okun, E. J. Hinman, R. C. Northcutt, R. J. Griep, and W. G. Walker. Renal Toxicity of Oral Cholecystographic Media. J.A.M.A. 186: 107 (1963).

24. D. Littmann and F. I. Marcus. Coronary Insufficiency Associated with Oral Administration of Gall-Bladder Dye. N. Engl. J. Med. 258: 1248 (1958).

25. R. M. Rone and S. M. Mellinkoff. Renal Insufficiency after Oral Administration of a Double Dose of a Cholecystographic Medium. New Eng. J. Med. 261: 589 (1959).

26. R. M. Taketa, R. N. Berk, J. H. Lang, E. C. Lasser, and C. R. Dunn. The Effect of pH on the Intestinal Absorption of Telepaque. Amer. Journ. Roentgenol. 114: 767 (1972).

27. E. W. McChesney and J. O. Hoppe. Observations on the Metabolism of Iodopanoic Acid. Arch. Int. Pharmacodyn. Ther. 99: 127 (1954).

28. L. E. Goldberger, R. N. Berk, J. H. Lang, and P. M. Loeb. Biopharmaceutical Factors Influencing the Intestinal Absorption of Iopanoic Acid. Invest. Radiol. 9: 16 (1974).

29. K. H. Holmdahl and H. Lodin. Absorption of Iopanoic Acid and its Sodium Salt. Acta. Radiol. 51: 247 (1959).

30. R. Peterhoff. Cholecystography with the Sodium Salt of Iopanoic Acid. Acta Radiol. 46: 719 (1956).

31. P. A. Shore, B. B. Brodie, and C. A. M. Hogben. The Gastric Secretion of Drugs: A pH Partition Hypothesis. J. Pharmacol. Exp. Ther. 119: 361 (1957).

32. L. S. Schanker, P. A. Shore, B. B. Brodie, and C. A. M. Hogben. Absorption of Drugs from the Stomach In The Rat. J. Pharmacol. Exp. Ther. 120: 528 (1957).

33. C. A. M. Hogben, D. J. Tocco, B. B. Brodie, and L. S. Schanker. On the Mechanism of Intestinal Absorption of Drugs. J. Pharmacol. Exp. Ther. 125: 275 (1959).

34. J. A. Nelson, A. A. Moss, H. I. Goldberg, L. F. Benet, and J. Amberg. Gastrointestinal Absorption of Iopanoic Acid. Invest. Radiol. 8: 1 (1973).

35. R. I. Reinke and R. N. Berk. The Mode of Telepaque Absorption from the Intestine. Am. J. of Roent. 113: 578 (1971).

36. J. H. Lang and E. C. Lasser. Binding of Roentgenographic Contrast Media to Serum Albumin. Invest. Radiol. 2: 391 (1967).

37. A. J. Levi, F. Gatmaitan, and I. M. Arias. Two Hepatic Cytoplasmic Protein Fractions, Y and Z, and their Possible Role in the Hepatic Uptake of Bilirubin, Sulfobromophthalein and Other Anions. J. Clin. Invest. 48: 2156 (1969).

38. J. Sokaloff, R. N. Berk, and J. H. Lang, and E. C. Lasser. The Role of the Y and Z Hepatic Proteins in the Excretion of Radiographic Contrast Materials. Radiology. 106: 519 (1973).

39. C. Cornelius, J. Ben-Ezzer, and I. M. Arias. Binding of Sulfobromophthalein Sodium (BSP) and Other Organic Anions by Isolated Hepatic Cell Plasma Membranes in vitro. Proc. Soc. Exp. Biol. Med. 124: 665 (1967).

40. F. J. Sanen. Considerations of Cholecystographic Contrast Media. Am. J. Roentgenol. 88: 797 (1962).

41. L. J. Schoenfield and W. T. Foulk. Studies of Sulfobromophthalein Sodium (BSP) Metabolism in Man. II. The Effect of Artificially Induced Fever, Norethandralone (Nilevar), and Iopanoic Acid (Telepaque). J. Clin. Invest. 43: 1419 (1964).

42. H. W. Fischer. Attempts to Improve Iodipamide Intravenous Cholangiography. Am. J. Roentgenol. 96: 477 (1966).

43. N. Kaplowitz, G. Clifton, and J. Kuhlenkamp. Hepatic Glutathione (GSH) S-Transferases: A Group of Enzymes with Similarities to Ligandin. Clinical Research. 22: 362A (1974).

44. N. Kaplowitz, I. W. Peroy-Robb, and N. B. Javitt. Role of Hepatic Anion-Binding Protein in Bromosulphthalein Conjugation. J. Exp. Med. 138: 483 (1973).

45. J. O. Hoppe and S. Archer. Observations on a Series of Aryl Triiodo Alkanoic Acid Derivatives with Particular Reference to a New Cholecystographic Medium, Telepaque. Am. J. Roentgenol. Radium Ther. Nucl. Med. 69: 631 (1953).

46. E. W. McChesney and W. F. Banks, Jr. Urinary Excretion of Three Oral Cholecystographic Agents in Man. Proc. Soc. Exp. Biol. Med. 119: 1027 (1965).

47. P. Millburn, R. L. Smith, and R. T. Williams. Biliary Excretion of Foreign Compounds. Biophenyl, stilbestrol, and Phenolphthalein in the Rat; Molecular Weight, Polarity, and Metabolism as Factors in Biliary Excretion. Biochem. J. 105: 1275 (1967).

48. R. L. Smith. Species Differences in the Biliary Excretion of Drugs. Proc. Europ. Soc. Study Drug Toxicity. 11: 19 (1970).

49. F. T. A. Aziz, P. C. Hirom, P. Millburn, R. L. Smith, and R. T. Williams. Biliary Excretion of Anions of Molecular Weight 300-800 in the Rat, Guinea Pig, and Rabbit. Biochem. J. 125: 25P (1971).

50. E. J. Mroszcyzak. "The Biliary Excretion and Enterohepatic Circulation of Diethylstibestrol and Diethylstilbestrol Monglucuronide in the Rhesus Monkey." Ph.D. Thesis, University of California, San Francisco, California, (1974).

51. J. A. Nelson (Department of Radiology, University of Utah Medical Center) Personal Communication (1973).

52. L. Andren and G. Theander. Residual Contrast Medium in the Bowel in Cholecystography with Iopanoic Acid and Certain Related Substances. Acta. Radiol. 53: 371 (1960).

53. H. E. Fink, Jr., W. J. Roenigk, and G. P. Wilson. An Experimental Investigation of the Nephrotoxic Effects of Oral Cholecystographic Agents. Am. J. Med. Sci. 247: 201 (1964).

54. E. E. Seedorf and W. N. Powell. Experience with Five Orally Given Cholecystographic Mediums. J.A.M.A. 159: 1361 (1955).

55. J. S. Schroder and D. Rooney. Excretion of 3-(3-Amino-2,4,6-Triiodophenyl)-2-Ethylpropanoic Acid (Telepaque) by Man. Proc. Soc. Exp. Biol. Med. 83: 544 (1953).

56. P. L. Perlman, R. E. Kosinski, and D. Sutter. Studies on the Absorption and Excretion of a New Cholecystographic Agent, Teridax. J. A. Ph. A. 44: 69 (1955).

57. A. A. Moss, J. R. Amberg, and R. S. Jones. Relationship of Bile Salts and Bile Flow to Biliary Excretion of Iopanoic Acid. Invest. Radiol. 7: 1 (1972).

58. C. R. Dunn and R. N. Berk. The Pharmaco-Kinetics of Telepaque Metabolism. The Relation of Blood Concentration and Bile Flow to the Rate of Hepatic Excretion. Am. J. Roentgenol. 114: 758 (1972).

59. R. N. Berk, L. E. Goldberger, and P.M. Loeb. The role of Bile Salts in the Hepatic Excretions of Iopanoic Acid. Invest. Radiol. 9: 17 (1974).

60. J. A. Nelson, H. W. Pepper, H. I. Goldberg, A. A. Moss, and J. R. Amberg. Effect of Phenobarbital on Iodipamide and Iopanoate Bile Excretion. Invest. Radiol. 8: 126 (1973).

61. M. R. Blum. "Pharmacokinetic Studies of Diphenylhydantoin," Ph.D. Thesis, University of California, San Francisco, California, 1974.

62. H. O. Wheeler, R. M. Epstein, R. R. Robinson, and E. S. Snell. Hepatic Storage and Excretion of Sulfobromophthalein Sodium in the Dog. J. Clin. Invest. 39: 236 (1960).

63. H. O. Wheeler, J. I. Meltzer, and S. E. Bradley. Biliary Transport and Hepatic Storage of Sulfobromophthalein Sodium in the Unanesthetized Dog, in Normal Man, and in Patients with Hepatic Disease. J. Clin. Invest. 39: 1131 (1960).

64. G. Segre. Saturation Phenomena and Zero Order Reactions in "Liver and Drugs," ed. F. Orland and A. M. Jezequel, Academie Press, New York, 1972, pp. 96-98.

65. N. McIntyre, Rosemary Mulligan, and E. Carson. BSP Tm and S, A Critical Re-Evaluation, in "The Liver. Quantitive Aspects of Structure and Function," Karger, Basel, 1973, pp. 417-427.

66. M. Rowland. Effect of Some Physiologic Factors on Bioavailability of Oral Dosage Forms, in "Current Concepts in the Pharmaceutical Sciences: Dosage Form Design and Bioavailability." Ed. James Swarbrick, Lea & Febiger, Philadelphia, 1973, pp. 181-222.

67. L. Kaufman, Carol J. Wilson, J. A. Nelson, and D. M. Shames. Techniques for in vitro and in vivo Elemental Quantitation by Fluorescent Excitation, in "Semiconductor Detectors in Medicine," U.S. Atomic Energy Commission, Office of Information Services, Washington, 1973, pp. 127-147.

68. W. Sadee (School of Pharmacy, University of California at San Francisco), Personal Communication (1973).

69. R. S. Jones, T. K. Yee, and C. E. Michielsen. A Modified Thomas Cannula for Gastric and Intestinal Fistulas. J. Appl. Physiol. 30: 427 (1971).

70. S. I. Seldinger. Catheter Replacement of the Needle in Percutaneous Arteriography. Acta Radiol. 39: 368 (1953).

71. Lee S. Monroe and William J. Longmore. Inhibition of Sulfobromophthalein (BSP) Conjugation with Glutathionine by Iopanoic Acid (Telepaque). Gastroenterology. 50: 396 (1966).